THE UNIVERSITY OF MICHIGAN

INDUSTRY PROGRAM OF THE COLLEGE OF ENGINEERING

INELASTIC BEHAVIOR OF MULTISTORY BUILDING FRAMES SUBJECTED TO EARTHQUAKE MOTION

Subhash C. Goel

A dissertation submitted in partial fulfillment
of the requirements for the degree of
Doctor of Philosophy in the
University of Michigan
Department of Civil Engineering
1967

December, 1967

IP-805

INELASTIC BEHAVIOR OF MULTISTORY BUILDING FRAMES SUBJECTED TO EARTHQUAKE MOTION

Subhash Chandra Goel

ABSTRACT

This dissertation presents a study of the inelastic behavior of unbraced multistory building frames when subjected to earthquake motion. A step-by-step numerical procedure which computes the response of the structure to a horizontal component of ground motion parallel to the plane of the frame is developed for use on a high-speed digital computer. The columns are assumed to behave elastically while the girders have a stable hysteresis behavior, characteristic of welded steel frames, which supplies the energy dissipation. A Ramberg-Osgood type moment-curvature relationship is assumed for the girders and a special hysteresis law is defined to describe their transient response during the lateral oscillation of the structure. In the later phase of the study the procedure is modified to include a form of viscous damping in the structure, the P-Δ effect and the axial deformation of columns.

Test frames of 10, 25, and 40 stories are analyzed while using a fairly wide range of structural parameters. Three accelerograms with distinctly different spectrum characteristics are used. The results of these analyses lead to an evaluation of the influence of various structural properties and the characteristics of ground motion upon the inelastic response of multistory building frames of the particular type investigated herein.

The following aspects of the results seem worthy of emphasis:

- The assumption of elastic behavior of columns is well documented by the inelastic response of the multistory frames subjected to severe earthquakes.
- The hysteresis behavior of girders can be a potential source of energy dissipation in typical multistory structures during a severe earthquake.
- The elastic fundamental period of a multistory structure and the general features of the elastic velocity response spectrum of the earthquake have a marked influence upon the inelastic response of the structure.
- Height or the number of stories of typical structures does not seem to be a very significant factor to influence the amount and distribution of ductile deformations resulting from a strong earthquake.
- The P-Δ effect does not appear to have a significant influence on the earthquake response of the structures analyzed. But the axial deformation of columns may affect the response by as much as 10 to 20 percent.
- Interfloor viscous damping as small as one percent of critical in the elastic fundamental mode of the structure can cause a considered reduction in its inelastic response to a strong earthquake.

INELASTIC BEHAVIOR OF MULTISTORY BUILDING FRAMES SUBJECTED TO EARTHQUAKE MOTION

Subhash Chandra Goel

A dissertation submitted in partial fulfillment
of the requirements for the degree of
Doctor of Philosophy in the
University of Michigan
1967

Doctoral Committee:

Professor Glen V. Berg, Co-chairman
Assistant Professor Robert D. Hanson, Co-chairman
Associate Professor John R. Hall, Jr.
Professor Bruce G. Johnston
Professor Finn C. Michelsen

To

My Elders

ACKNOWLEDGMENTS

The author wishes to express his deep and profound gratitude to Professor Glen V. Berg, co-chairman of his doctoral committee, for introducing him to the field of earthquake engineering and suggesting the problem for this dissertation. His continuous advice and guidance have been extremely valuable without which this dissertation could not have been completed. Special thanks are due to Professor R. D. Hanson, co-chairman of the doctoral committee, who supervised the research work in its later stages during the absence of Professor Berg. Professor Hanson's critical appreciation of the author's work and giving numerous suggestions, and his efforts of reviewing the manuscript have been extremely valuable. The author also wishes to thank all the other members of his doctoral committee for their helpful suggestions.

This dissertation is part of ORA Project 06889, "Response of Steel Frame Structures to Earthquake Motion," administered by the University of Michigan's Office of Research Administration, and directed by Professor Glen V. Berg with whom the author had the privilege of working. The project was sponsored by the American Iron and Steel Institute as its Project No. 119. Fellowships were also provided by the Graduate School of the University of Michigan. The author gratefully acknowledges the financial support received from both the institutions.

The Computing Center of the University of Michigan made available their IBM 7090 computer and the calcomp 763/780 digital plotter for the numerical computations and plotting of some of the results. Miss Reta Teachout and Miss Jean Goss typed the first draft. The final

typing and reproduction was done by the Office of Research Administration and partly by the Industry Program of the College of Engineering. Mr. Robert Anoff did the final drafting of the figures. The author wishes to thank all the individuals who have helped in the production of this dissertation.

The author also wishes to express his special appreciation for his wife, Madhuri Goel, for showing a keen interest and exceptional patience during his two and one half years of graduate study at the University of Michigan.

TABLE OF CONTENTS

		Page
ACKNOWLEDGMENTS		iii
LIST OF TABLES		vii
LIST OF FIGURES		viii
NOMENCLATURE		xii
CHAPTER		
1	INTRODUCTION	1
2	METHOD OF ANALYSIS	5
	2.1 General	5
	2.2 Assumptions	6
	2.3 Outline of Procedure	7
	2.4 Ramberg-Osgood Hysteresis Model	9
	2.5 Ramberg-Osgood Girder Stiffness	14
	2.6 Size of the Time Interval	20
	2.7 Check on Accuracy	25
	2.8 Elastic and Elasto-Plastic Girders	27
3	PROGRAM OF INVESTIGATION	29
	3.1 General	29
	3.2 Structures Considered	29
	3.3 Mathematical Models of the Test Frames	30
	3.4 Response Parameters	39
	3.5 Ground Motion Characteristics	42
4	DISCUSSION OF RESULTS	47
	4.1 General	47
	4.2 Inelastic Behavior of Girders	47
	4.3 Fundamental Period of Structure Versus Period Characteristics of Ground Motion	51
	4.4 Duration of Ground Motion	56
	4.5 Height of Frame	56
	4.5.1 Standard Models	58
	4.5.2 Constant Period Models	59
	4.5.3 Portion of Structure	59
	4.6 Stiffness-Strength Taper	60
	4.7 Yield Strength of Members	61

TABLE OF CONTENTS (Continued)

		Page
5	SOME ADDITIONAL CONSIDERATIONS	106
	5.1 General	106
	5.2 Sidesway Effect of Gravity Loads, the P-Δ Effect	108
	5.2.1 Procedure	108
	5.2.2 Results	111
	5.3 Axial Deformation of Columns	119
	5.3.1 Procedure	119
	5.3.2 Results	123
	5.4 Damping	130
	5.4.1 Procedure	130
	5.4.2 Results	135
6	SUMMARY AND CONCLUSIONS	144
APPENDIX - HYSTERESIS LAW		150
REFERENCES		154

LIST OF TABLES

Table		Page
3.1	Properties of the Standard 40-story Frame	36
3.2	Member Properties, Uniform Models	38
3.3	Values of I_o , Inches	46
4.1	Maximum Input Energy, 10-story Models	55
4.2	Maximum Input Energy, 25-story Models	55

LIST OF FIGURES

Figure		Page
2.1	Ramberg-Osgood Hysteresis Model	10
2.2	Ramberg-Osgood Girder	15
2.3	Moment-Rotation Skeleton Curve	18
2.4	M-θ Discrepancy and Stiffness Modification	22
2.5	A Typical Girder Response	26
3.1	Single-Bay Frame Equivalent to a Multi-Bay Structure	31
3.2	I_x Versus S_x for 14 WF Column Sections	33
3.3	I_x Versus Z_x for 18 WF-36 WF Girder Sections	34
3.4	Yield Criterion	41
3.5	The Three Accelerograms	44
3.6	Undamped Velocity Spectra for the Modified Accelerograms	45
4.1	Effect of Inelastic Action of Girders N = 10, T = 1.25 sec, Taft 1952	63
4.2	Effect of Inelastic Action of Girders N = 25, T = 2.27 sec, El Centro 1940	65
4.3	Elastic Versus Inelastic Response N = 10, T = 1.25 sec, Taft 1952	67
4.4	Elastic Versus Inelastic Response N = 25, T = 2.27 sec, El Centro 1940	68
4.5	Energy Versus Time N = 10, T = 1.25 sec, Taft 1952	69
4.6	Energy Versus Time N = 25, T = 2.27 sec, El Centro 1940	70
4.7	Ramberg-Osgood (r = 10) Versus Elasto-Plastic Response, N = 25, T = 2.27 sec, El Centro 1940	71

Figure		Page
4.8	Effect of Fundamental Period of Structure, N = 10, r = 10, Taft 1952	72
4.9	Effect of Fundamental Period of Structure, N = 25, r = 10, Taft 1952	74
4.10	Effect of Fundamental Period of Structure, N = 10, r = 10, Alameda Park 1962	76
4.11	Effect of Fundamental Period of Structure, N = 25, r = 10, Alameda Park 1962	78
4.12	Effect of Fundamental Period of Structure, N = 10, r = 10, El Centro 1940	80
4.13	Effect of Fundamental Period of Structure, N = 25, r = 10, El Centro 1940	82
4.14	Input Energy Versus Time for the Three Accelerograms, N = 10, r = 10	84
4.15	Input Energy Versus Time for the Three Accelerograms, N = 25, r = 10	85
4.16	Effect of Height on the Inelastic Response, Standard R-0 Models, El Centro 1940	86
4.17	Effect of Height on the Inelastic Response, Standard R-0 Models, Taft 1952	88
4.18	Effect of Height on the Inelastic Response, Standard R-0 Models, Alameda Park 1962	90
4.19	Effect of Height on the Inelastic Response, T = 2.27 sec, r = 10, El Centro 1940	92
4.20	Response of Top 10 Stories, Standard R-0 Models, El Centro 1940	94
4.21	Response of Top 10 Stories, Standard R-0 Models, Taft 1952	96
4.22	Response of Top 10 Stories, Standard R-0 Models, Alameda Park 1962	98
4.23	Effect of Stiffness-Strength Taper N = 10, r = 10, T = 1.25 sec, Taft 1952	100

Figure		Page
4.24	Effect of Stiffness-Strength Taper N = 25, r = 10, T = 2.27 sec, El Centro 1940	102
4.25	Effect of Strength on the Inelastic Response, N = 25, r = 10, T = 2.27 sec, El Centro 1940	104
5.1	P-Δ Effect in Single-Story Frame	109
5.2	P-Δ Effect in Multi-Story Frame	109
5.3	Effect of P-Δ on the Elastic Response, N = 10, T = 1.25 sec, Taft 1952	112
5.4	Effect of P-Δ on the Inelastic Response, N = 10, r = 10, T = 1.25 sec, Taft 1952	113
5.5	Effect of P-Δ on Input and Dissipated Energy, N = 10, Elastic and r = 10, T = 1.25 sec, Taft 1952 ...	115
5.6	Effect of P-Δ on Lateral Response, N = 10, Elastic and r = 10, T = 1.25 sec, Taft 1952	116
5.7	Effect of P-Δ on the Inelastic Response, N = 10, r = 10, T = 1.25 sec, El Centro 1940	117
5.8	Effect of P-Δ on the Inelastic Response, N = 25, r = 10, T = 2.27 sec, El Centro 1940	118
5.9	Girder Bending with Vertical Joint Displacements	122
5.10	Area Versus Moment of Inertia for 14 WF Sections	124
5.11	Effect of Axial Deformation of Columns on the Inelastic Response, N = 10, r = 10, T = 1.25 sec, Taft 1952	125
5.12	Maximum Vertical Joint Displacements and Column Loads, N = 10, r = 10, T = 1.25 sec, Taft 1952	127
5.13	Combined Effect of P-Δ and Axial Deformation of Columns on the Inelastic Response, N = 10, r = 10, T = 1.25 sec, Taft 1952	128
5.14	Effect of Period Change Equivalent to Axial Deformation of Columns on the Inelastic Response, N = 10, r = 10, Taft 1952	131
5.15	Effect of Column Axial Deformation on Inelastic Response, N = 10, r = 10, Taft 1952	132

Figure		Page
5.16	Effect of Column Axial Deformation on Lateral Response, N = 10, r = 10, Taft 1952	133
5.17	Interfloor Viscous Damping	134
5.18	Effect of Damping on the Inelastic Response, N = 10, r = 10, T = 1.25 sec, Taft 1952	136
5.19	Effect of Damping on Input and Dissipated Energy, N = 10, r = 10, T = 1.25 sec, Taft 1952	137
5.20	Effect of Damping on the Lateral Displacements, N = 10, r = 10, T = 1.25 sec, Taft 1952	138
5.21	Effect of Earthquake Duration on Energy Dissipation, N = 10, r = 10, T = 1.25 sec, Taft 1952	139
5.22	Effect of Damping Ratio on Energy Dissipation, N = 10, r = 10, T = 1.25 sec, Taft 1952	140
A	General Hysteresis Behavior	151

NOMENCLATURE

M	moment
ϕ	curvature
M_y, ϕ_y	characteristic moment and curvature in the Ramberg-Osgood function
r	Ramberg-Osgood exponent
$\| \|$	absolute value
N	number of stories
m_i	lumped mass of the i-th floor
$\ddot{x}_i$	acceleration of the i-th mass relative to base
Q_i	restoring force on the i-th mass
$\ddot{y}$	ground acceleration
θ	joint-rotation
θ_y	characteristic joint rotation corresponding to ϕ_y
Δ	incremental value of the argument
x_i	displacement of the i-th mass relative to base
EI	elastic stiffness in flexure
L	bay width
K	girder stiffness
Δt	time step
T	elastic fundamental period in lateral vibration
H	story height
EI_o	common stiffness factor
E	modulus of elasticity
I_x	moment of inertia of a member section about the axis of bending (major axis)

S_x	elastic section modulus about the major axis
Z_x	plastic section modulus about the major axis
d	nominal depth of girder section
σ_y	nominal yield stress
M_{max}	maximum moment in a column
μ	girder ductility ratio
θ_{max}	maximum rotation of girder ends
ϵ	excursion ratio
S_V	maximum relative velocity response of an elastic undamped single-degree-of-freedom system
I_o	spectrum intensity
P-Δ	sidesway effect of gravity loads
V	shear in columns
M^1, M^2	end moments in columns
y_i	vertical displacement of the i-th joint
A	area of column cross-section
$[K'_{xx}]$	lateral stiffness matrix
[D]	damping matrix
[m]	mass matrix
$\{\dot{x}\}$	vector of velocity of floor masses relative to base
β	fraction of critical damping in the elastic fundamental mode
S	damper force per unit velocity

CHAPTER 1

INTRODUCTION

Soon after the results of linear dynamic analysis of the response of building structures subjected to strong motion earthquakes were known, it became obvious that the linear elastic analysis overestimates the response by as much as several hundred percent as compared with the forces that the typical building codes specify for their design.[1,2] Yet the code specifications are favored by the fact that they lead to economical designs which have successfully withstood severe earthquakes in the past with little or no damage at all.[3] This discrepancy between the design forces as specified by the building codes and those predicted by the linear elastic analyses cannot be reconciled even with a relatively large amount of damping and the uncalculated reserve strength of the structure.

Behavior of structures during a strong motion earthquake is far from being linear. Structural and non-structural components of common buildings can dissipate quite large amounts of energy through inelastic deformations before failure. The survival of actual structures during strong motion earthquakes is commonly explained by large amounts of energy being dissipated through the inelastic deformation of the structural and the non-structural components. In the low traditional types of buildings heavy partition walls of concrete or masonry may claim a significant share of the total dissipated energy, thereby reducing the burden of inelastic deformation on the main load-carrying frame. But in the modern tall and slender buildings, the non-structural elements

are greatly reduced for the obvious need of minimizing the dead loads. This presents a great need for a more thorough understanding of the inelastic dynamic behavior of tall building frames, as more and more reliance has to be placed on their capacity to dissipate energy through ductile deformations.

Code procedures and design specifications commonly are based on the results of elastic analyses. By specifying reduced design forces use is made (though implicity) of the capacity of structures to absorb sufficient amounts of energy through damping and inelastic deformation. But explicit recommendations in regard to the damping and ductility requirements of structures and structural materials are lacking in the building codes of today (1967). The reason seems to be the obvious lack of enough experimental and analytical information regarding the exact behavior of structural materials and elements under reversed cyclic loading far into the inelastic range and their damping properties. This together with the formidable amount of computational effort which is required for performing any non-linear earthquake analysis of a multistory structure are sufficient reasons to explain why the building codes have not been able to base their recommendations upon the results of more realistic types of analyses.

A tall building excited into oscillation by earthquake ground motion is an extremely complex problem. In an attempt to compute the inelastic response of such a system two things are absolutely necessary--a calculating machine and a knowledge of the force-deformation behavior of the structural members. With the aid of modern electronic digital computers several investigations (several on single-degree-of-freedom

systems and only a few on the multiple-degree-of-freedom systems) have been made in the past to compute the inelastic response of structures subjected to some past strong motion earthquakes.[4,5,6,7,8,9,10] Among other simplifying assumptions they used relatively simple and idealized force-deformation hysteresis models such as elasto-plastic and bi-linear.

Currently very little is known about the actual hysteresis behavior of structural members and connections under reversed cyclic loading. Some recent experiments at the University of California, Berkeley, on welded steel beam-to-column connections have shown that the hysteresis loops remain remarkably stable even under cyclic extreme-fiber strains as large as 2 1/2 percent.[11] The load-strain behavior is neither elasto-plastic nor bi-linear--rather it is curvilinear which gradually deviates from linearity and leans toward the plastic branch as the strains become large. This behavior can be expressed by a simple mathematical function of the Ramberg-Osgood type in either the force-displacement or the moment-curvature terms. This type of hysteresis model in force-displacement terms has been used by Jennings[12] and Berg[13] in their studies of single-degree-of-freedom systems.

The present study employs this curvilinear type of hysteresis behavior for the members of multistory building frames when subjected to earthquake motion. The objective was to evaluate the inelastic response of a class of multistory structures while studying more thoroughly the influence of various significant structural parameters and characteristics of ground motion. The structures considered in this investigation were unbraced, open moment-resisting frame type of multistory buildings.

This research work was divided into two phases:

The first phase began with the development of an analytical procedure for computing the response of a multistory building frame subjected to a prescribed ground motion utilizing a high-speed electronic digital computer. The columns of the frame were assumed to behave elastically while energy dissipation was permitted in the girders, whose moment-curvature behavior was expressed by a Ramberg-Osgood function. An extensive parameter variation was then scheduled in order to obtain a wide range of results. The development and results of this phase of study are described in Chapters 2, 3, and 4.

In the second phase, several factors were investigated which were not included in the analyses performed in the first phase. These factors were the overturning effect of gravity loads acting through the sidesway displacements (commonly called the P- Δ effect), axial deformation of columns, and damping. The method developed in the first phase was modified to include these factors with the viscous damping introduced as interfloor dashpots providing a specified percentage of critical damping in the elastic fundamental mode. A good number of analyses were performed with relevant modifications made in the procedure. A comparison of the new results with the corresponding response results taken from the first phase leads to an evaluation of the influence of these factors. This information is presented in Chapter 5.

Finally, in Chapter 6 a summary of the entire study together with the significant conclusions derived therefrom is presented.

CHAPTER 2

METHOD OF ANALYSIS

2.1 General

A multistory building responding to an earthquake type ground motion is an extremely complex system. An attempt to compute the earthquake response of such a system, especially when the inelastic behavior of structural members has to be considered, is an exceedingly difficult problem involving huge computational effort. With the development of modern powerful and large capacity digital computers some recent efforts have been made to evaluate the inelastic earthquake response of multistory structures. They employ idealized elasto-plastic or bilinear type hysteresis behavior for the frame members, along with other assumptions to convert the actual structure into a suitable mathematical model which can be conveniently handled by available numerical techniques.

This chapter presents a numerical procedure which was developed to compute the inelastic dynamic response of a multistory building frame subjected to an arbitrary base motion. Accelerograms of some past earthquake records were used for the base motion and the computations were performed on the IBM 7090 computer available at the University of Michigan Computing Laboratory. The procedure employs a curvilinear hysteresis behavior which is typical of the structural steel members. In spite of all precision used in the computation it must be remembered that the results represent only the response of an idealized mathematical model.

2.2 Assumptions

The development of the method of analysis, which is described in the subsequent sections of this chapter, was based upon the following assumptions:

1. An actual structure can be ideally represented as an equivalent single-bay, multistory, rigid-jointed frame which is symmetrical about its vertical center line. This conversion is equivalent to assuming that all joints at one floor level of the original structure deflect and rotate by equal amounts at all times during the response.
2. The mass of the structure is lumped at the floor levels, each story mass representing the entire mass of the floor and half the mass of the walls and columns in the stories immediately above and below. Also, only the lateral response of the structure to the horizontal component of ground acceleration parallel to the plane of the frame is considered. Thus the number of degrees of freedom is reduced to N, the number of stories in the frame.
3. The girders follow the non-linear moment-curvature behavior as defined by the Ramberg-Osgood function of the form

$$\frac{\phi}{\phi_y} = \frac{M}{M_y} \left\{1 + \left| \frac{M}{M_y} \right|^{r-1}\right\}$$

M_y, ϕ_y and r being the characteristic parameters of the function.

4. The columns behave elastically. This assumption is partly based upon the results of earlier bi-linear studies,[10] which showed that columns of typical building frames under a strong earthquake motion do remain elastic except in a few top stories in some cases.

5. Only the flexural resistance of the bare frame members is considered. Damping resistance - structural or non-structural, effects of shear and axial strains, and the P-Δ effect have not been considered in the analysis for the first phase of the study. However, the effect of some of these factors is described in Chapter 5.

2.3 Outline of Procedure

The method of analysis, which was developed for use on a high-speed digital computer, in essence is a step-by-step numerical solution of a set of simultaneous differential equations of lateral motion of the form,

$$m_i \ddot{x}_i + Q_i = - m_i \ddot{y} \qquad (2.1)$$

where,

m_i = mass of the ith floor

$\ddot{x}_i$ = acceleration of the ith mass relative to base

Q_i = restoring force at the ith mass

and $\ddot{y}$ = ground acceleration.

The number of such equations will be equal to N, where N is the number of story masses. These differential equations were solved by the Gill's version of the fourth-order Runge-Kutta numerical procedure[14] using a finite increment of time. The conditions at the end of a time step are found as a superposition of the conditions at the beginning of the step and the changes occurring during that time step. The restoring force, Q_i, at each floor level is found from the column end-moments which exist at the beginning of each sub-step of the Runge-Kutta sub-routine.

The essential steps in the sequence of computation are as follows:

1. The incremental lateral displacements of the floor masses relative to the base, Δx's, occurring in a time interval are computed by the Runge-Kutta sub-routine.
2. By a static stiffness-matrix analysis the incremental joint rotations, $\Delta\theta$'s, at the ends of the girders are computed from the known values of Δx's. This involves computation of the girder stiffnesses relevant to the time interval. This is explained in a subsequent section. Because the columns are assumed to behave elastically, their stiffnesses are computed only once, whereas the girder stiffnesses vary in each time interval. Because the single-bay frame is assumed to be symmetrical about its vertical axis, the slopes and moments at the two ends of each girder will be equal at all times.

3. The incremental moments, ΔM's , at the ends of all members are computed from the known values of incremental joint deformations, Δx's and $\Delta\theta$'s , using appropriate stiffness factors. The incremental restoring forces, ΔQ's , at the floor levels are then computed from the incremental moments at the column ends.
4. The forces and deformations in the frame members at the end of the time interval are obtained by adding the changes during this time interval to the corresponding beginning values.

A repetition of this cycle of computations gives a progressive numerical solution of the dynamic problem. The method of analysis implicitly assumes a stable hysteresis behavior of the girders.

2.4 Ramberg-Osgood Hysteresis Model

The non-linear behavior of girders is represented by a three-parameter Ramberg-Osgood function in moment-curvature terms as given in Equation (2.2).

$$\frac{\phi}{\phi_y} = \frac{M}{M_y} \left\{1 + \left|\frac{M}{M_y}\right|^{r-1}\right\} \qquad (2.2)$$

M_y , ϕ_y and r are the three characteristic parameters of the function. Equation (2.2) in dimensionless form is graphically shown in Figure 2.1(a). For given values of M_y and ϕ_y , it is the exponent r that governs the sharpness of the break away from the elastic branch (straight line tangential to the curves at the origin 0). The Ramberg-Osgood function includes as special limiting cases the linear case, obtained by setting $r = 1$, and the conventional elasto-plastic case, which is obtained as r tends to infinity.

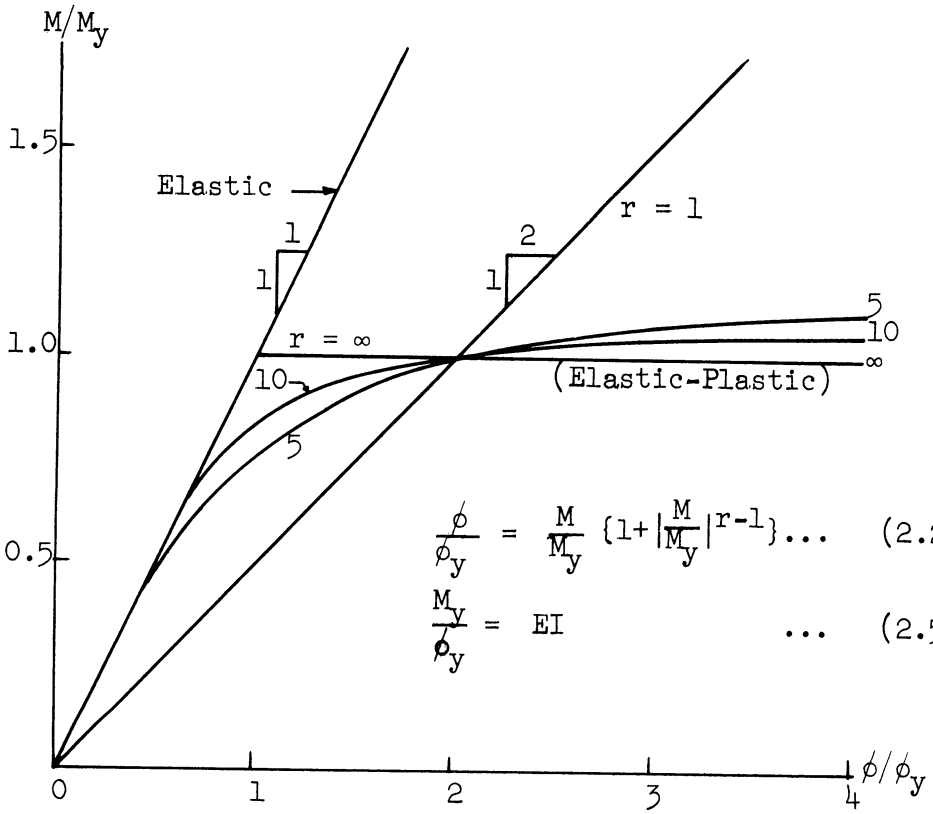

a. Ramberg-Osgood Function

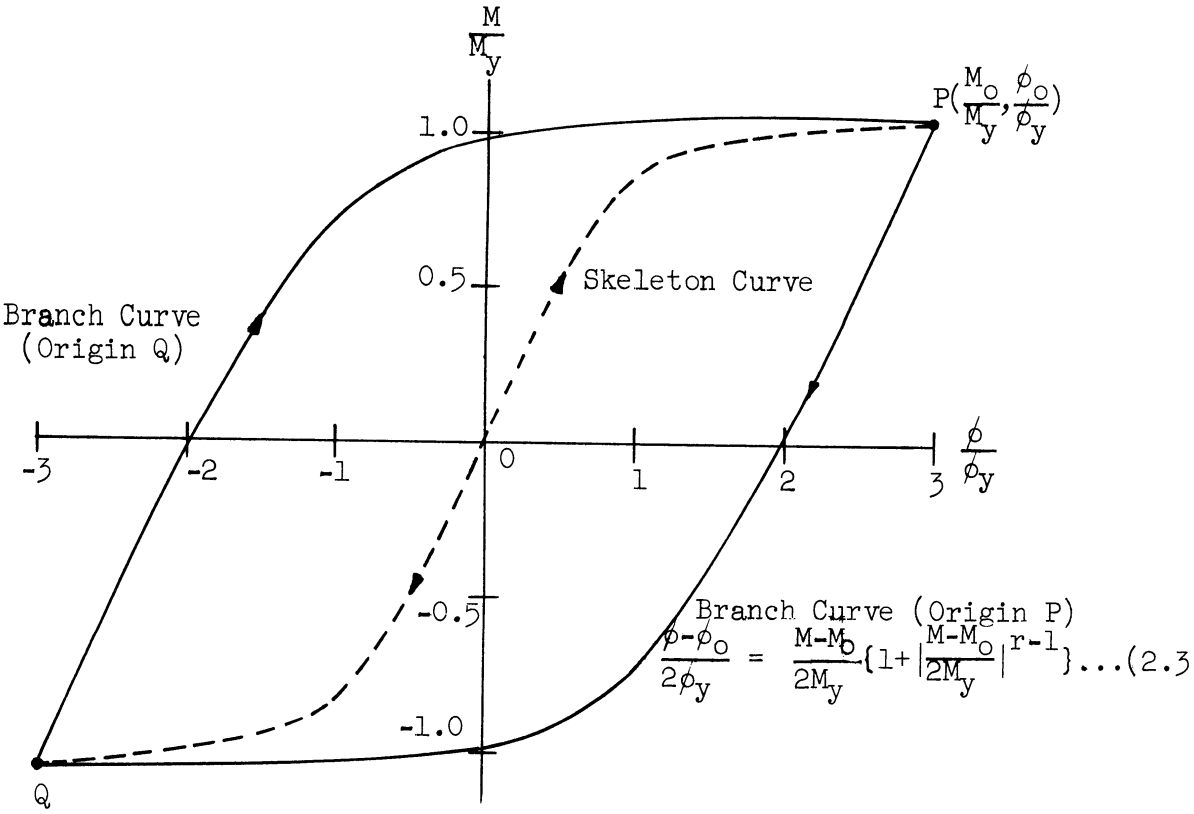

b. Ramberg-Osgood Hysteresis

Figure 2.1. Ramberg-Osgood hysteresis model.

Equation (2.2) expresses the M-ϕ relation only for the curves originating from the origin O, i.e., the curves of first loading. Such a curve is called the skeleton curve or the virgin curve. The former term is used here for the curve given by Equation (2.2). Suppose on the first loading of the cross-section of a member a point P has been reached on the skeleton curve, the reversed loading will follow the descending branch curve given by

$$\frac{\phi - \phi_o}{2\phi_y} = \frac{M - M_o}{2M_y} \left\{1 + \left|\frac{M - M_o}{2M_y}\right|^{r-1}\right\} \qquad (2.3)$$

where

$$\left(\frac{\phi_o}{\phi_y}, \frac{M_o}{M_y}\right)$$

are the coordinates of P, the point of origin of the descending branch curve. See Figure 2.1(b).

An examination of Equation (2.3) will reveal that this is a curve which is twice as large as the skeleton curve (Equation (2.2)) with the point of origin shifted from the origin O to the point P. Also, the descending branch curve has the property that it becomes tangential to the descending skeleton curve OQ at the point Q which is the symmetrically opposite point to P. Let the coordinates of the point Q be

$$\left(\frac{\phi_1}{\phi_y}, \frac{M_1}{M_y}\right),$$

where $\phi_1 = -\phi_o$ and $M_1 = -M_o$. A further reversal at point Q will generate the ascending branch curve which again can be given by Equation (2.3) if the coordinates of point Q are substituted in place of those of P. Thus, the equation for the ascending branch curve becomes

$$\frac{\phi - \phi_1}{2\phi_y} = \frac{M - M_1}{2M_y}\left\{1 + \left|\frac{M - M_1}{2M_y}\right|^{r-1}\right\} \qquad (2.4)$$

It is therefore clear that Equation (2.3) serves equally well for ascending or descending branch curve where

$$\left(\frac{\phi_o}{\phi_y}, \frac{M_o}{M_y}\right)$$

are recognized as the coordinates of the starting or the originating point of the curve. It can easily be seen that the ascending curve of Equation (2.4) will become tangential to the original skeleton curve at the point P , thus closing the hysteresis loop which started at the same point.

A hysteresis loop obtained by the two branch curves, as shown in Figure 2.1(b), describes the moment-curvature hysteresis behavior of a member cross-section in a steady-state vibration of a constant amplitude. But structural vibrations due to an earthquake type excitation are far from being steady-state. Hence a more general type of law, which can be applied to any random type of vibration, was needed for the study reported here. Such a general hysteresis law, which was developed by Berg for his single-degree-of-freedom studies,[13] is given in the Appendix. This hysteresis law was used in the present stduy to describe the hysteresis behavior of the girders of a multistory building frame responding to an earthquake motion.

This type of Ramberg-Osgood function, as expressed by Equations (2.2) and (2.3), gave a very close mathematical fit[13] to the remarkably stable experimental hysteresis loops obtained

by Popov on welded steel beam-to-column connections.[11] The slope at the point of origin for the skeleton as well as the branch curves, M_y/ϕ_y , was taken as the elastic stiffness of the member corss-section and the parameter M_y was assumed to be equal to its fully plastic moment.[15] Thus,

$$\frac{M_y}{\phi_y} = EI \tag{2.5}$$

where E is the modulus of elasticity and I the moment of inertia of the cross-section about the axis of bending. Thus the value of the two parameters M_y and ϕ_y in the Ramberg-Osgood function was fixed, while the exponent r was given a standard value of 10 which was the most representative value obtained from the experimental curves.

Equation (2.3), with the parameters M_y , ϕ_y and r , fixed as above, gives a very close fit to the branch curves of the experimental hysteresis loops. But the virgin loading curve was not well represented by the skeleton curve of Equation (2.2) with the same values of the parameters.[13] It is the author's opinion that the virgin loading curve would show a sharper transition from the elastic to the elasto-plastic branch than would be predicted by the skeleton curve of Equation (2.2) because of the lack of Bauschinger effect in the first loading. However, since the deformations grow rather gradually in the earthquake excited structural vibrations the effect of the first few oscillatins would perhaps make the skeleton curve look more like the one of Equation (2.2) for the gradually developing hysteresis loops. This was seen in the hysterssis loops for copper and mild steel under progressively increasing or decreasing amplitude as reported by Popov.[16]

It may, therefore, be observed that the Ramberg-Osgood formulation is a very realistic and convenient model to represent the actual hysteresis behavior of structural steel members subjected to large cyclic bending strains.

2.5 Ramberg-Osgood Girder Stiffness

Since the single-bay frame is assumed to be symmetrical about its vertical axis, the girders will have equal moments and rotations at both ends, so that the point of inflexion will be located at center span of each girder. Let the bending moment, curvature and the bent axis of such an antisymmetrical girder be shown in Figure 2.2. M, ϕ and θ are the moment, curvature and slope at the ends of this girder. M and ϕ will satisfy the Ramberg-Osgood relationship -- Equation (2.2) or (2.3) depending upon whether the loading is on the skeleton curve or a branch curve. For the following discussion let the girder be considered to be loaded the first time, i.e., the moment and curvature at every cross-section are given by

$$\frac{\phi}{\phi_y} = \frac{M}{M_y}\left\{1 + \left|\frac{M}{M_y}\right|^{r-1}\right\} \tag{2.2}$$

The relation between the end-moment M and the end-slope θ of the girder can be derived from the moment-area principle as follows.

At a section a distance x from the center

$$M_x = M \cdot \frac{x}{L/2} \tag{2.6}$$

and from Equation (2.2)

$$\phi_x = \phi_y \frac{M_x}{M_y}\left\{1 + \left|\frac{M_x}{M_y}\right|^{r-1}\right\} \tag{2.7}$$

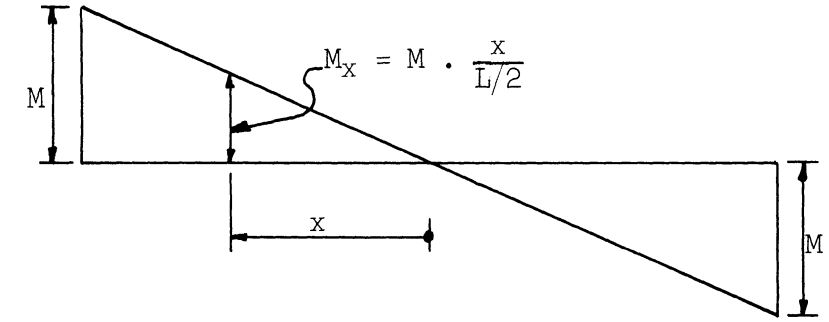

a. Moment

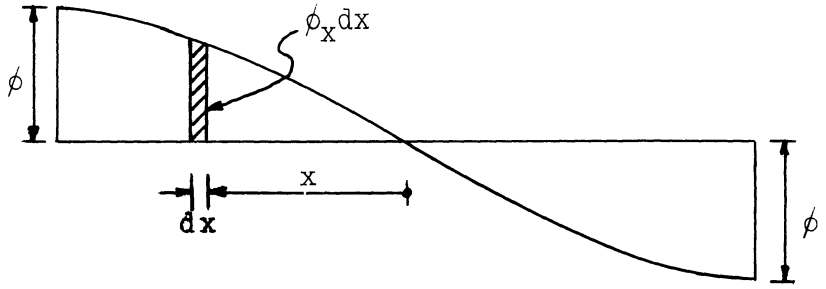

b. Curvature

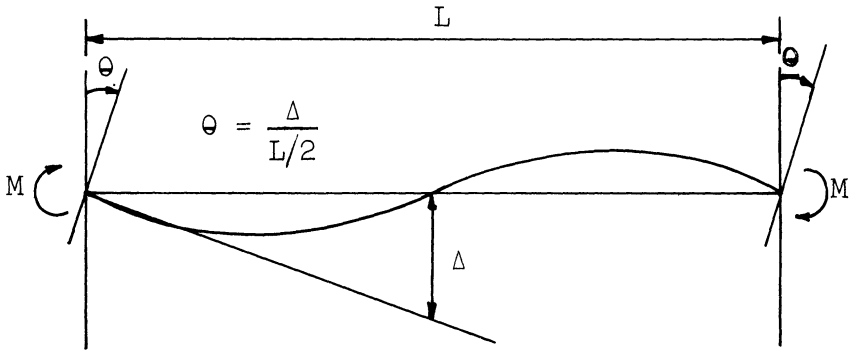

c. Bending

Figure 2.2. Ramberg-Osgood girder.

Substituting Equation (2.6) into (2.7) gives

$$\phi_x = \phi_y \cdot \frac{M}{M_y} \cdot \frac{x}{L/2} \left\{1 + \left|\frac{M}{M_y} \cdot \frac{x}{L/2}\right|^{r-1}\right\}$$

which can be rewritten as

$$\phi_x = \phi_y \cdot \frac{M}{M_y} \cdot \left(\frac{x}{L/2}\right) \left\{1+\left|\frac{M}{M_y}\right|^{r-1} \left(\frac{x}{L/2}\right)^{r-1}\right\} \qquad (2.8)$$

Now, from the relation

$$\frac{dy}{dx} = \int \frac{d^2y}{dx^2}\, dx$$

one gets

$$\theta = \frac{1}{L/2} \int_0^{L/2} \phi_x \cdot x\, dx \qquad (2.9)$$

Combining Equations (2.8) and (2.9), we get the expression

$$\theta = \int_0^{L/2} \phi_y \left(\frac{M}{M_y}\right) \left(\frac{x}{L/2}\right)^2 \left\{1 + \left(\frac{x}{L/2}\right)^{r-1} \left|\frac{M}{M_y}\right|^{r-1}\right\} dx \qquad (2.10)$$

Let $x/(L/2) = y$, so that Equation (2.10) can be written as

$$\theta = \frac{\phi_y L}{2} \cdot \frac{M}{M_y} \int_0^1 \left\{y^2 + y^{r+1} \left|\frac{M}{M_y}\right|^{r-1}\right\} dy$$

When the integral is evaluated, the expression for the end-moment and end-slope takes the form

$$\theta = \left(\frac{\phi_y \cdot L}{6}\right) \cdot \frac{M}{M_y} \left\{1 + \frac{3}{r+2} \left|\frac{M}{M_y}\right|^{r-1}\right\} \qquad (2.11)$$

The term $(\phi_y \cdot L)/6$ can be recognized as the end-rotation at $M = M_y$, if the member were elastic. Let this elastic rotation be denoted as θ_y . Thus,

$$\theta_y = \frac{\phi_y L}{6} \qquad (2.12)$$

and the M-θ relation takes the form

$$\frac{\theta}{\theta_y} = \frac{M}{M_y}\left\{1 + \frac{3}{r+2}\left|\frac{M}{M_y}\right|^{r-1}\right\} \qquad (2.13)$$

Comparing Equations (2.2) and (2.13) it will be noticed that the two have essentially the same form except for an additional factor $3/(r+2)$ in the latter which in the M-ϕ relation (2.2) is equal to 1. Equation (2.13), therefore, describes the moment-rotation behavior at the ends of the girder whose cross-sections follow the Ramberg-Osgood moment-curvature behavior - Equation (2.2) for the skeleton curve. The M-θ skeleton curve, as defined by Equation (2.13), is shown in Figure 2.3.

A similar analysis for the branch curves of the M-ϕ hysteresis loops as defined by

$$\frac{\phi - \phi_o}{2\phi_y} = \frac{M - M_o}{2M_y}\left\{1 + \left|\frac{M - M_o}{2M_y}\right|^{r-1}\right\} \qquad (2.3)$$

will show that the expression for the corresponding branch curve in M-θ terms can be written as

$$\frac{\theta - \theta_o}{2\theta_y} = \frac{M - M_o}{2M_y}\left\{1 + \frac{3}{r+2}\left|\frac{M - M_o}{2M_y}\right|^{r-1}\right\} \qquad (2.14)$$

where (θ_o, M_o) are the coordinates of the point of origin of the branch curve on the M-θ plot. Thus, a complete hysteresis behavior at the ends of a Ramberg-Osgood girder can be expressed by Equations (2.13) and (2.14).

An expressinn for the stiffness coefficient can be obtained by differentiating, with respect to θ, Equations (2.13) and (2.14) for the skeleton and the branch curves respectively. Thus, for

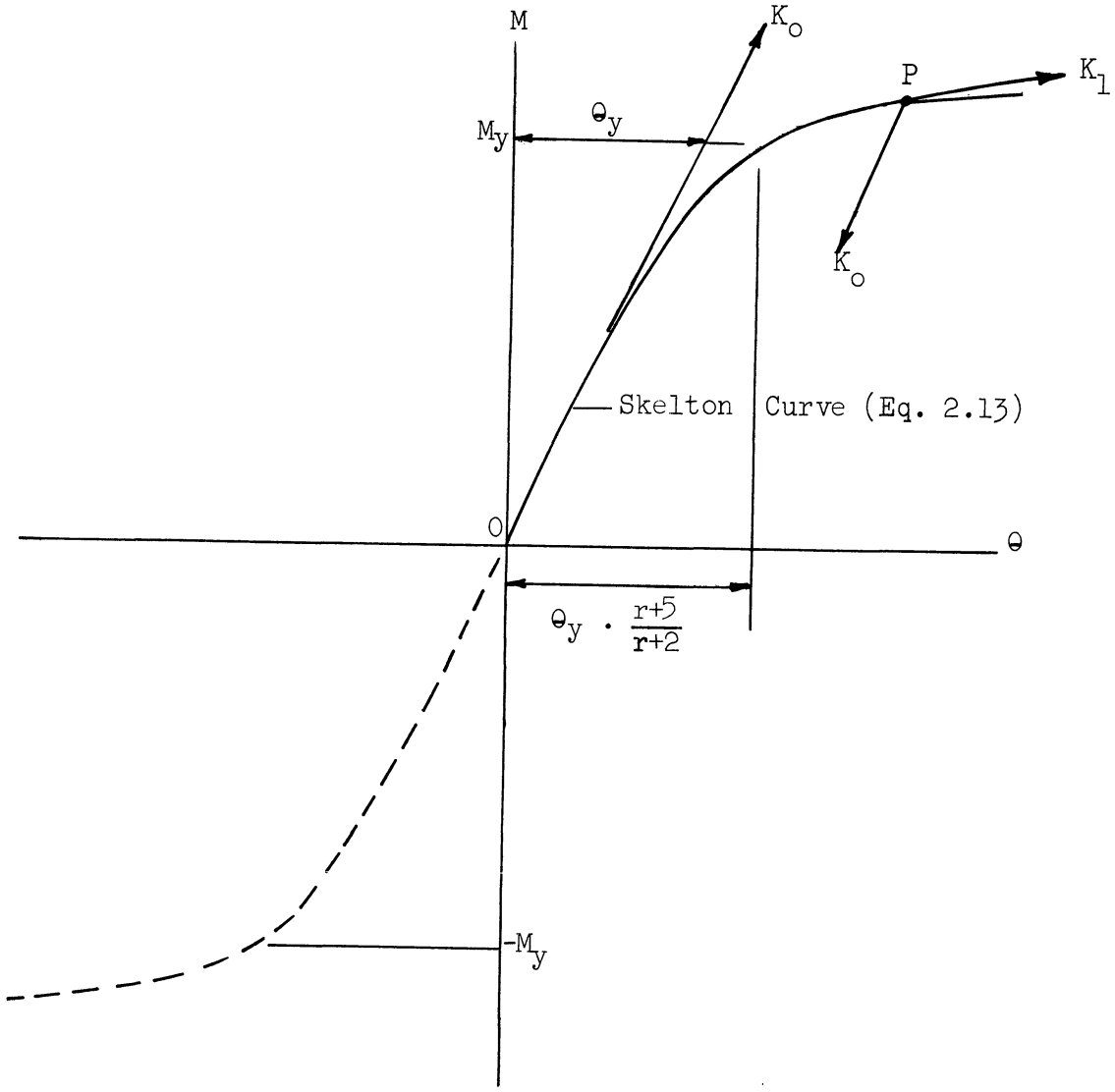

Figure 2.3. Moment-Rotation skeleton curve.

skeleton curve

$$K_1 = \frac{M_y}{\theta_y} \cdot \frac{1}{\left\{1 + \frac{3r}{r+2} \left|\frac{M}{M_y}\right|^{r-1}\right\}} \tag{2.15}$$

and for a branch curve,

$$K_1 = \frac{M_y}{\theta_y} \cdot \frac{1}{\left\{1 + \frac{3r}{r+2} \left|\frac{M - M_o}{2M_y}\right|^{r-1}\right\}} \tag{2.16}$$

Equations (2.15) and (2.16) represent the slope of the tangent at a point on the M-θ curves. The stiffness given by these two equations will, therefore, be valid only if the incremental rotation $\Delta\theta$ at the ends of a girder in a time interval is positive for ascending and negative for descending the M-θ curves. If a reversal occurs at a point P on an M-θ curve (Figure 2.3), the girder stiffness at that instant will be given by the slope of the skeleton M-θ curve at the origin. Thus, the stiffness K_o at a point of reversal is given by

$$K_o = \frac{M_y}{\theta_y} \tag{2.17}$$

The point P then becomes the origin of the new branch curve.

Since the direction of joint rotations at a floor, which in turn determines the appropriate girder stiffness to be used in a time interval, can not be predicted at the beginning of the step, an iteration has to be performed in each time interval. At the beginning of each step it is assumed that the direction of joint rotation is the same as it was in the previous time interval. Girder

stiffnesses are thus determined from Equation (2.15) or (2.16), as the case may be, and the computations are performed. A check at the end of step (2) of the procedure is made to see if the sign of $\Delta\theta$ at each floor is consistent with the assumed direction of movement on the respective M-θ curve. In case a reversal is detected by this check at one or more floor levels, the girder stiffnesses at these levels are changes to K_o and new values of $\Delta\theta$'s are computed by repeating the computations involved in the step (2). This iteration is complete when a set of $\Delta\theta$ values has been obtained which are consistent with the girder stiffnesses used in that time interval. Control is then switched over to step (3) of the procedure.

2.6 Size of the Time Interval

The procedure, as outlined in the preceding sections, will give exact results only if the size of the time interval in the numerical process is of an infinitesimal order. But in actual computations the interval will have to be of a finite size. Hence the claim on the exactness of the solution is lost. In order to compute the changes occurring in a time interval the conditions (including the stiffness of the girders) at the beginning of the time step are used. This will no longer lead to exact results since the stiffness of the girders is not actually constant during a finite size of the time interval because of the curvilinear nature of the M-ϕ or the M-θ curves. Thus, in step (3) of the sequence of computations when ΔM's at the ends of the girders are computed from the known $\Delta\theta$ values, the points along the ascending branches of the hysteresis loops will always lie above the corresponding theoretical curves as given by Equations (2.13) and (2.14). This is shown in

Figure 2.4(a). The opposite will be true for the descending branches of the $M-\theta$ curves. What is worst about this discrepancy is the fact that the departure from the theoretical $M-\theta$ curves will go on increasing unitl the next point of reversal. Moreover, since the $M-\theta$ points generated by the numerical procedure lie away from the theoretical curves given by Equations (2.13) and (2.14), the points of reversals as predicted by the analysis will not be the true ones. Thus, the hysteresis loops consisting of several straight line segments as generated by the numerical procedure will satisfy equilibrium but not the Ramberg-Osgood $M-\theta$ equations.

The above mentioned discrepancy is a direct consequence of the finite size of time step used in the numerical solution. Obviously, one could think of minimizing the error simply by reducing the step size. This technique was tried in a few trial runs of the program and it was found that the gain in accuracy of the results was discouragingly slow as compared with the increase in the computation time involved. In order to obtain results of an acceptable accuracy with reasonable machine time required a method of modifying the girder stiffnesses in each time interval was devised. This scheme of stiffness modification, which produced excellent results, is illustrated in Figure 2.4(b) and the explanation follows.

At the beginning of a time step, which involves no reversal, let the $M-\theta$ values for a girder correspond to a point P in Figure 2.4(b). P' is the point on the true $M-\theta$ curve for the moment M and the end rotation is θ' which satisfies the Equation (2.13) or (2.14), as the case may be. Using the girder stiffness K,

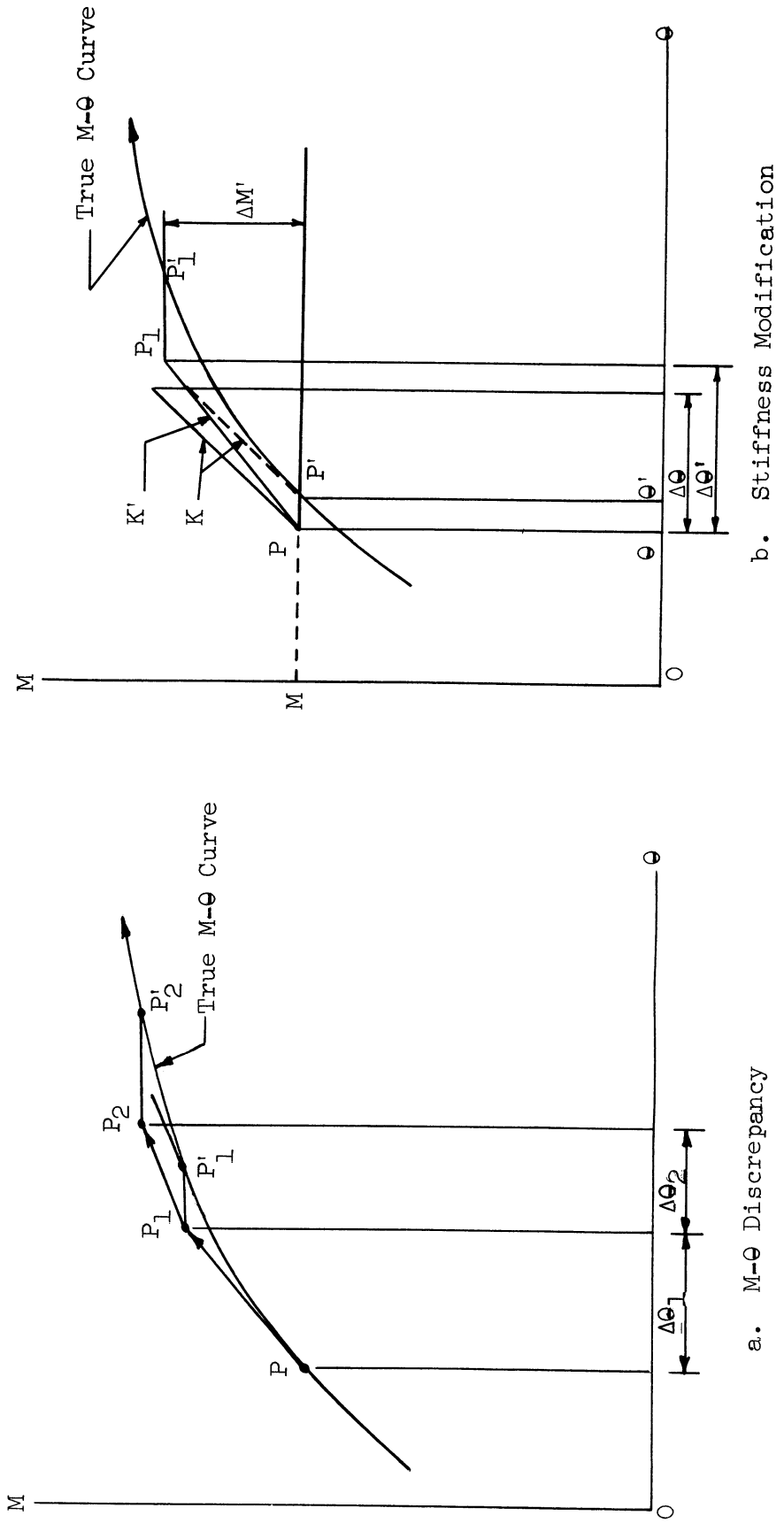

Figure 2.4. M-θ discrepancy and stiffness modification.

which is the slope of the tangent to the M-θ curve at the point P', compute the Δx's and $\Delta\theta$'s from steps (1) and (2). At this stage the girder stiffness K is modified to K' by multiplying it by the ratio

$$\left\{\frac{\Delta\theta - (\theta' - \theta)}{\Delta\theta}\right\}$$

and the control transferred to step (2) again. The new values of $\Delta\theta'$ and $\Delta M'$ as computed this time from steps (2) and (3) by using the modified K' values will be closer to the theoretical M-θ curve.

This is a very simple device which pulls the moment-rotation points nearer to the theoretical M-θ curves as the solution proceeds and keeps the discrepancy between the two from growing out of practical bounds. It should be noted that this modification of girder stiffness is applied only to those floors where no reversal of moment is detected in that time interval by the relevant test which was described in Section 2.5. This is because at such floors the stiffness had already been modified to K_0 when the reversal was detected and since at the point of reversal θ and θ' take the same value the multiplying factor becomes equal to unity.

In the same procedure, after modifying the girder stiffnesses to K', if the control is transferred to step (1) instead of step (2) and fresh values of Δx's, $\Delta\theta$'s and ΔM's are computed with the modified stiffnesses better results should be expected. This was done in a trial case, but the improvement in the results was so little that it did not warrant the necessity of re-entering the Runge-Kutta subroutine in the same time interval. Rather, the earlier scheme

of bypassing step (1) after stiffness modification was used which resulted in a saving of about 25 percent of the total machine time required for one analysis at the cost of a nearly negligible loss of accuracy.

The actual size of the time interval to be chosen for the numerical procedure as described in this chapter should be a function of the fundamental period of vibration T of the structure. Also the hysteresis curves of the Ramberg-Osgood function show a sharper transition from the elastic to the plastic zones for larger values of the exponent r (Figure 2.1(a)). Thus, a smaller time step would be required for large values of r in order to traverse the theoretical hysteresis curves with reasonable closeness. An increase in the number of stories N of the structure would increase the influence of the higher modes on the total response. So the time interval should be smaller for a taller structure having more stories in it. These factors helped in the choice of a suitable size of the time interval Δt for the Ramberg-Osgood analyses. The following empirical formula was used:

$$\Delta t = \frac{T}{(8 + 0.2r)N} \tag{2.18}$$

The value of Δt as given by Equation (2.18) was used as the normal size of the time step. However, a smaller calue had to be used whenever a peak on the accelerogram (which consisted of straight line segments) was encountered within a normal length of the time step. The Runge-Kutta method used for the numerical intergation of the differential equations of motion provides an excellent facility to vary the length of the time interval as the solution proceeds.

2.7 Check on Accuracy

As a check on the accuracy of the method of analysis and the results obtained therefrom, the following three tests can be applied at any instant during the computations.

1. The conditions of static equilibrium of the deformed structure must be satisfied at every instant of time.
2. The energy input to the structure at any instant can be computed by intergrating the product of base shear and the ground velocity. This must check with the sum of the dissipated energy up to that instant plus the recoverable strain energy and the kinetic energy present in the structure at that instant of time.
3. The girders must generate the true M-θ hysteresis loops as defined by Equations (2.13) and (2.14).

The first of these tests is a check on the statics involved in the analysis and was applied in the initial testing of the computer program. The other two tests were used throughout all computations. The energy test proved to be a very versatile check and helped in detecting errors in the procedure which could not have been detected by the static test. The procedure, using the size of the time interval as given by Equation (2.18), gave results so that the energy balance was within one percent and the generated M-θ curves were reasonably close to the corresponding theoretical curves. A typical girder response obtained from one of the analyses is shown in Figure 2.5.

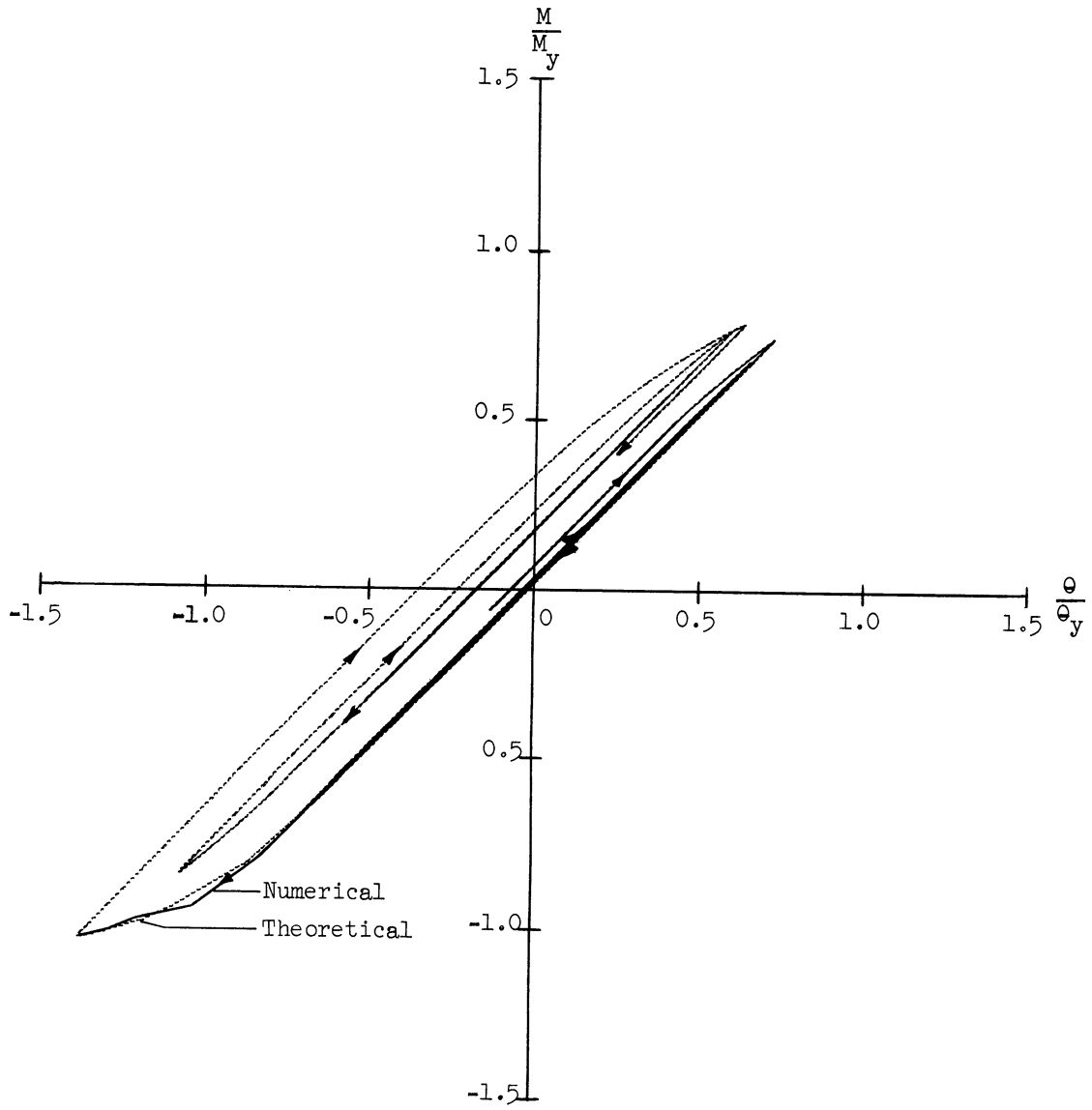

a. $\frac{M}{M_y}$ vs. $\frac{\theta}{\theta_y}$

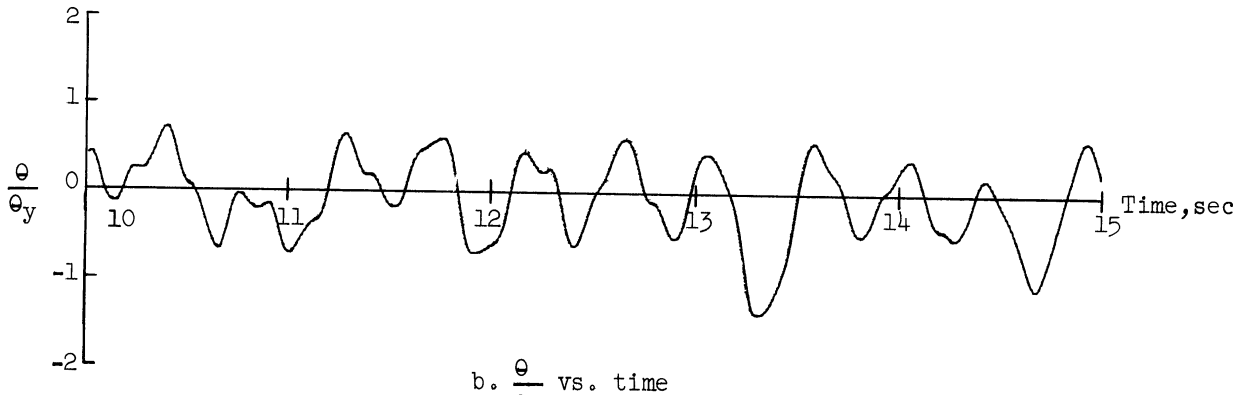

b. $\frac{\theta}{\theta_y}$ vs. time

Figure 2.5. Typical girder response

2.8 Elastic and Elasto-Plastic Girders

The evaluation of the effect of the inelastic behavior of girders upon the earthquake response of multistory structures was an important feature of the study. This involved the comparison of the response of a structure to a given earthquake when the degree of plasticity on the girders ranged from nil, i.e., elastic to the fully elasto-plastic case. The Ramberg-Osgood girders with $r = 5$ or 10 represent the cases of intermediate degree of plasticity and perhaps the more realistic ones. The Ramberg-Osgood function covers all these cases if the exponent r is considered as a variable, the strength and stiffness being fixed by the other two parameters M_y and ϕ_y (Figure 2.1(a)). But the case of real elastic girders is obtained by setting $r = 1$ and multiplying the resulting linear stiffness by two. The factor of two is necessary because the real elastic case has stiffness equal to twice that obtained for $r = 1$ (Figure 2.1(a)).

Thus, the computer program written for analyzing a multistory frame with Ramberg-Osgood girders could as well have been used for the elastic and the elasto-plastic cases. But the case of elastic girders needs the girder stiffnesses to be computed only once in the analysis and the simulation of elasto-plastic girders by putting a very large value of r in the Ramberg-Osgood analysis involved numerical problems. Therefore, for convenience and better efficiency a separate program was written for these two cases. This program was obviously simpler than the general Ramberg-Osgood program and required less computation time than required for the same cases to be analyzed as special cases by the general Ramberg-Osgood program.

An elasto-plastic girder has a special problem of sharp kink in the hysteresis loops when a negative or a positive plastic hinge forms at the two ends of the member. Before the formation of such a hinge a girder is assumed to have its elastic stiffness and the step-by-step elastic analysis proceeds until the absolute value of the end moment in a girder exceeds its M_y value at the end of any time interval. The analysis then goes back to the beginning of that interval and the computations performed with a smaller time interval which was taken equal to one-tenth of the normal size. The next time such an excess in the end moment is encountered the stiffness of that member is set to zero, the moment set to its yield moment M_y , the time interval restored to its normal value and the analysis continues. Reversal in the end rotation of a girder is detected in the same manner as was explained before in Section 2.5. The girder stiffness is restored to its elastic value if it was zero before the reversal was detected. The same program was used for the case of elastic girders by omitting the portions relevant to the appearance or disappearance of a plastic hinge. A normal size of the time interval equal to T/80 and T/100 was used for the 10- and 25- story frames respectively and the first two tests as given in Section 2.7 were applied to maintain the same degree of accuracy of the results as for the Ramberg-Osgood analyses.

CHAPTER 3

PROGRAM OF INVESTIGATION

3.1 General

The importance of energy absorption through inelastic ductile deformations in limiting the earthquake response of buildings has been recognized for several years, but attempts to evaluate quantitatively the inelastic response of multistory buildings have been very few and recent. The knowledge of the expected amount and distribution of inelastic deformation and the energy dissipation in multistory structures during strong motion earthquakes is still inadequate. Analyses for this investigation were scheduled to yield some information on this basic question and to evaluate the influence of various significant structural properties and characteristics of ground motion upon the inelastic response.

This chapter describes the types of structural models and their variable parameters, the maximum response parameters recorded, and the types of earthquake records used in the present study. The variables were selected to cover a fairly wide, practical range of values, but the number of analyses made was limited in order to keep the total machine computation time within a reasonable limit.

3.2 Structures Considered

This study deals with regular, rectangular buildings only. Any irregularities, such as setbacks, eccentricities, appendages or discontinuities were not considered because the primary purpose was to study the influence of the basic structural parameters upon the

earthquake behavior of multistory buildings. The basic types of structures analyzed were typical, open, moment-resistant frames. In addition, two 10- and 25- story frames,having uniform girder and column properties, were also analyzed in order to compare their response with that of the corresponding standard frames having normal stiffness-strength taper for the same earthquake motion.

3.3 Mathematical Models of the Test Frames

For the purpose of response computation, an actual structure was approximated by a single-bay frame symmetrical about its vertical center line, having the same number of stories as in the real structure. As was mentioned in Chapter 2, this approximation can be justified on the assumption that the lateral deflections and rotations of all joints at one floor level in the actual structure are identical at all times. A replacement of a typical three-bay structure by a one-bay frame is shown in Figure 3.1. It may be noted that the single-bay frame has column stiffnesses equal to that of the outer columns of the three-bay structure, the girder stiffnesses remaining the same.

A model of such a 40-story, symmetrical, single-bay frame was developed with the following data:

Story Height: 13.5 feet (uniform)

Bay Width: 20.0 feet

Frame Spacing: 20.0 feet

Story Weight: 44.0 kips (@ 110 psf--Dead load of the finished structure per story)

Girder and Column Stiffness Ratios:

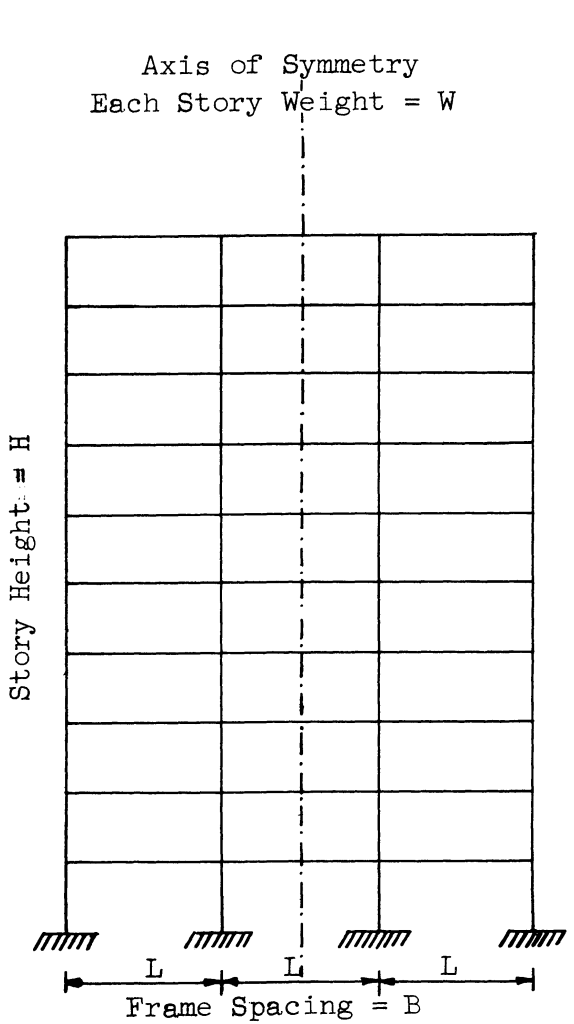

Actual 3-Bay Frame

Stiffness Ratio, EI/EI_o

Columns		Girders
Exterior	Interior	
1.0	2.0	2.0
1.25	2.5	
1.5	3.0	3.0
1.75	3.5	
2.0	4.0	

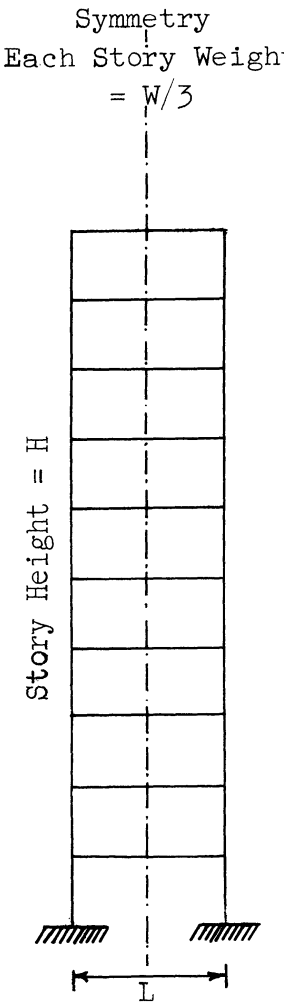

Equivalent Single-Bay Frame

Stiffness Ratio, EI/EI_o

Columns	Girders
1.0	2.0
1.25	
1.5	3.0
1.75	
2.0	

Figure 3.1. Single-bay frame equivalent to a multi-bay structure.

Ratio of top to bottom column stiffness--1:15

(Linearly tapering in steps of two stories).

Ratio of top to bottom girder stiffness--2:11

(Linearly tapering in steps of five stories).

For columns 14 WF sections both with and without cover plates were used. The sections for girders started with a nominal size of 18 WF at the top and were increased by three inches in nominal depth in steps of 5 stories up to a maximum of 36 inches. The columns were assumed to have infinite stiffness in a length equal to the depth of the girder at each connection. But the girders, however, were assumed to have uniform stiffness from center to center of the columns. The same assumption was incorporated in the response computation procedure (described in Chapter 2), where the maximum moments and shears in the columns were recorded at the ends of these rigid stubs.

The value of the common stiffness factor EI_o was computed for a selected value of 3.0 seconds for the elastic fundamental period of lateral vibration, T, using the above data. Selecting the elastic modulus for steel, E, as 29000 ksi, the required values of the moments of inertia, I_x, for various members were computed. Empirical Equations (3.1) and (3.2) (Figures 3.2 and 3.3) were established using the data from the Handbook of Structural Steel Sections for sections with the nominal sizes selected above.

$$S_x = \frac{I_x}{7}\left(1 - \frac{1}{3}\log\frac{I_x}{1200}\right) \qquad (3.1)$$

$$Z_x = \frac{I_x}{.45d} \qquad (3.2)$$

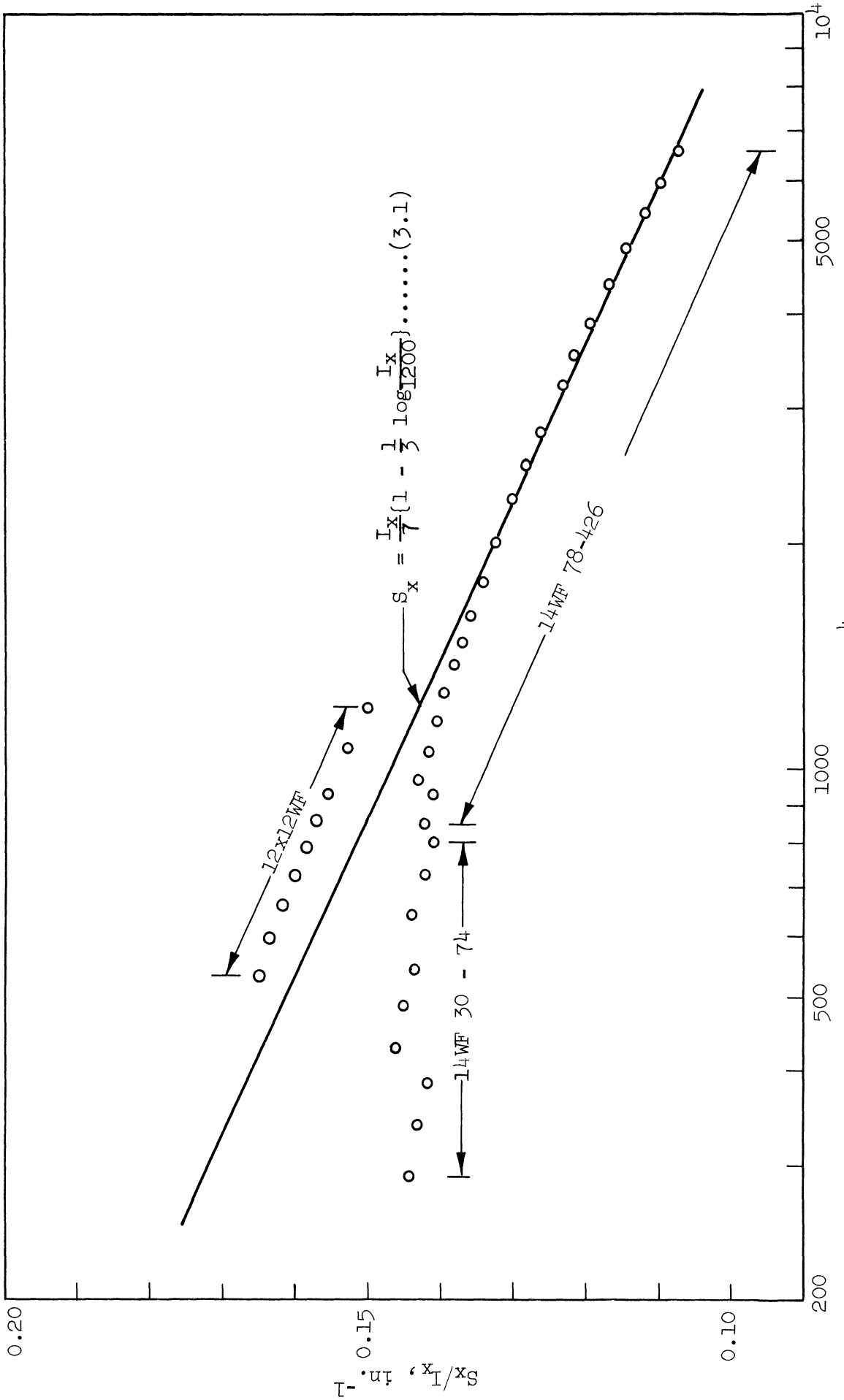

Figure 3.2. I_x vs. S_x for 14WF column sections.

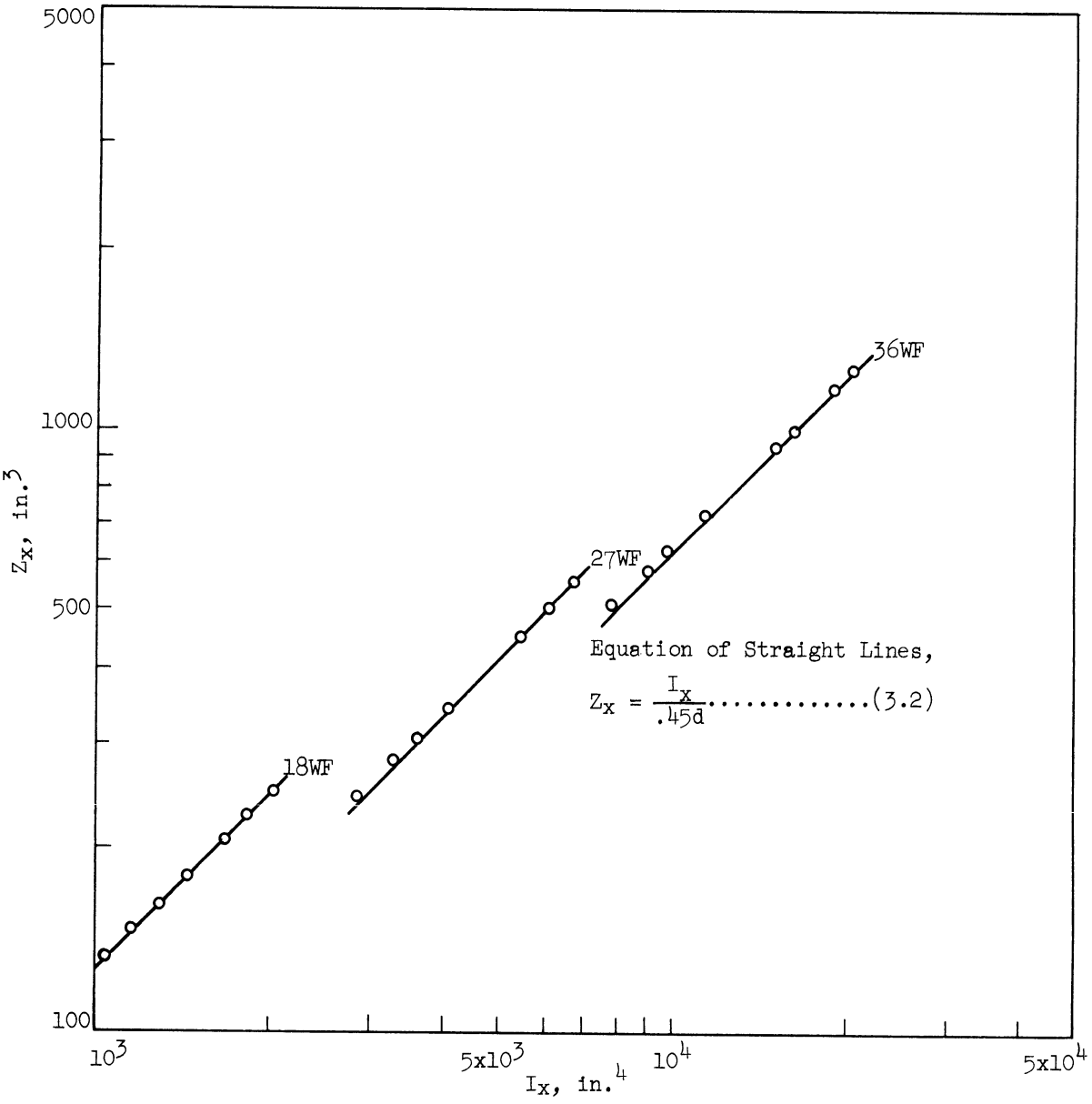

Figure 3.3. I_x vs. Z_x for 18WF-36WF girder sections.

where, S_x = elastic section modulus for 14 WF sections, $in.^3$

Z_x = plastic section modulus for girder sections 18 WF - 36 WF, $in.^3$

I_x = moment of inertia of the cross section, $in.^4$

and d = the nominal size of the girder section in inches.

Equations (3.1) and (3.2) were used to establish the values of elastic section modulii for column sections and plastic section modulii for the girder sections from their moment of inertia values. The proportions of the standard 40-story model, as generated by this procedure, are given in Table 3.1. The values of the required section modulii for various members appear reasonable and lie well within the range provided by their respective nominal sizes, except for columns in the lower half of the structure. Here the 14 WF core needs cover plates, but this is a normal situation in the design of such tall frames. It was further assumed that the M_y parameter for a Ramberg-Osgood WF beam section could be approximated by its fully plastic moment[15] for a nominal yield stress σ_y, taken as 36 ksi in this standard case. Since the columns were assumed to behave as linearly elastic, their maximum moments were recorded as ratios to their respective initial yield moments, $(\sigma_y \cdot S_x)$.

After the model of the 40-story standard frame was proportioned, the top 10 and 25 stories of this frame were used as standard models of 10- and 25-story frames. The fundamental period for the 10-story frame was computed as 1.25 seconds and that for the 25-story frame as 2.27 seconds. In order to study the effect of a variation in stiffness upon the response of these structures, analyses were made of similar

TABLE 3.1

MEMBER PROPERTIES, STANDARD 40-STORY FRAME

Single-bay Frame: Story Weight = 44 kips; Story Height = 13.5 feet

N = 40, T = 3.0 secs.

Stories	Columns			Girders		
	I_x, in.^{4}	S_x, in.^{3}	Nom. Size	I_x, in.^{4}	Z_x, in.^{3}	Nom. Size
39-40	868.22	130.20				
37-38	1507.97	280.92		1736.45	214.37	18 WF
35-36	2147.71	281.85				
33-34	2787.46	350.77		2852.74	301.88	21 WF
31-32	3427.20	416.62				
29-30	4066.94	480.00	14 WF			
				3969.02	367.51	24 WF
27-28	4706.69	541.28				
25-26	5346.43	600.77				
23-24	5986.17	658.65		5085.31	418.55	27 WF
21-22	6625.92	715.13				
19-20	7265.66	770.33				
				6201.60	459.38	30 WF
17-18	7905.41	824.36				
15-16	8545.15	877.32				
13-14	9184.90	929.29		7317.89	492.78	33 WF
11-12	9824.64	980.34	14 WF + Cover Plates			
9-10	10464.38	1030.53		8434.18	520.63	36 WF
7-8	11104.13	1079.90				
5-6	11743.87	1128.52				
3-4	12383.62	1176.41				
				9550.46	589.54	36 WF
1-2	13023.36	1223.61				

structures having the same dimensions and weights, but with their stiffnesses altered to produce variations in their fundamental periods according to the following schedule:

		Number of Stories		
		10	25	40
T, seconds =	0.50	x		
	1.25	(x)	x	
	2.27	x	(x)	x
	3.00		x	(x)

The circled values of T correspond to the three standard models 10 , 25 , and 40 stories high.

The influence of the height of the structure was studied by comparing the response of the three standard models as well as that of the three models having a common fundamental period of 2.27 seconds. The earthquake motion was the same in each comparison. This general scheme also provided an additional basis for comparing the response of a smaller frame with that of the corresponding top portion of a taller one subjected to the same ground motion. It was partly for this purpose that the story height was kept uniform.

In addition to the above standard models in which the member stiffnesses have a typical taper, two uniform stiffness-strength models of 10 and 25 stories were also generated. The nominal size for columns was still kept at 14 WF while the girders were 21 WF in 10-story and 27 WF in the 25-story model. The stiffness ratio, EI/EI_o , for columns was 1 and that for girders 2 in both frames. Other dimensions and the

story weights were the same as for the standard taper models. The common stiffness factor EI_o was then adjusted to give the standard fundamental period of 1.25 seconds for the 10-story and 2.27 seconds in the 25-story structure. The cross-sectional properties of the frame-members of these two uniform models are shown in Table 3.2 below.

TABLE 3.2

MEMBER PROPERTIES, UNIFORM MODELS

N	Columns			Girders		
	Nom. Size	I_x, in.^{4}	S_x, in.^{3}	Nom. Size	I_x, in.^{4}	Z_x, in.^{3}
10	14 WF	1539.26	211.97	21 WF	3078.52	325.77
25	14 WF	2793.04	350.21	27 WF	5586.08	459.76

It may be noted that all the above models of multistory structures were proportioned to have lumped masses equivalent to the full dead load of the finished structure per story and assuming that the fire-proofing concrete around columns, floor slabs and other non-structural elements do not contribute to their lateral strength or stiffness. This was assumed because during a strong earthquake motion the contribution of such elements to the strength and stiffness would probably deteriorate rapidly. The fundmental period of the basic 40-story frame, which was the controlling factor in the design of the test frame by the described procedure, was chosen from the consideration that all the needed stiffness and strength was provided by the bare frame alone. The fundamental periods of 1.25, 2.27 and 3.0 seconds for the

10-, 25-, and 40-story standard frames were kept longer than the observed periods of buildings of comparable heights, because earlier investigations[17,18,19] have shown that for small vibrations the computed period of a bare steel frame could be as much as 25 to 100 percent greater than the observed period of the finished structure.

3.4 Response Parameters

The following significant parameters were chosen to characterize the maximum earthquake response of the test structures as obtained from the computer analyses:

1. Maximum lateral displacement of the floors relative to base.
2. Maximum relative story displacements.
3. Maximum absolute acceleration of the floor masses--recorded as fractions of gravity.
4. Maximum shear force in the columns of a story--recorded as fraction of the total weight of the structure.
5. Column ductility ratio--defined as the ratio of the maximum column moment in a story to its initial yield moment M_y . The analysis treats the columns to behave as linearly elastic so that this ratio is the same as the ratio of maximum curvature to the initial yield curvature. Therefore, this ratio does not imply any inelastic behavior of the columns.
6. Girder Ductility Ratio, μ .

   There can be more than one possible definition for the ductility ratio of a member having a curvilinear

moment-rotation behavior as adopted in this study. No definition claims any special merit over the others. In the absence of any standard definition, the girder ductility ratio has been defined as the maximum absolute joint rotation divided by the yield rotation. This definition has been used more frequently than any other and is denoted by μ . Thus, μ is given by the expression

$$\mu = \frac{|\theta|_{max}}{\theta_y}$$

The yield rotation θ_y corresponds to the parameter ϕ_y in the Ramberg-Osgood moment-curvature relationship.

7. Excursion Ratio, ϵ .

The excursion ratio for a Ramberg-Osgood girder is defined as the sum of all joint rotations in the yield regions during the entire response divided by θ_y . This parameter is chosen to express the total plastic deformation suffered by each girder. In the Ramberg-Osgood curvilinear hysteresis model there is no distinct yield point; hence, there is no single definition for the yield region. The yield criterion used in this study is illustrated in Figure 3.4(c). A parallel criterion was used for an elastic or elasto-plastic moment-rotation behavior as illustrated in Figures 3.4(a) and 3.4(b) respectively.

8. Hysteresis energy dissipated at each floor.

The total energy dissipated by each girder at the end of the earthquake is a singificant parameter which was

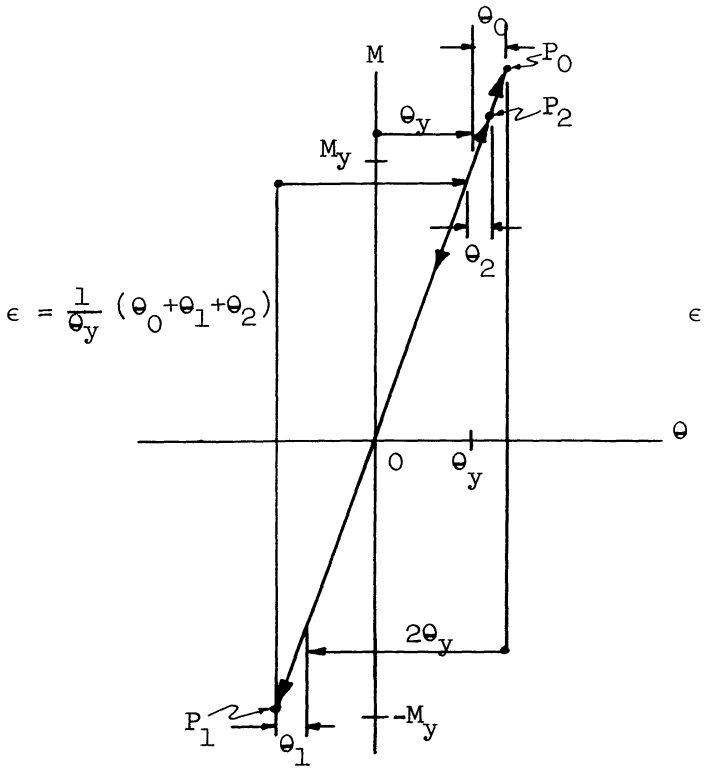

a. Elastic

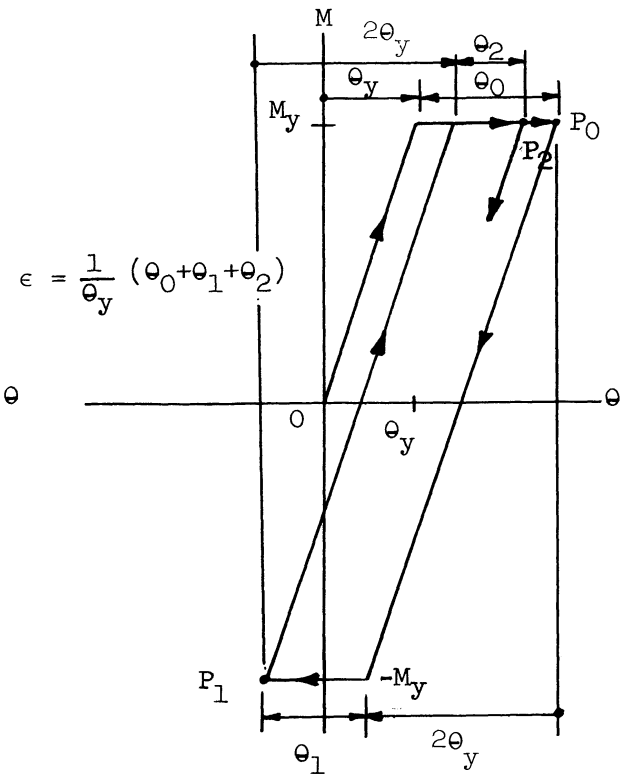

b. Elasto-Plastic

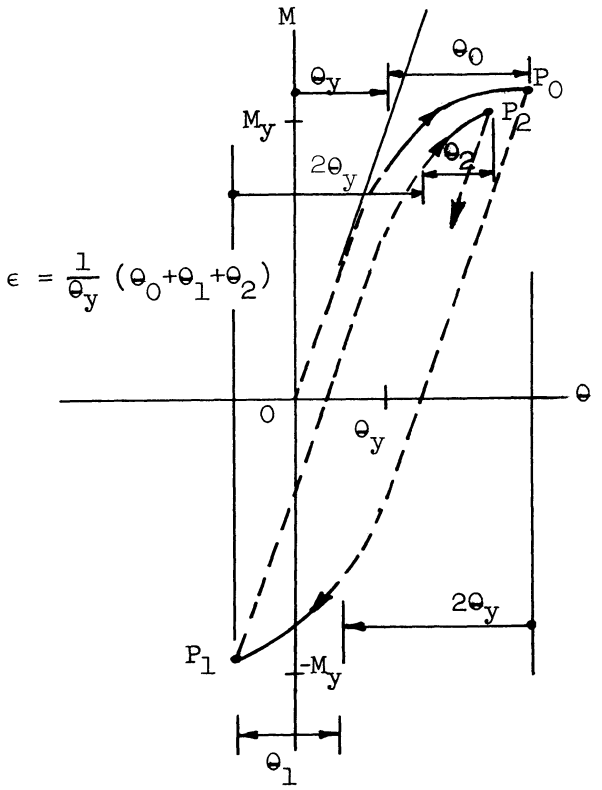

c. Ramberg-Osgood

Solid lines mark the yield regions

P_0, P_1, and P_2 are the reversal points

Figure 3.4. Yield criterion

recorded for the inelastic response of the structure. This was normalized by dividing it by the factor $M_y \cdot \theta_y$ for the respective girder section. This ratio is exactly equal to 2ϵ in the elasto-plastic hysteresis case but not for the Ramberg-Osgood case.

9. Maximum Input Energy

The maximum energy input to the structure is a parameter which characterizes the magnitude of its entire earthquake response. This was recorded and expressed as the energy per unit of total mass of the structure.

All of these maximum response parameters will be referred to simply as response parameters in order to avoid an excessive retitition of the word maximum.

3.5 Ground Motion Characteristics

In addition to the influence of various structural parameters, like the height and stiffness of the structure and the inelastic action of the girders, the influence of the characteristics of earthquake ground motion upon the structural response was an important aspect of the study. The most significant characteristics, which also governed the choice of the earthquake records to be used in the study, are given below.

(i) Period Characteristics and Intensity

The period characteristic of an accelerogram, as it is reflected in its velocity response spectrum, was an important factor in selecting suitable earthquake records for this investigation. The N-S component of El Centro, California, 1940 earthquake was chosen as a standard

accelerogram because it has almost uniform velocity-spectrum peaks over the range of the fundamental periods of various test frames. As it was decided to use a stronger earthquake than the ones recorded to date, the acceleration ordinates of the El Centro record were multiplied by a factor of 1.5.

Two other accelerograms, one having spectrum peaks in the short period range (0.5-1.0 second) and the other in the longer period range (2.0-3.0 seconds), were also selected. These were Taft, California, July 1952, S21°W component and Alameda Park, Mexico, May 11, 1962, N10°46'W component. The spectrum intensity, defined as the area under the undamped velocity spectrum between 0.5 and 3.0 seconds, was used as a measure of the earthquake intensity.(20) In order to make the spectrum intensity of these two accelerograms nearly equal to that of the El Centro by 1.5, the acceleration ordinates of the Taft recorded were multiplied by a factor of 3.0 and those of Alameda Park by 2.4.

The three accelerograms used in the analysis are, therefore;

(a) El Centro, California, 1940, N-S component by 1.5

(b) Taft, California, July 1952, S21°W component by 3.0

(c) Alameda Park, Mexico, May 11, 1962, N10°46'W component by 2.4.

These modified accelerograms are shown in Figure 3.5 and their undamped velocity spectra are given in Figure 3.6. Table 3.3 shows the values of the spectrum intensity, $I_o = \int_{0.5}^{3.0} S_V \, dT$, of these accelerograms before and after multiplying by the corresponding factors.

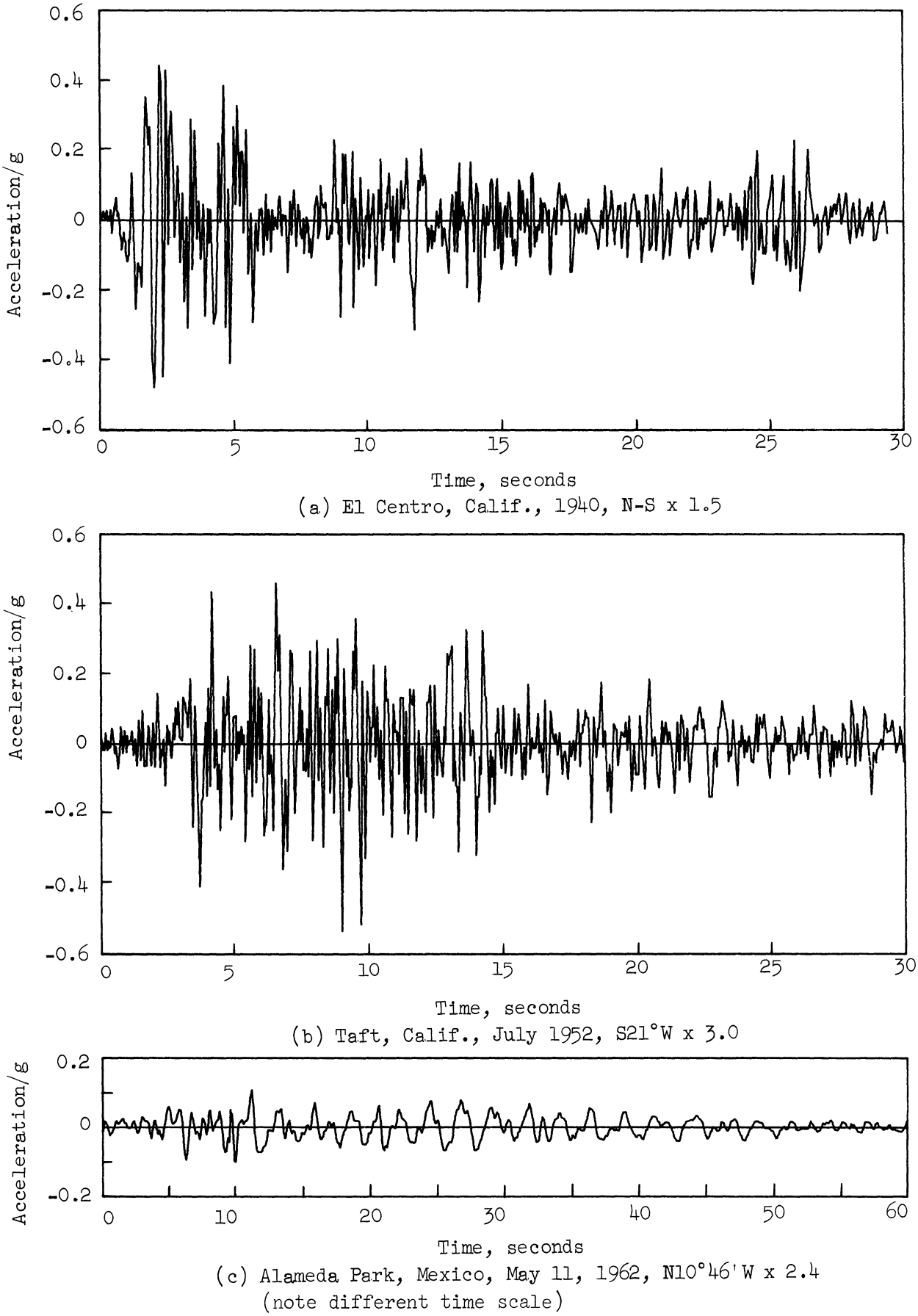

Figure 3.5. The three accelerograms.

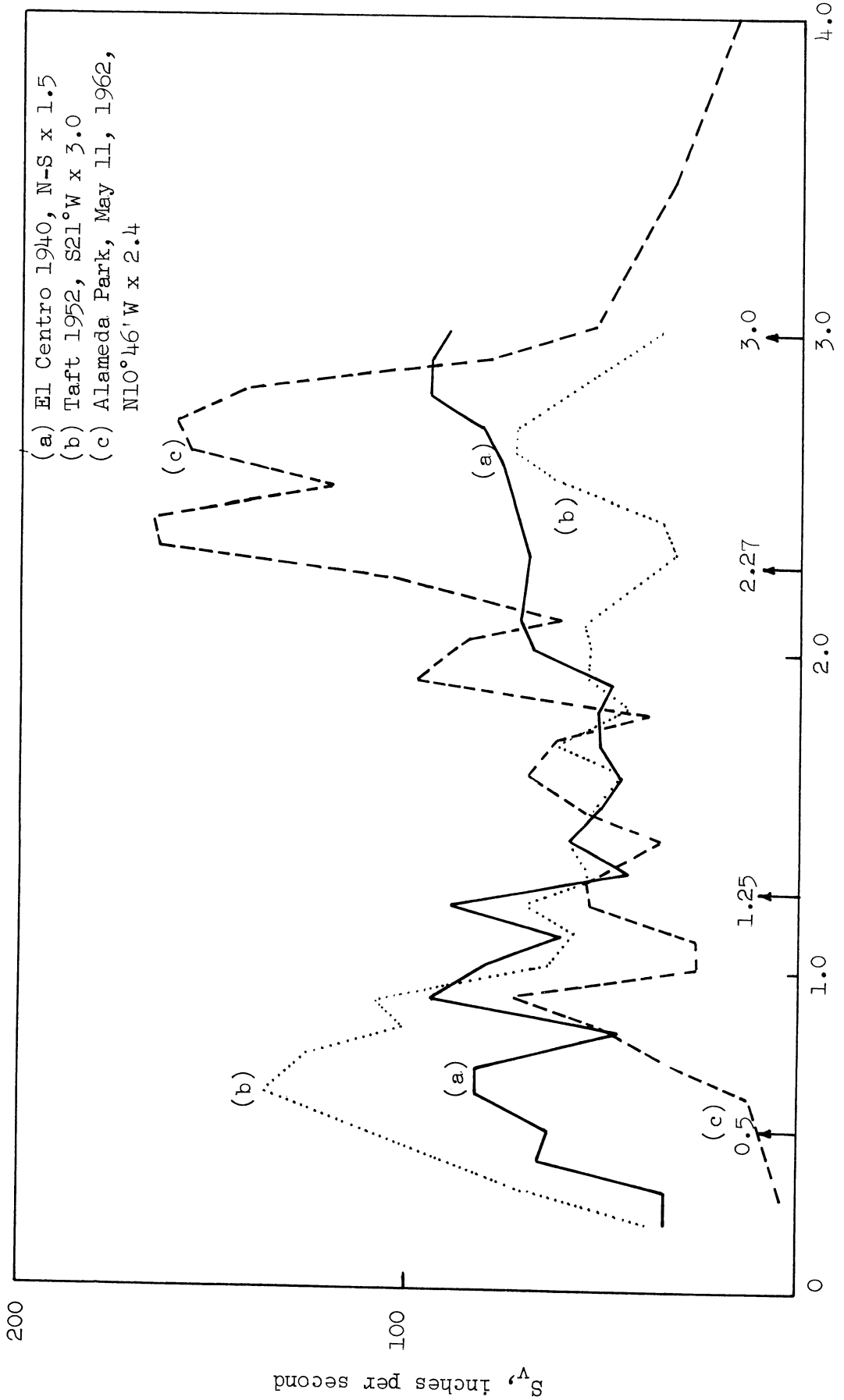

Figure 3.6. Undamped velocity spectra for the modified accelerograms

TABLE 3.3

VALUES OF I_o, INCHES

	El Centro, 1940 (N-S)	Taft, 1952 (S21°W)	Alameda Park, 1962 (N10°46'W)
Original	109.50	53.83	68.43
Modified	164.25	161.49	164.23

(ii) Duration

The first two accelerograms are 30 seconds long and the last record is 60 seconds long. The full length of these accelerograms was used in the analyses and the response of each model was recorded at five-second intervals to investigate the effect of duration of the ground motion upon some of the significant response parameters.

CHAPTER 4

DISCUSSION OF RESULTS

4.1 General

The results obtained from the computer analyses described earlier are presented and discussed in this chapter. The various structural and ground motion characteristics whose influence upon the structural response was investigated are as follows:

1. Inelastic Behavior of Girders.
2. Fundamental Period of Structure vs. the Period Characteristics of Ground Motion.
3. Duration of Ground Motion.
4. Height of the Frame
   a. Number of Stories.
   b. Portion of Structure.
5. Stiffness-Strength Taper.
6. Strength of Members.

4.2 Inelastic Behavior of Girders

As memtioned earlier in Chapter 2, the sharpness of the transition from elastic to plastic range depends upon the value of the Ramberg-Osgood exponent r in the M-ϕ relation. For the standard Ramberg-Osgood models, a value of ten has been used for r, which is a representative value[13] of some experimental results.[11] In this section the response of 10- and 25- story models having Ramberg-Osgood girders is compared with the corresponding elastic and elasto-plastic cases.

Four 10-story models with the standard fundamental period of 1.25 seconds and having elastic, Ramberg-Osgood $r = 5$, $r = 10$ and elasto-plastic (which is the same as Ramberg-Osgood with $r = \infty$) girders were analyzed for the Taft accelerogram. The resulting maximum response parameters, as plotted against the story level, are shown in Figure 4.1. A similar analysis was made with 25 story models, $T = 2.27$ seconds, except that the case of $r = 5$ was dropped. The remaining three models, i.e., with elastic, Ramberg-Osgood $r = 10$ and elasto-plastic girders were analyzed for the El Centro accelerogram and the response parameters are compared in Figure 4.2.

A study of these figures shows that the elastic response in general is markedly higher than any of the inelastic cases. The inelastic action of girders alone is responsible for lowering the response by about 50 percent as compared with the corresponding elastic response. In Figure 4.1 although there is little difference between the response of the three inelastic cases, it can be noticed that the response of the model with $r = 10$ lies almost in between that of the $r = 5$ and the elasto-plastic model. Similarly the elasto-plastic ($r = \infty$) response of the 25-story model is a little higher than the response of the standard Ramberg-Osgood ($r = 10$) case (Figure 4.2). Thus the inelastic response parameters show a gradual increase with increasing value of r in the Ramberg-Osgood M-ϕ relation. A very important item to note in Figures 4.1(d) and 4.2(d) is that the column ductility ratios in the inelastic models are generally less than one, thus justifying the assumption of elastic column behavior.

The elastic and the inelastic (R-O , r = 10) displacement-time response of some floors of the 10-story model are presented for comparison in Figure 4.3 and similarly for the 25-story model in Figure 4.4. The amplitude of lateral displacements of the inelastic models is considerably lower than that of the corresponding elastic model as a result of energy dissipation. It should also be noted that the elastic fundamental mode of vibration of the structure dominates the inelastic response.

The energy vs. time relationship for the elastic and the Ramberg-Osgood (r = 10) versions of the 10-story model are shown in Figure 4.5. Similar curves for the 25-story model subjected to the El Centro accelerogram are presented in Figure 4.6. A comparison of the toal input energy curves for the elastic and inelastic versions in both cases will show that the average growth of energy with time is at similar rates. However, the elastic models show wide fluctuations in the input energy which are very much damped out in the inelastic response. An important feature of the inelastic response, as revealed by Figures 4.5 and 4.6, is that the total energy dissipated by the girders through inelastic hysteresis behavior is a major part (about 80-90 percent) of the total input energy. Therefore, at any instant, the stored energy in the elastic structure is much larger than that in the corresponding inelastic model.

An interesting comparison of the response of the standard Ramberg-Osgood (r = 10) and the elasto-plastic version of the 25-story model subjected to the El Centro accelerogram is presented in Figure 4.7. In Figure 4.7(a) the input energy and the total

dissipated energy per unit mass vs. time for the two models are given. A close examination of these two sets of curves will show that the stored energy in the elasto-plastic model at any instant is higher than that in the Ramberg-Osgood case. The displacement-time curves for the top floor of the above two models are shown in Figure 4.7(b). It can be seen that the amplitude of lateral oscillation of the elasto-plastic model is considerably higher than that of the Ramberg-Osgood frame, accounting for the higher stored energy in the former. The shift of the equilibrium position of oscillation from the zero position is much more marked in the elasto-plastic model. This means that larger permanent lateral distortion of the structure may be expected with the assumption of the elasto-plastic hysteresis model than would occur with the Ramberg-Osgood type hysteresis behavior. This has been demonstrated earlier by Berg in his study of Ramberg-Osgood single degree of freedom systems.(13) This observation may be attributed to the fact that an elasto-plastic system will dissipate energy only at amplitudes larger than the yield amplitude whereas in the Ramberg-Osgood type hysteresis some energy is dissipated even at low amplitudes.

It may therefore be said that the inelastic hysteresis behavior of the girders alone in a multistory structure provides a major source of energy dissipation and thus can cause a considerable reduction of its response to a severe earthquake as compared with the results of elastic analysis. The assumption of the elastic column behavior seems to be very well documented by these results. The assumption of the elasto-plastic hysteresis behavior appears to

over-estimate the response as compared with the choice of a Ramberg-Osgood type hysteresis which is fairly typical of steel flexual members.

4.3 Fundamental Period of Structure Versus Period Characteristics of Ground Motion

The fundamental period of a structure is perhaps the most significant parameter which is commonly referred to in the evaluation of the elastic dynamic response of the structure to a particular earthquake motion. In the present study an attempt was made to evaluate the influence of the elastic fundamental period (or elastic stiffness) of the structure upon its inelastic response. The evaluation of this effect was made by giving appropriate consideration to the period characteristics of the earthquake motion, as reflected through the general features of its undamped velocity spectrum. This section, therefore, presents a study of the combined influence of the elastic fundamental period of the structure and the period characteristics of the earthquake motion.

The sitffness of the 10-story standard Ramberg-Osgood model ($r = 10$) was adjusted to produce three models having the fundamental periods of 0.5, 1.25 and 2.27 seconds. All other properties (including the M_y - values for the members) remained unchanged. A similar treatment was given to the 25-story frame to produce three models with periods 1.25, 2.27 and 3.0 seconds. These six models were then analyzed for each of the three accelerograms with the exception that the analysis of the 25-story short period model for the Alameda Park earthquake was dropped because of the excessive computation time needed for this case. The results of these analyses are presented in Figures 4.8 - 1

Figures 4.8 and 4.9 show the response parameters of the 10- and 25- story models respectively, subjected to the Taft accelerogram which has velocity spectrum peaks in the short period range (0.5 - 1.0 second). The story displacements and the relative story-to-story displacements increase with the period - a characteristic feature of the displacement spectrum. The absolute floor accelerations also show a tendency of increasing with the period but not as distinctly as the displacements. The response of the columns and girders show a definite trend to decrease with the increasing fundamental period - faithfully following the velocity spectrum.

Response results similar to above for the Alameda Park accelerogram are presented in Figures 4.10 and 4.11. The displacements and accelerations again show a tendency to increase with the increasing period of the structure. But the column and girder response increases with increasing period for the range 0.5 - 2.27 seconds in 10-story models (Figure 4.10(d) - (h)),whereas the columns and girders of the 3.0 second 25-story frame are affected less than those of the 2.27 second model (Figure 4.11(d) - (h)). This is again in accordance with the shape of the velocity spectrum of this accelerogram which has a marked peak zone around 2.5 seconds followed by low spectrum values on either side.

In the case of the El Centro earthquake, the response results (Figures 4.12 and 4.13) show that the displacments do increase with the increasing fundamental period of the structure, but all other response parameters show a mixed trend. This is perhaps due to the fact that the velocity specturm for this accelerogram has peaks in the short period as well as the long range upto 3.0 seconds. Thus, the

forces and deformations in the frame members seem to be very much influenced by the shape of the velocity spectrum of the ground motion.

The fundamental elastic period has the dominating influence upon the inelastic response of the structure. However, the important contribution of the higher modes can also be seen in some of these results. This contribution of the higher modes causes an accentuated response near the top of the structure, commonly referred to as the "whiplash" effect.[10] This effect can be clearly observed in the response of the longer period models to Taft and El Centro earthquakes. It is absent from the response of 0.5 second period 10-story model to these two earthquakes and almost all the cases subjected to the Alameda Park accelerogram.

The explanation is simply based upon the different features of the velocity spectra of these three accelerograms. The Taft and El Centro both have spectrum peaks in the short period range (0.5 - 1.0 second) so that the longer period structures will have second or higher mode periods occurring in this region, thus contributing significantly to the total response. The 0.5 second period 10-story model has higher modal periods which lie in the region of very low spectrum values, resulting in almost negligible contribution of the higher modes. Similarly, the Alameda Park accelerogram has a very pronounced but narrow width of spectrum peak region around 2.5 seconds, with low values on both sides. The structures considered here have their fundamental periods ranging from 0.5 to 3.0 seconds so that no model has higher modes whose period would be located in the peak zone of the velocity spectrum. This accounts for the absence

of the "whiplash" effect or of any significant contributions of the higher modes to the total response to that earthquake.

In Table 4.1 are given the values of the maximum input energy per unit mass for the three 10-story Ramberg-Osgood models analyzed for each of the three accelerograms. Also tabulated therein are the values of elastic spectral energy per unit mass $(1/2\ S_V^2)$ for those periods. These values represent the maximum input energy per unit mass for an elastic single-degree-of-freedom system of that natural period of vibration subjected to the given earthquake. Similar energy values are tabulated in Table 4.2 for the three 25-story models.

A comparison of the elastic and inelastic input energy values in each case shows a reasonable correspondence. What is more interesting is that the maximum input energy values for each accelerogram follow the same pattern of variation over the range of periods considered as do the elastic spectral energy values, $1/2\ S_V^2$. Furthermore, the inelastic energy values are generally lower than the elastic spectral values -- a characteristic feature of the spectra for energy dissipative systems. The general resemblance in the pattern of the maximum input energy values for the inelastic multistory structures and the elastic spectral values of these accelerograms again seems to support the observation that the elastic fundamental period of the structure and the general shape of the elastic velocity response spectrum of the earthquake have a great bearing upon the inelastic response of the structure.

TABLE 4.1

MAXIMUM INPUT ENERGY, 10-STORY MODELS

Accelerogram	Max. Input Energy per unit mass ($inch^2$--sec^{-2})	Fundamental Period (seconds)		
		0.5	1.25	2.27
(a) El Centro	Elastic (1/2 S_v^2)	1965	1800	2380
	Inelastic, r = 10	2200	1545	2101
(b) Taft	Elastic (1/2 S_v^2)	6660	1890	545
	Inelastic, r = 10	2063	1929	772
(c) Alameda Park	Elastic (1/2 S_v^2)	17	1460	9700
	Inelastic, r = 10	348	555	7046

TABLE 4.2

MAXIMUM INPUT ENERGY, 25-STORY MODELS

Accelerogram	Max. Input Energy per unit mass ($inch^2$--sec^{-2})	Fundamental Period (seconds)		
		1.25	2.27	3.0
(a) El Centro	Elastic (1/2 S_v^2)	1800	2380	4005
	Inelastic, r = 10	1477	1871	2490
(b) Taft	Elastic (1/2 S_v^2)	1890	545	612
	Inelastic, r = 10	1582	1119	966
(c) Alameda Park	Elastic (1/2 S_v^2)	1460	9700	1458
	Inelastic, r = 10	--	5028	1236

4.4 Duration of Ground Motion

In order to study the influence of the duration of ground motion upon the response of structures, the various response parameters were recorded at a regular interval of five seconds. Since the input energy per unit mass is the single parameter which gives the best indication of the entire structural reponse in general, its variation with time is presented here to show the general growth of the structural response with the duration of ground motion. In Figures 4.14 and 4.15 are plotted the envelopes of the local maximum input energy per unit mass in each five-second interval for the 10-story and 25-story analyses, respectively, as reported in Section 4.3.

Both figures show that for the El Centro earthquake the growth of energy and consequently the maximum response occurs the earliest and that the Alameda Park earthquake produces the slowest energy growth of any of the three earthquake motions. The interaction between the fundamental period of the structure and the perid characteristics of ground motion, as was discussed in Section 4.3, can be very clearly noticed from these energy curves.

4.5 Height of Frame

The influence of the height or the number of stories of a multistory building frame upon its response to earthquake was an important feature of the study. The study of the influence of this important parameter was made in three ways. First, the three standard Ramberg-Osgood ($r = 10$) models, 10, 25, and 40 stories high with fundamental periods, $T = 1.25$, 2.27 and 3.0 seconds, respectively, were considered. As was mentioned earlier in Chapter 3,

the 10- and 25- story standard models were identical with the top 10 and 25 stories of the standard 40-story frame. Their fundamental periods were determined on this basis. These three standard models of different heights and different fundamental periods but having the same stiffness and strength of the members were analysed for each of the three accelerograms. The results are presented in Figures 4.16 - 4.18. This was intended to represent a normal situation where a taller structure has a longer period than a shorter structure.

Next, the stiffness of the standard 10- and 40-story frames was adjusted to a common fundamental period of 2.27 seconds, same as that of the standard 25-story model. The response of these three models to the El Centro earthquake is shown in Figure 4.19. The idea of this comparison was to study the effect of height by eliminating the difference of period. It may be noted that in accomplishing this the shorter structure becomes less stiff and the taller stiffer as compared with their respective standard models.

In the third comparison the response of top 10 stories of the standard 25- and 40- story models is plotted against the response of the standard 10-story frame. This is again done for each of the three accelerograms and the results are shown in Figures 4.20 - 4.22. This, therefore, becomes a basis to study how the same structural assemblage (10 stories here) will respond to the same earthquake when it forms the top part of a taller structure as compared with its behavior as a complete structure based directly on the moving ground.

A discussion of these results is given in the following paragraphs:

4.5.1 Standard Models

The response of the three standard models to the El Centro, Taft and Alameda Park earthquakes is shown in Figures 4.16, 4.17 and 4.18 respectively. The various response parameters are plotted against vertical position in the structure, expressed as percent of height. A few interesting observations can be made from a study of these figures. The lateral displacements show a tendency to increase with increasing height (or period) except for the Taft and Alameda Park earthquakes, where the 25- and 40- story frames have similar displacements. This can again be correlated with the spectrum features of these accelerograms. El Centro has a steadily increasing displacement spectrum whereas the displacement spectrum values for Taft beyond 0.6 second and those for Alameda Park beyond about 2.5 seconds are nearly constant because of the downward slope of their velocity spectra in these regions. However, the 40-story model shows more accentuated displacements near the top than the 25-story model, because of the greater contribution of the higher modes in the former. This effect can be seen, to a larger or smaller extent, in almost all of these figures for the 40-story model, but is not as pronounced for the Alameda Park earthquake as for the other two.

The floor accelerations, story shears per unit weight of the structure, and the ductility ratio in the columns decrease with increasing height. The girder response shows a rather mixed trend for the El Centro earthquake, being largest for the 10-story model in the Taft earthquake and for the 25-story model in the Alameda Park earthquake. This again shows that the girder response is more

influenced by the features of the velocity spectrum of the earthquake and the fundamental period of the structure than by the height of the structure.

4.5.2 Constant Period Models

Figure 4.19 shows the response of the three 10- , 25- and 40- story models of the same period, 2.27 seconds, subjected to the El Centro earthquake. The lateral displacements and acclerations of the floor masses are almost the same for the 25- and 40- story frames, those for the 10-story model being a little higher. But the difference is not very significant. Story shears per unit weight of the structure and the column ductility ratios are definitely lower as the structure becomes taller. On the other hand the girder response shows a definite increase with the height of the frame. When this is compared with the relatively mixed trend of the girder response of the three standard models to the same El Centro earthquake (Figure 4.16(f) - (h)) the difference in the behavior appears to be due to the increased stiffness of the 40-story and the reduced stiffness of the 10-story frame as compared with the stiffnesses of their respective standard versions.

4.5.3 Portion of Structure

Figures 4.20, 4.21 and 4.22 compare the response of the top 10 stories of the standard 10-, 25- and 40- story frames for the three earthquakes. The response of these top 10 stories (which are the identical structural assemblage in every case) to the Taft and El Centro earthquakes does not seem to be significantly affected by the fact that they form the upper parts of the structures of different heights. The velocity spectrum for the Taft earthquake has peaks in

the short period range so that the 10-story frame should have greater response than the same members forming the top of 25- and 40- story frames of longer periods. But higher modes become more significant in the latter cases so that the response of these 10-story members is similar. In Figure 4.22 for the Alameda Park earthquake the response of the 10 stories of the 25-story frame is distinctly higher than the other two cases. This again indicates that for the Alameda Park earthquake the influence of the fundamental period of the structure is more predominant and the higher modes are less significant in the response of the top portions of tall frames.

All the above discussion of results presented in this section leads to the significant conclusion that the inelastic response of a multistory structure is predominantly controlled by its fundamental period and by the spectrum features of the earthquake motion rather than by the height of the structure or its number of stories. However, the column moments and the seismic base shear coefficients can be expected to be smaller in taller structures. The accentuation of the response in the upper portion of the structures, the "whiplash" effect, seems to depend upon the velocity spectrum values of the earthquake in the region of the first few higher modal periods of the structure.

4.6 Stiffness - Strength Taper

In this section a comparison is made between the inelastic response of the standard taper 10- and 25- story frames and that of the corresponding models having equal fundamental periods and uniform stiffness and strength. As was mentioned in Chapter 3, the uniform

models have member size and strength corresponding to the middle portion of the respective standard model. The 10-story frames were analyzed for the Taft and the 25-story frames for the El Centro earthquake with the results presented in Figures 4.23 and 4.24 respectively.

It can be seen from the two figures that the lateral displacements are generally larger for the uniform models whereas the accelerations and the story shears are not affected by the stiffness distribution. The column and girder responses in the uniform models are larger near the bottom with a very sharp taper upwards, while those for the standard models are relatively more uniformly distributed. Calculations show that in both instances the uniform and the standard models dissipated almost equal amounts of the total energy but in the uniform models the concentration of ductile deformations was at the lower levels. The "whiplash" effect, of course, is absent from the response of the uniform structures. The columns in every case behave elastically.

4.7 Yield Strength of Members

In this section a comparison in made between the response of two 25-story Ramberg-Osgood ($r = 10$) frames -- one with the member yield moments for $\sigma_y = 36$ ksi and the other for which the member strength was set to $\sigma_y = 18$ ksi . The accelerogram used was the El Centro and the results are shown in Figure 4.25.

The weaker frame has smaller lateral displacements and floor accelerations. The shears in the columns are cut down almost in proportion to the reduction in strength. The column ductility ratios have increased in the weaker frame but not in inverse proportion to

the strength, so that the column moments are less in the weaker structure - a consequence of weaker girders. The columns, however, behaved elastically even though the yield level was reduced by one-half. The girder ductility ratios in the weaker frame are about double and the yield excursion ratios about four times those of the stronger frame. The total energy dissipated is smaller in the weaker frame but it makes up a larger fraction of the total input energy, being 0.97 for the weaker and 0.94 for the stronger frame. The maximum input energy for the weaker frame was 4514 kip inches and that for the stronger one 5330 kip-inches. It would be quite reasonable to expect greater input energy in a stronger structure because an elastic structure represents the one of infinite yield strength and suffers the maximum energy input from the same earthquake motion. This observation for the multistory structures also agrees with the results of the earlier studies of single-degree-of-freedom elasto-plastic systems.[8]

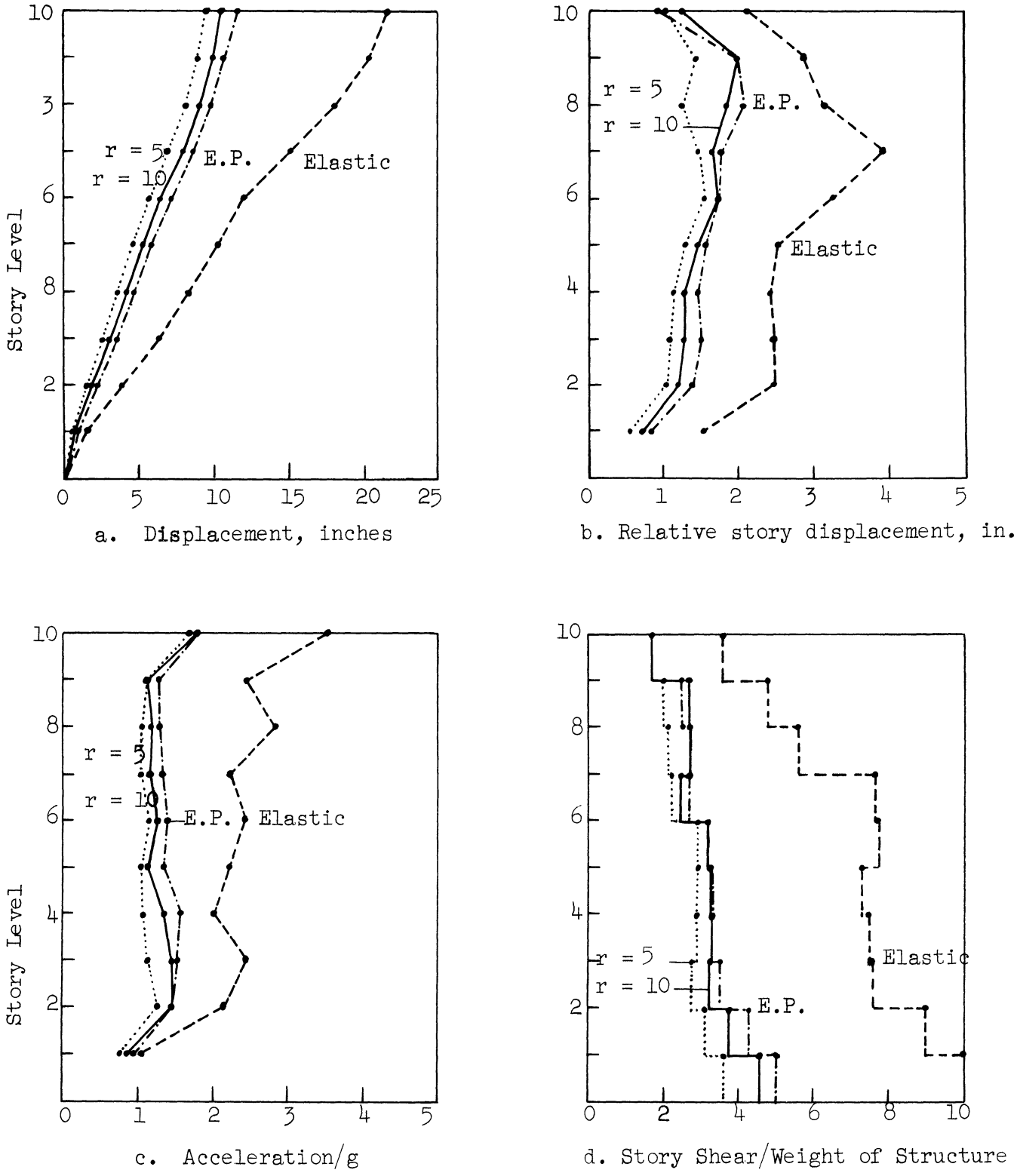

10 Story Standard Models, T = 1.25 sec; Taft 1952, S21°W x 3.0

Figure 4.1. Effect of inelastic action of girders.

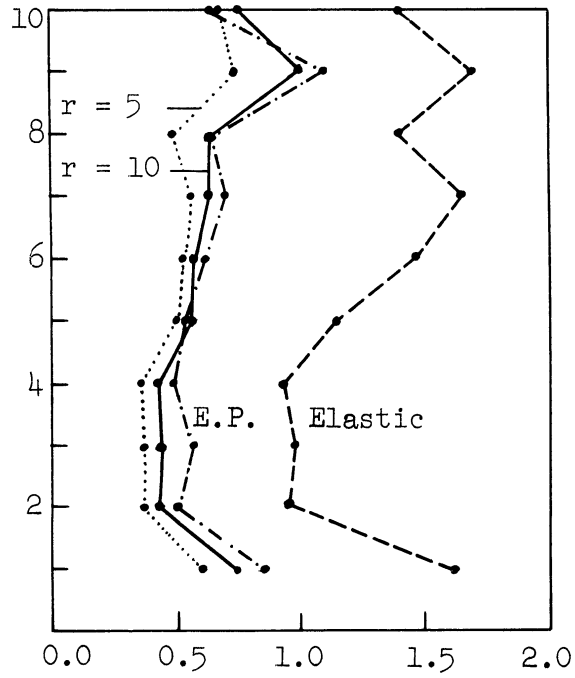

e. Column Ductility, M_{max}/M_y

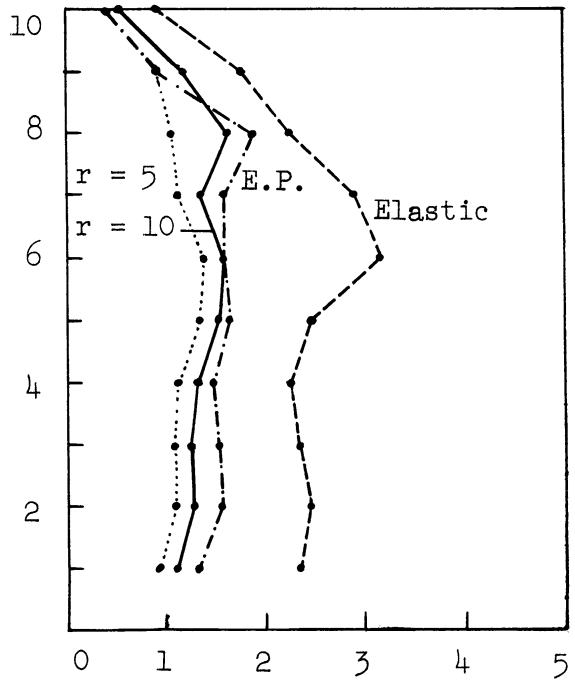

f. Girder Ductility Ratio

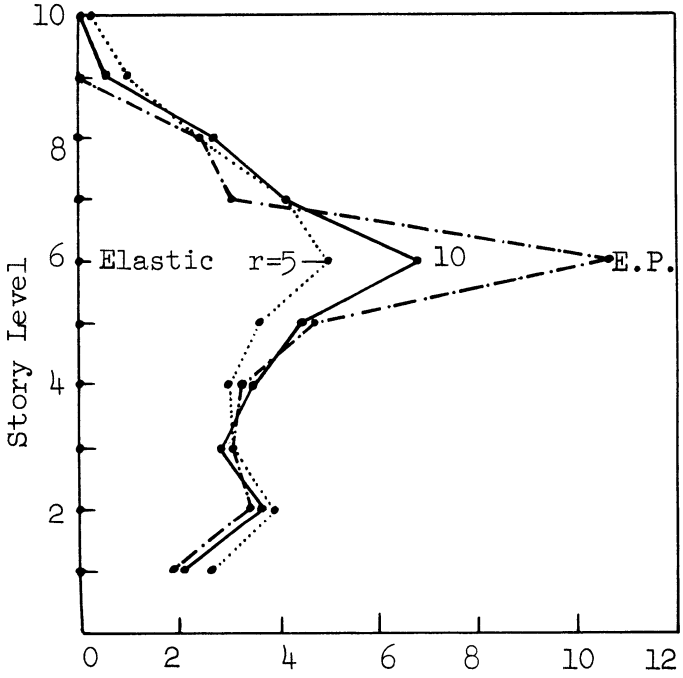

g. Hysteresis Energy/$(M_y.\theta_y)$

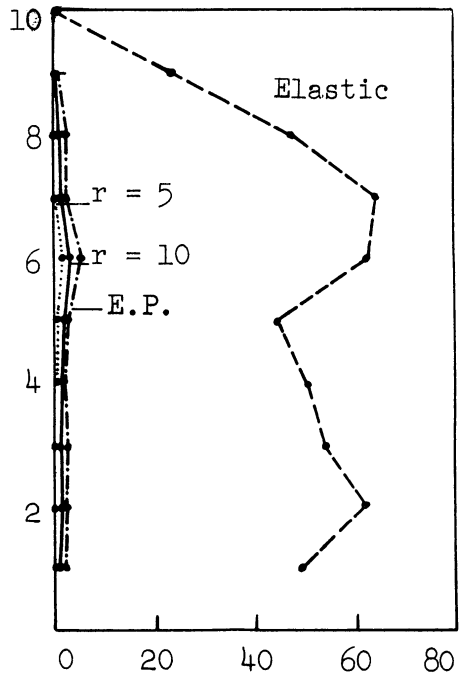

h. Yield Excursion Ratio, ϵ

10-Story Standard Models, T = 1.25 sec; Taft 1952, S21°W x 3.0

Figure 4.1. (Concluded).

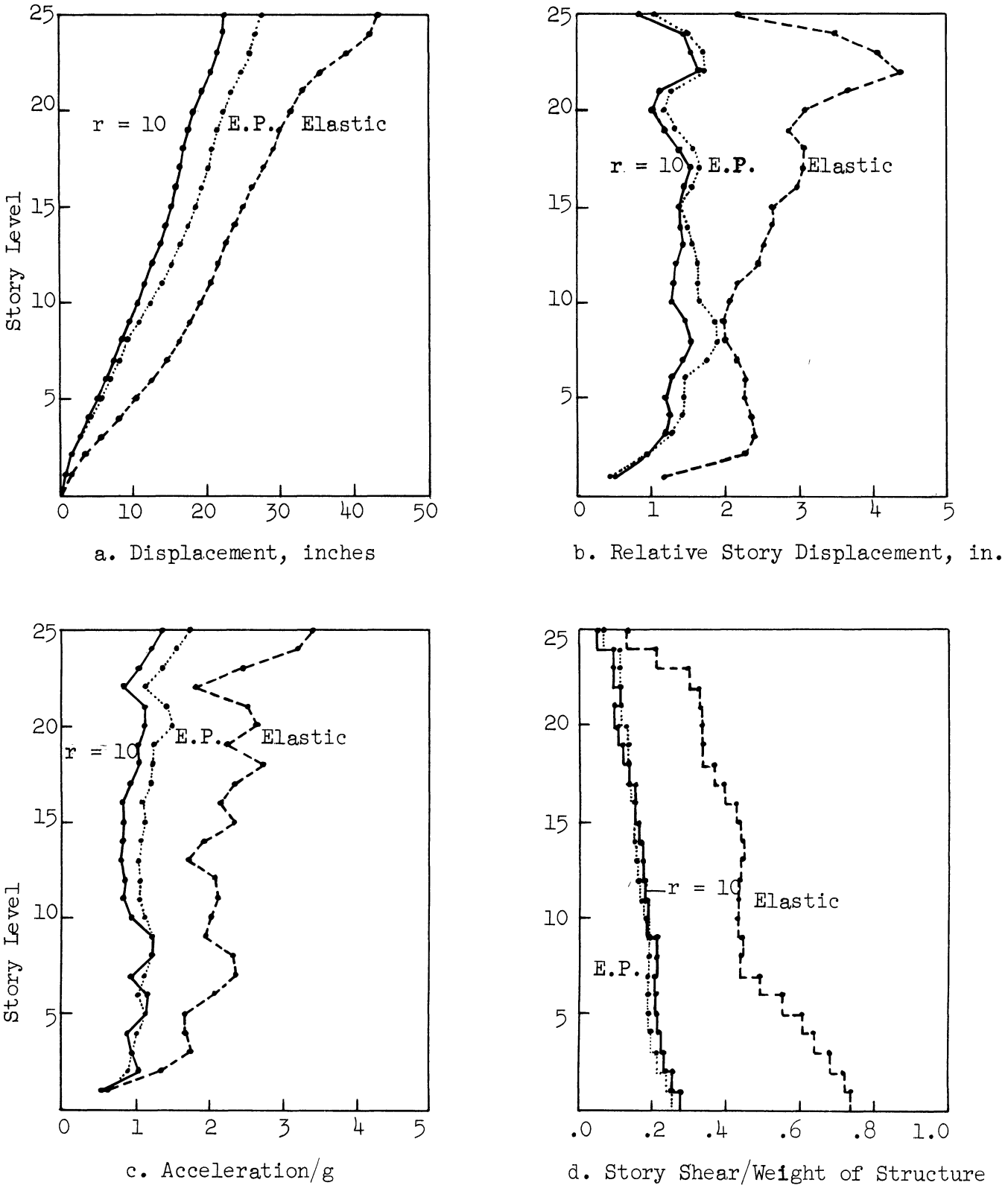

25-Story Standard Models, T = 2.27 Sec; El Centro 1940, N-S x 1.5

Figure 4.2. Effect of inelastic action of girders.

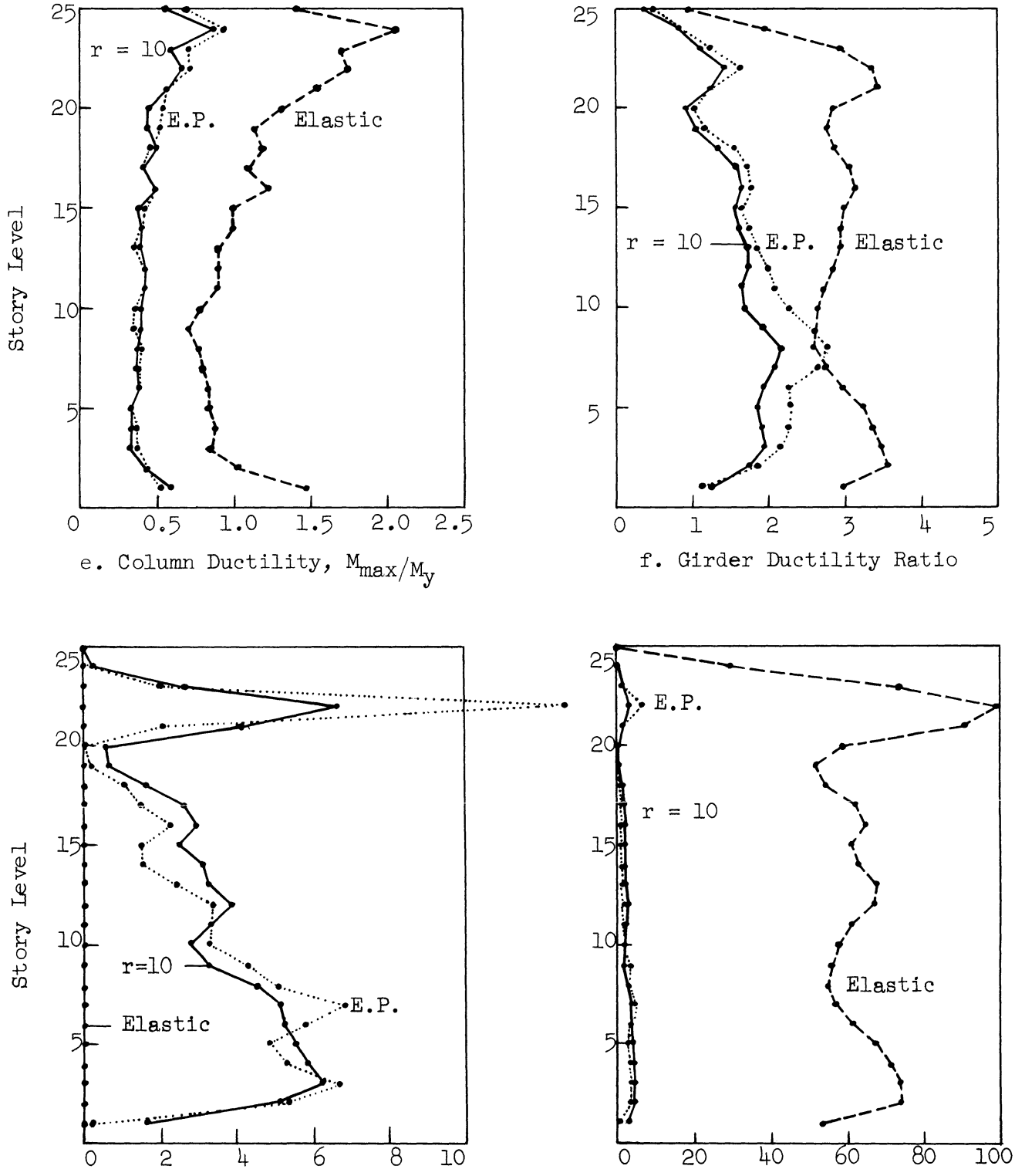

25-Story Standard Models, T = 2.27 Sec; El Centro 1940, N-S x 1.5

Figure 4.2. (Concluded)

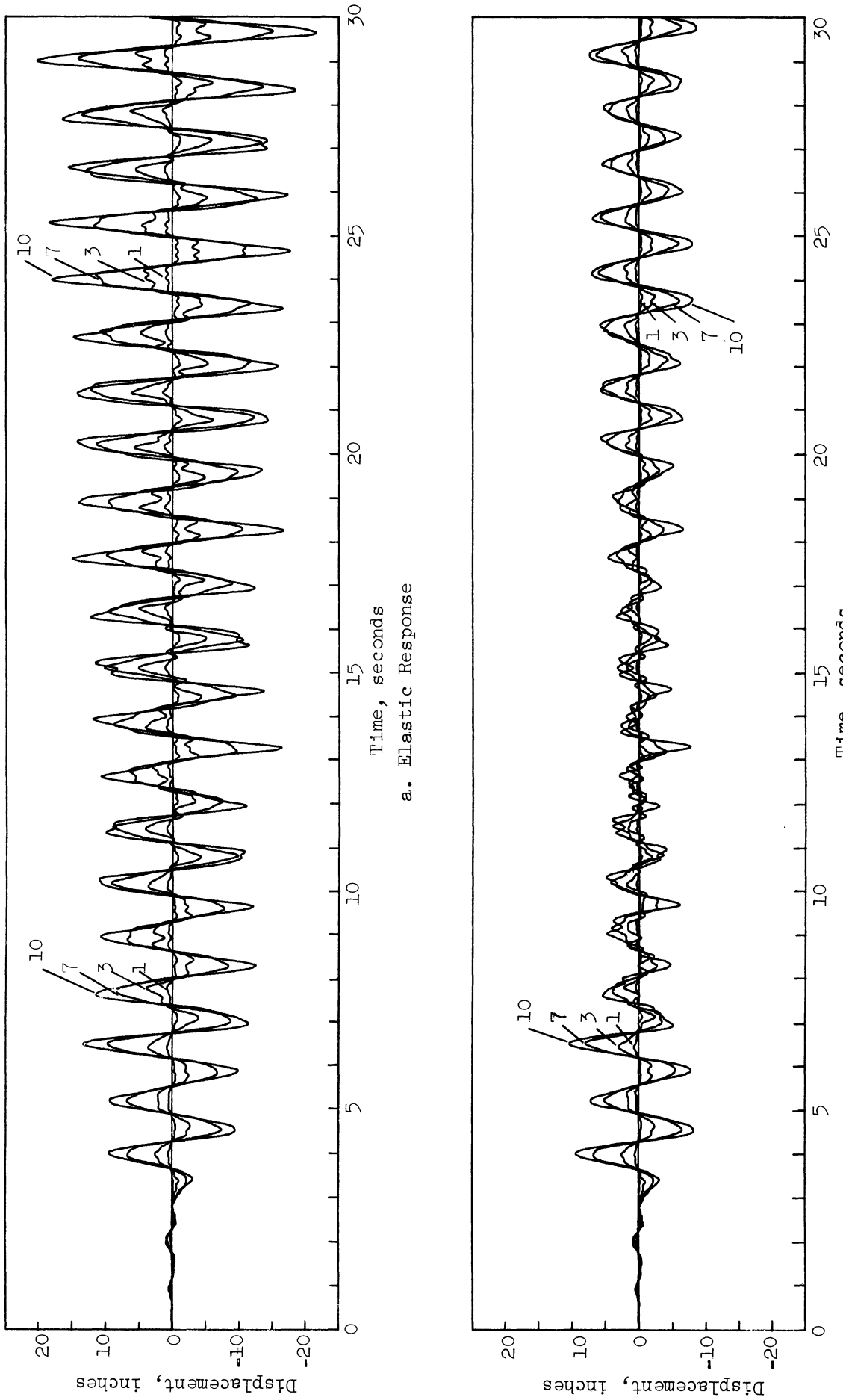

Figure 4.3. Elastic vs. inelastic response, 10-story frame (T=1.25 sec), Taft 1952, S21°W x 3.0.

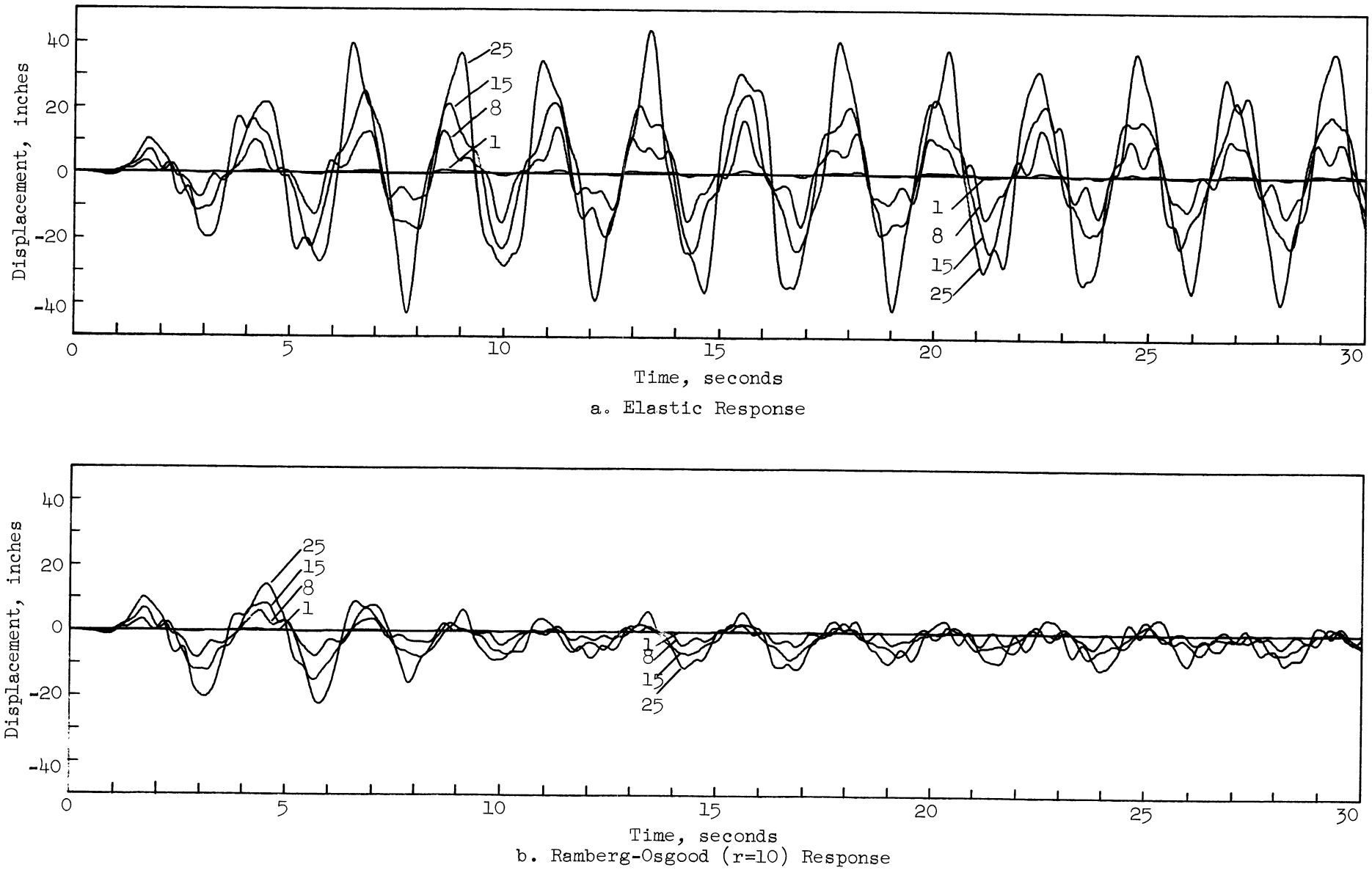

Figure 4.4. Elastic vs. inelastic response, 25-story frame (T=2.27 sec), El Centro 1940, N-S x 1.5.

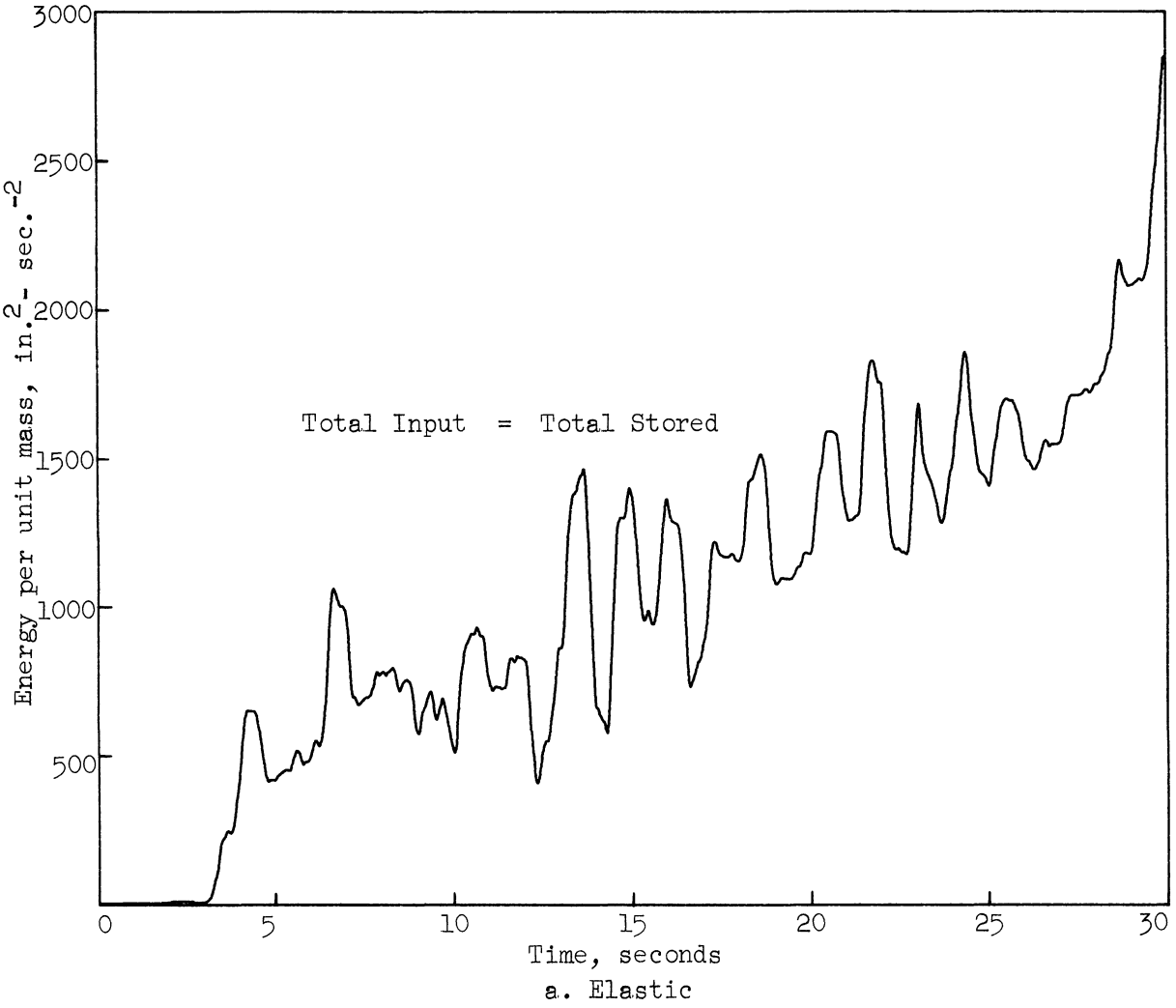

a. Elastic

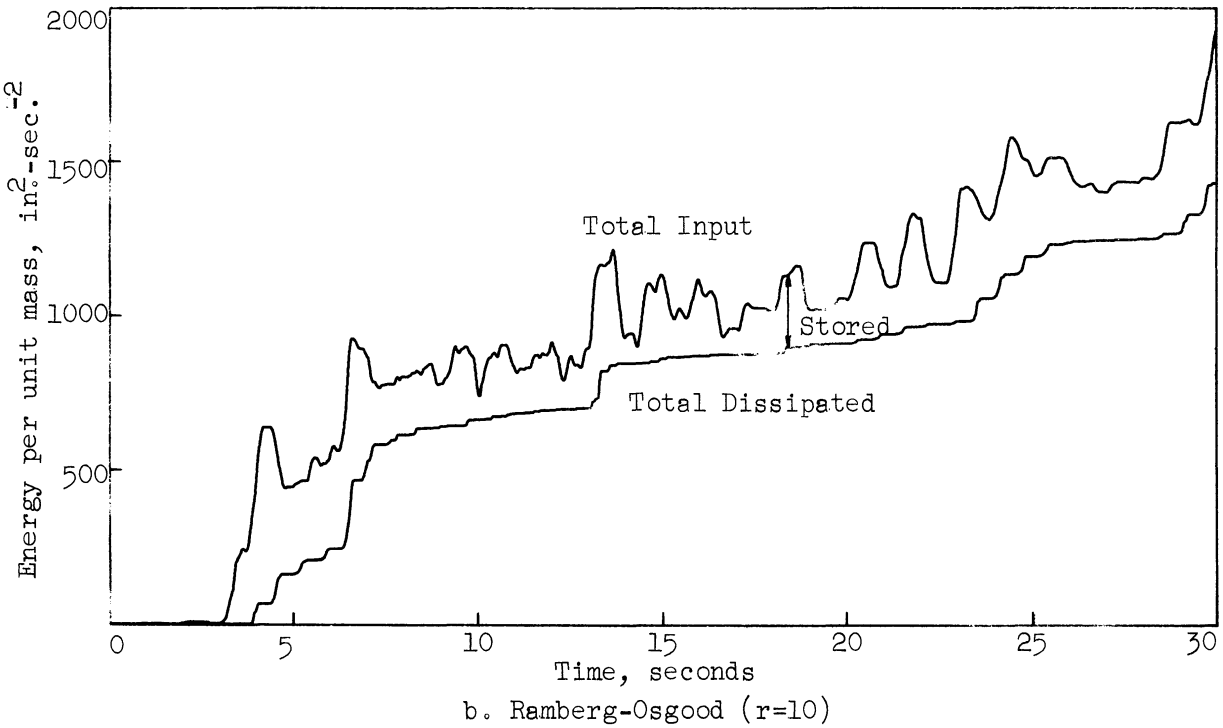

b. Ramberg-Osgood (r=10)

Figure 4.5. Energy vs. time, N=10, T=1.25 sec; Taft 1952, S21°W x 3.0.

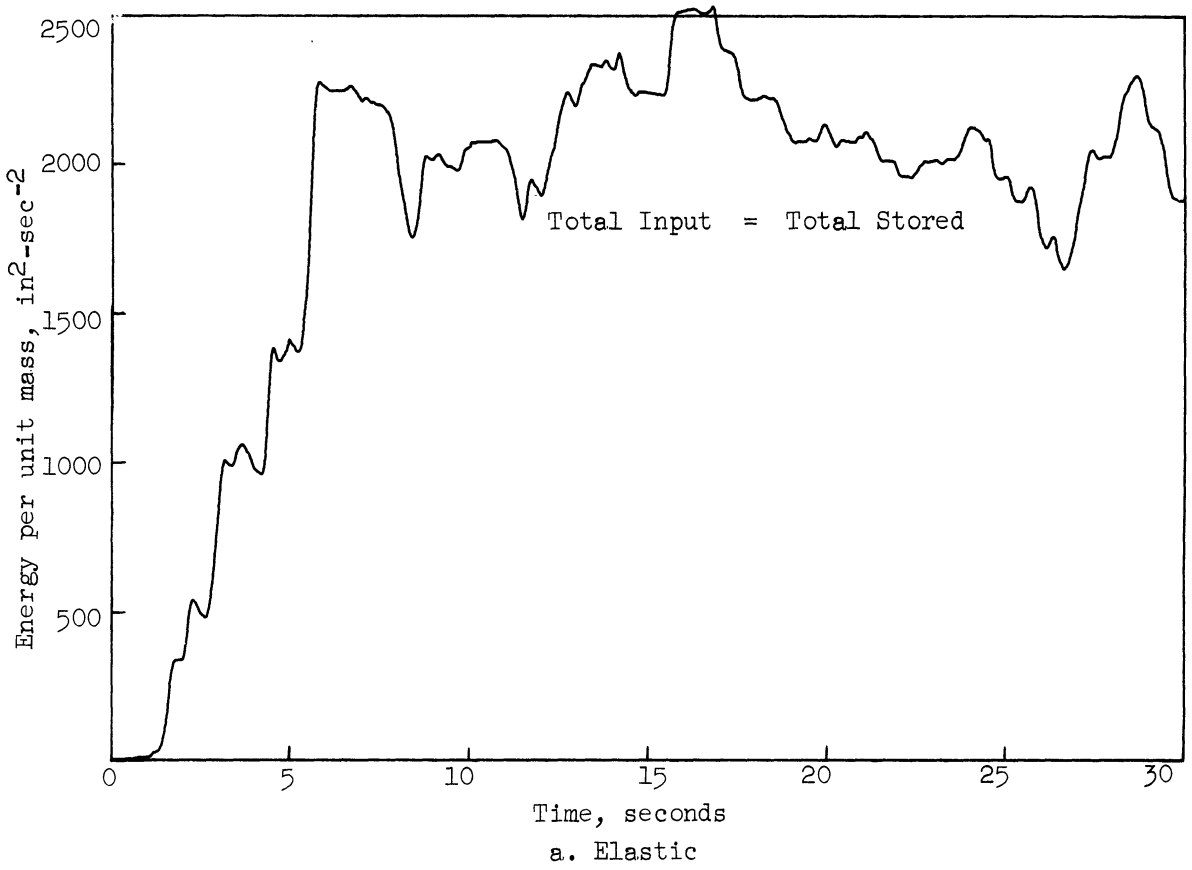

a. Elastic

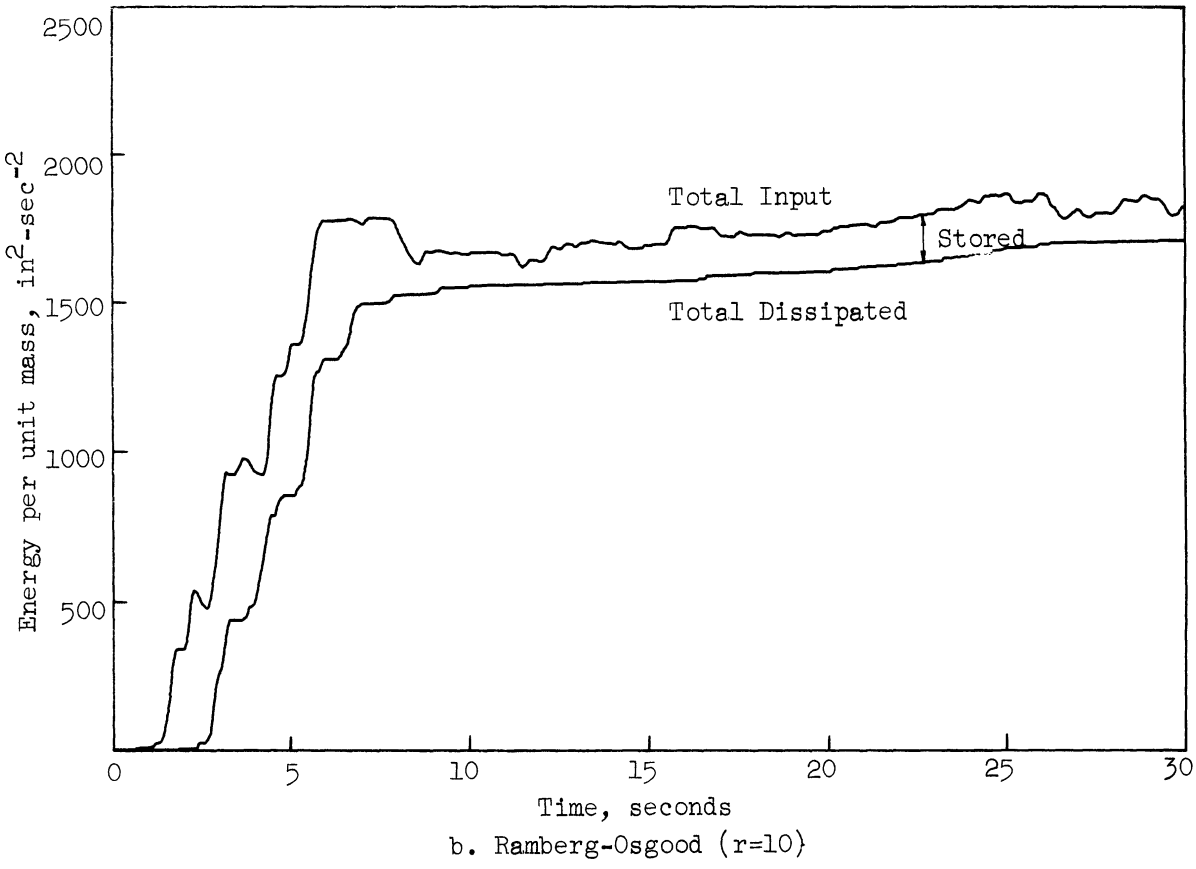

b. Ramberg-Osgood (r=10)

Figure 4.6. Energy vs. time, N=25, T=2.27 sec.; El Centro 1940, N-S x 1.5.

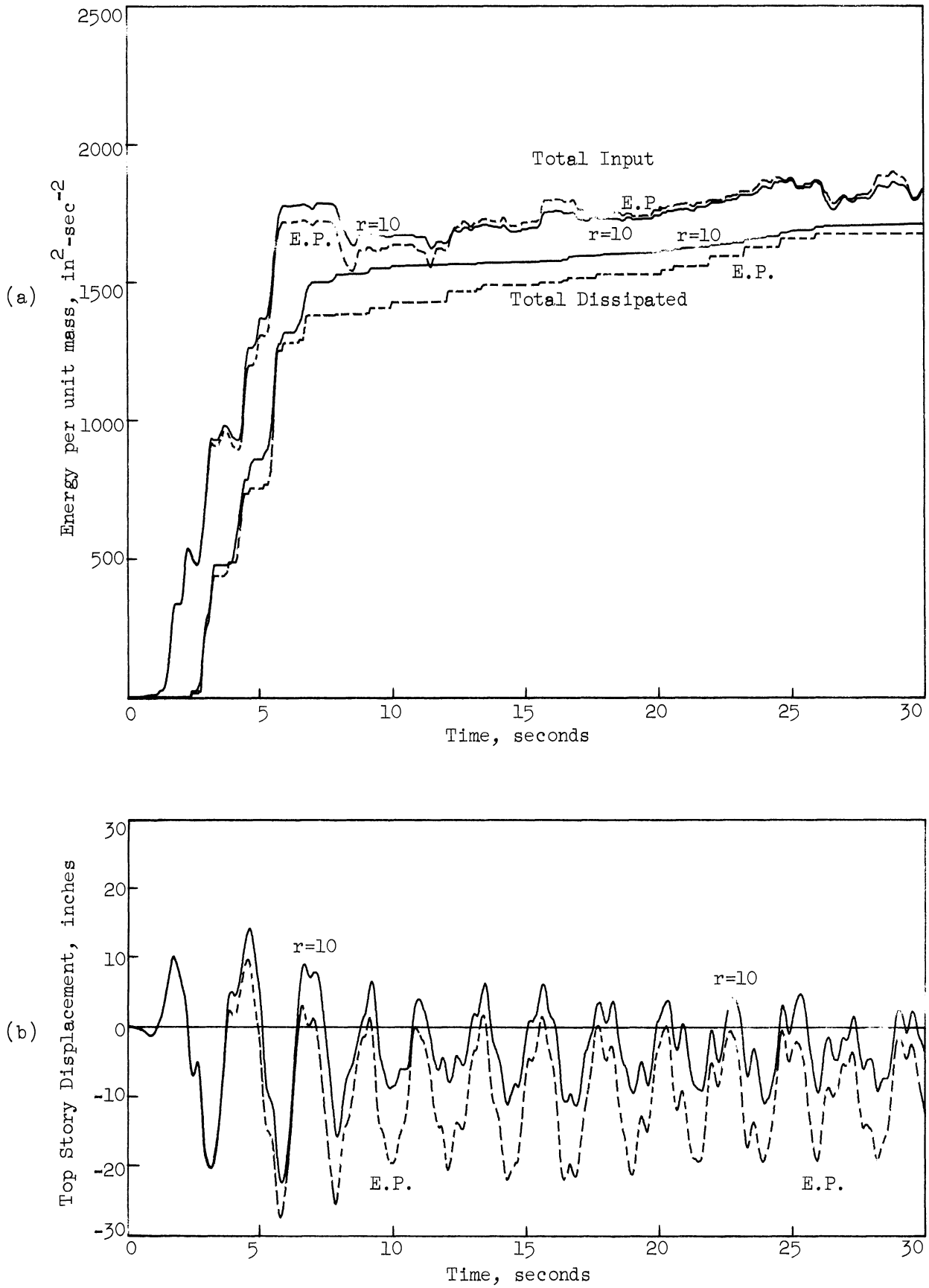

25-Story Model, T=2.27 seconds, El Centro 1940, N-S x 1.5

Figure 4.7. Ramberg-Osgood (r=10) vs. elasto-plastic response.

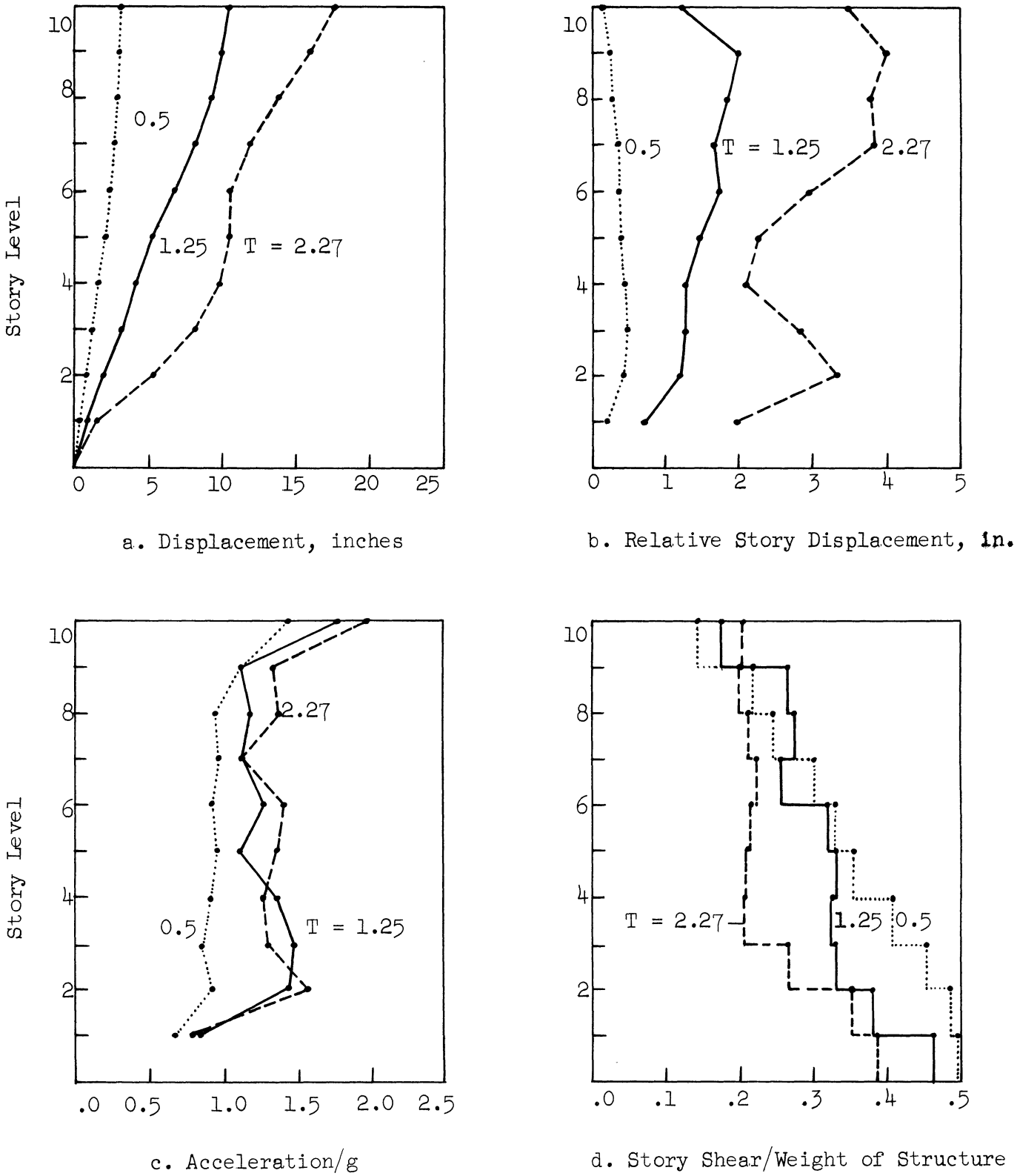

10-Story Ramberg-Osgood Models (r=10); Taft 1952, S21°W x 3.0

Figure 4.8. Effect of fundamental period of structure.

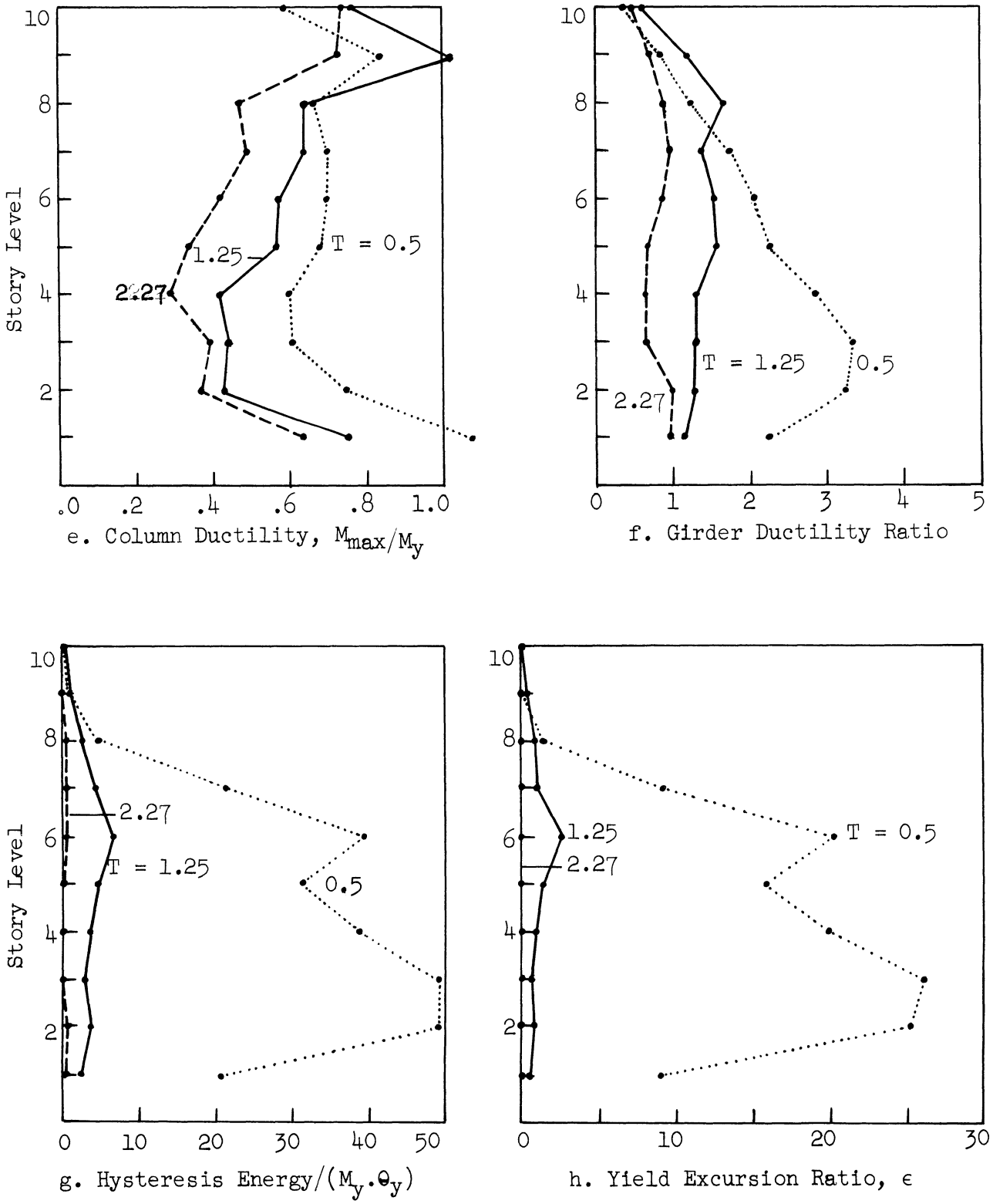

10-Story Ramberg-Osgood Models (r = 10); Taft 1952, S21°W x 3.0

Figure 4.8. (Concluded)

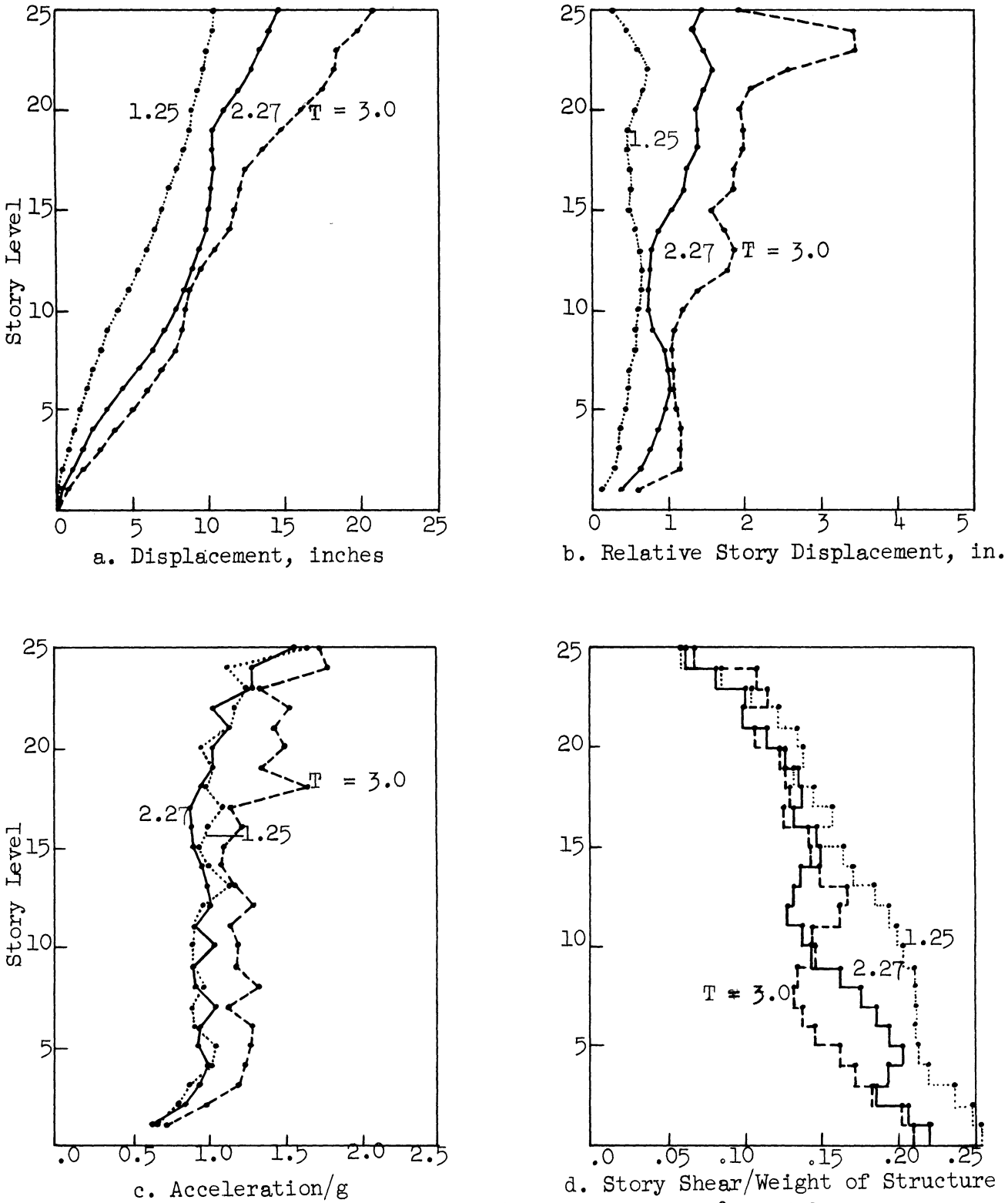

25-Story Ramberg-Osgood Models (r = 10); Taft 1952, S21°W x 3.0.

Figure 4.9. Effect of fundamental period of structure.

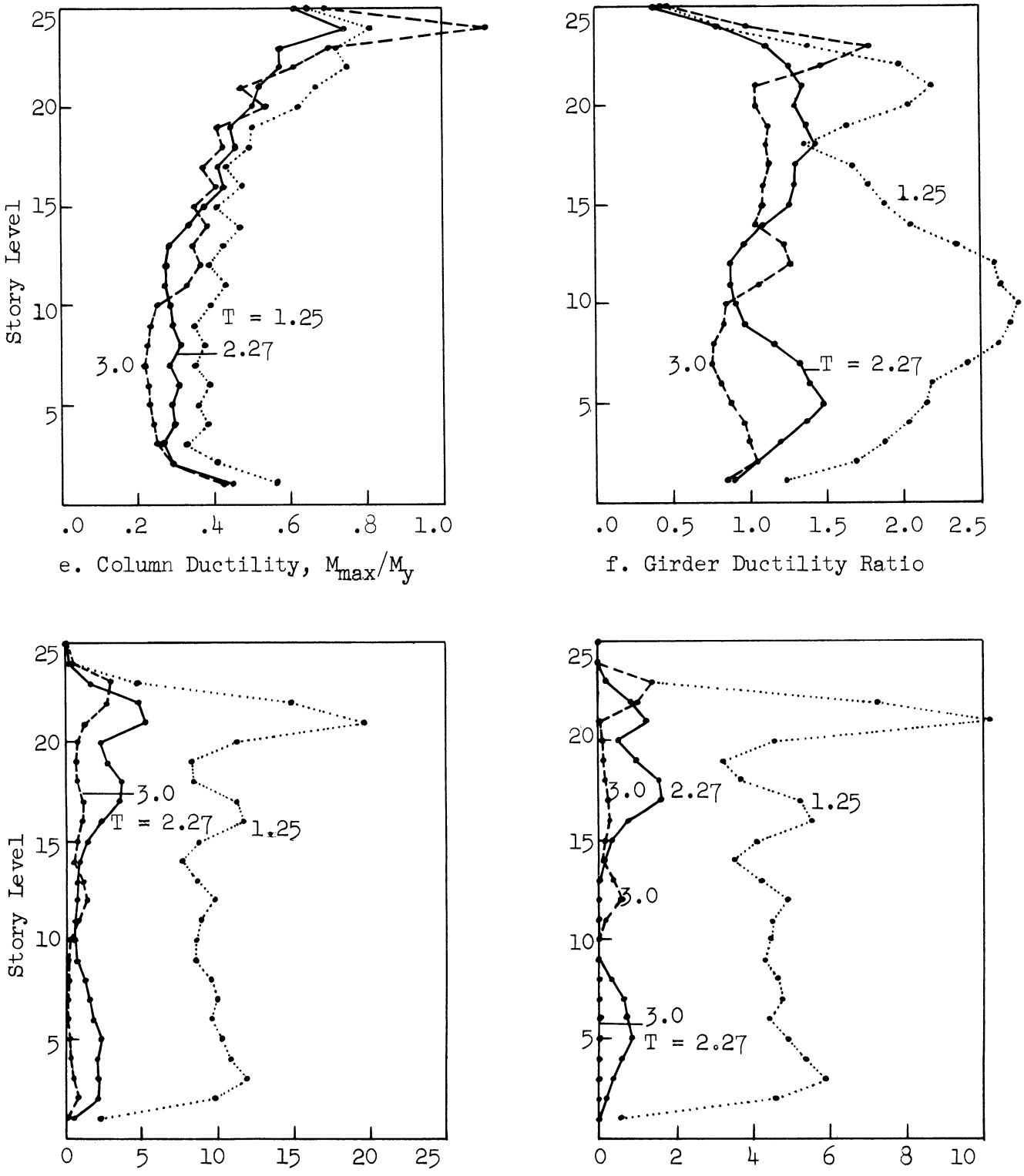

e. Column Ductility, M_{max}/M_y

f. Girder Ductility Ratio

g. Hysteresis Energy/$(M_y.\theta_y)$

h. Yield Excursion Ratio, ϵ

25-Story Ramberg-Osgood Models (r=10); Taft 1952, S21°W x 3.0

Figure 4.9. (Concluded)

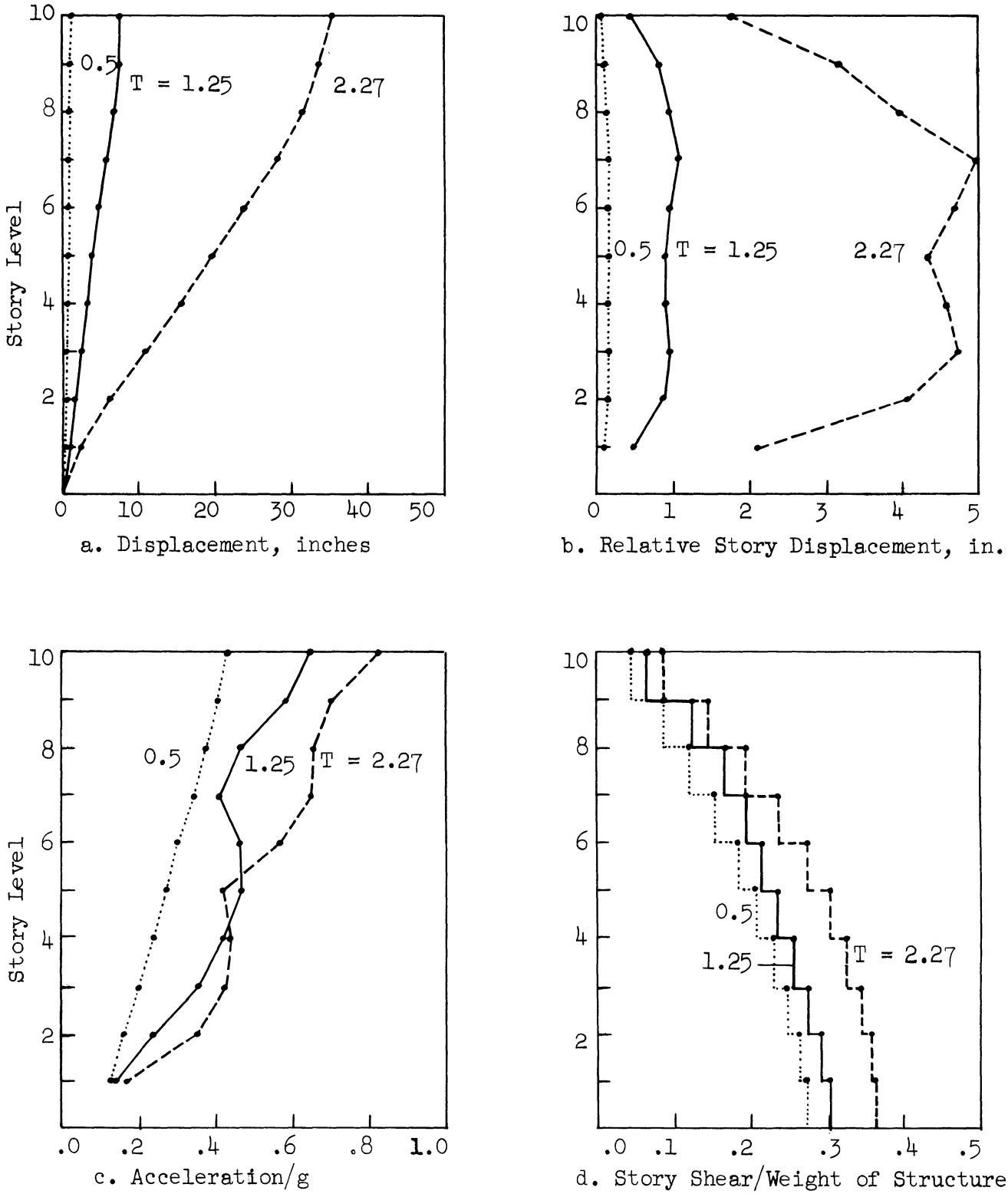

10-Story Ramberg-Osgood Models (r=10); Alameda Park 1962, N10°-46'W x 2.4

Figure 4.10. Effect of fundamental period of structure.

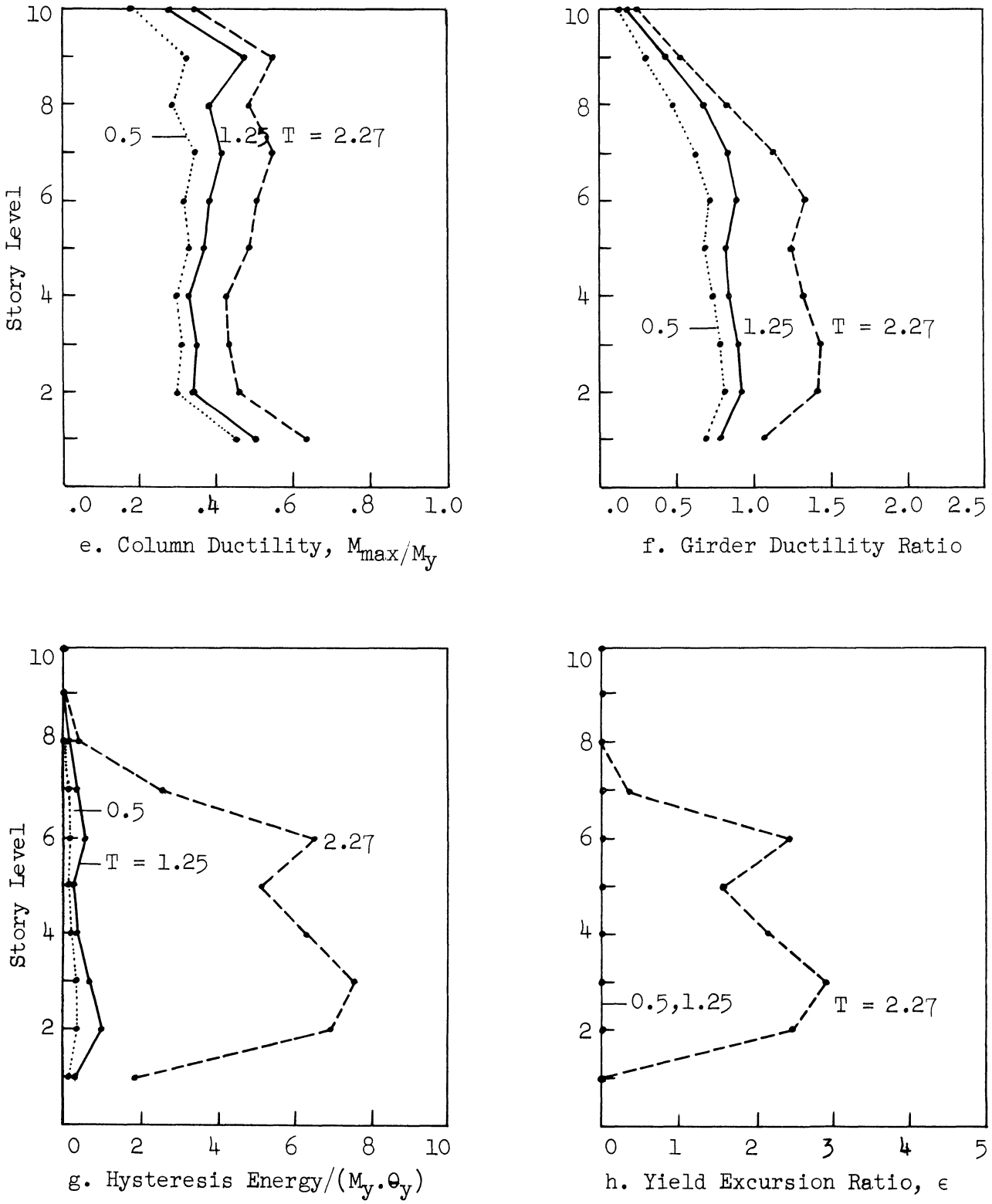

10-Strong Ramberg-Osgood Models (r=10); Alameda Park 1962, N10°-46'W x 2.4

Figure 4.10. (Concluded).

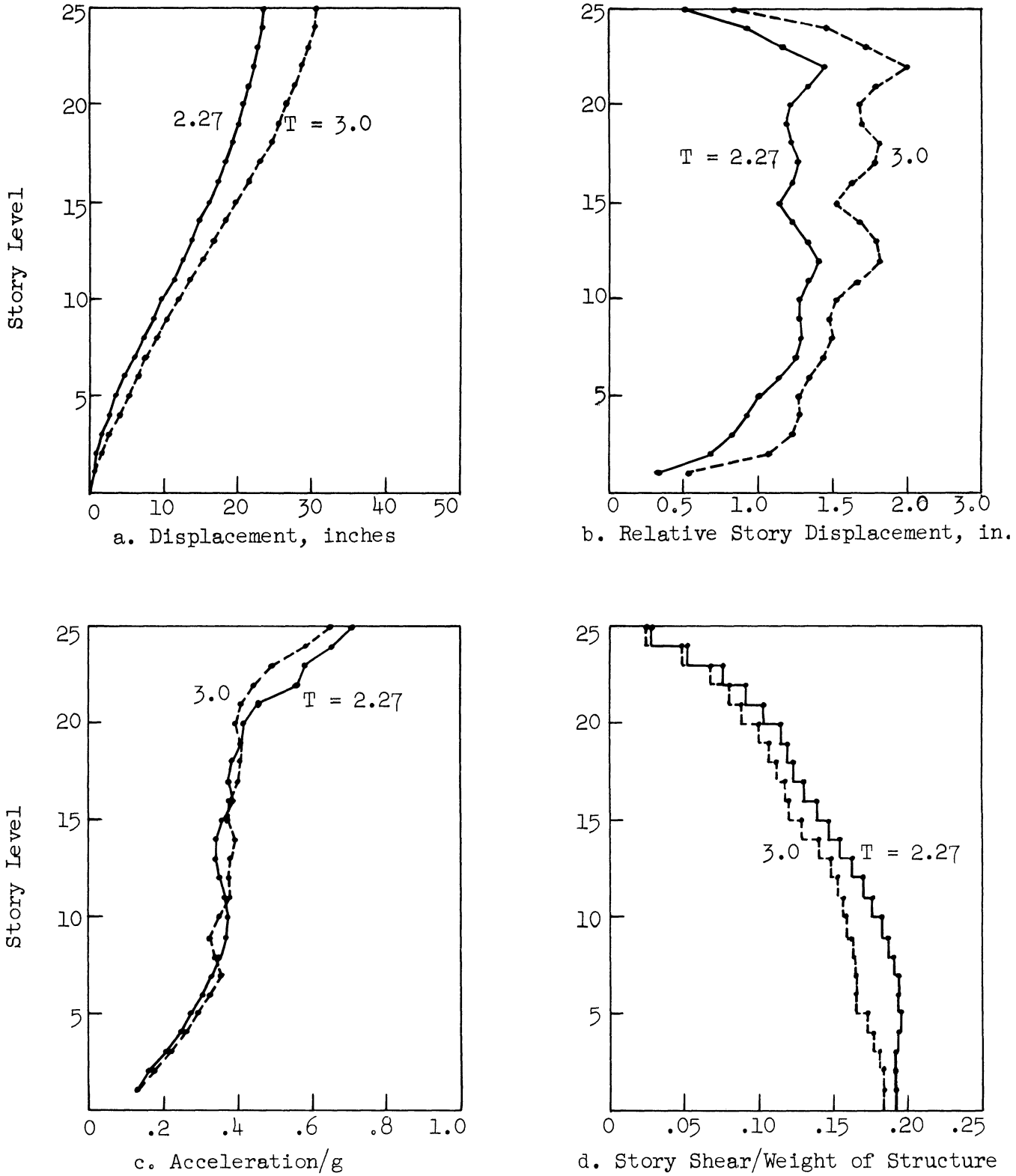

25-Story Ramberg-Osgood Models (r=10); Alameda Park 1962, N10°-46'W x 2.4

Figure 4.11. Effect of fundamental period of structure.

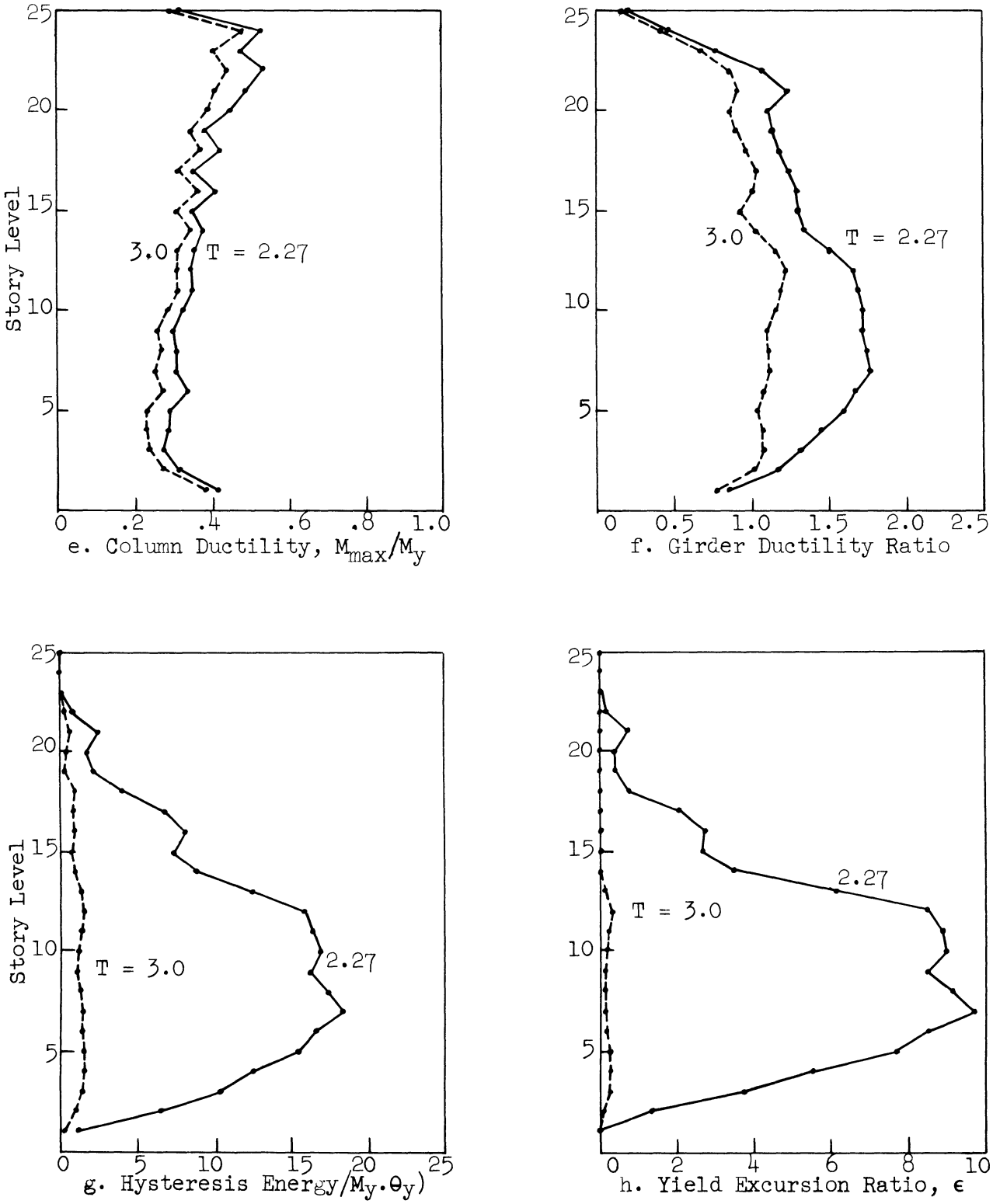

25-Story Ramberg-Osgood Models (r=10); Alameda Park 1962, N10°-46'W x 2.4

Figure 4.11. (Concluded)

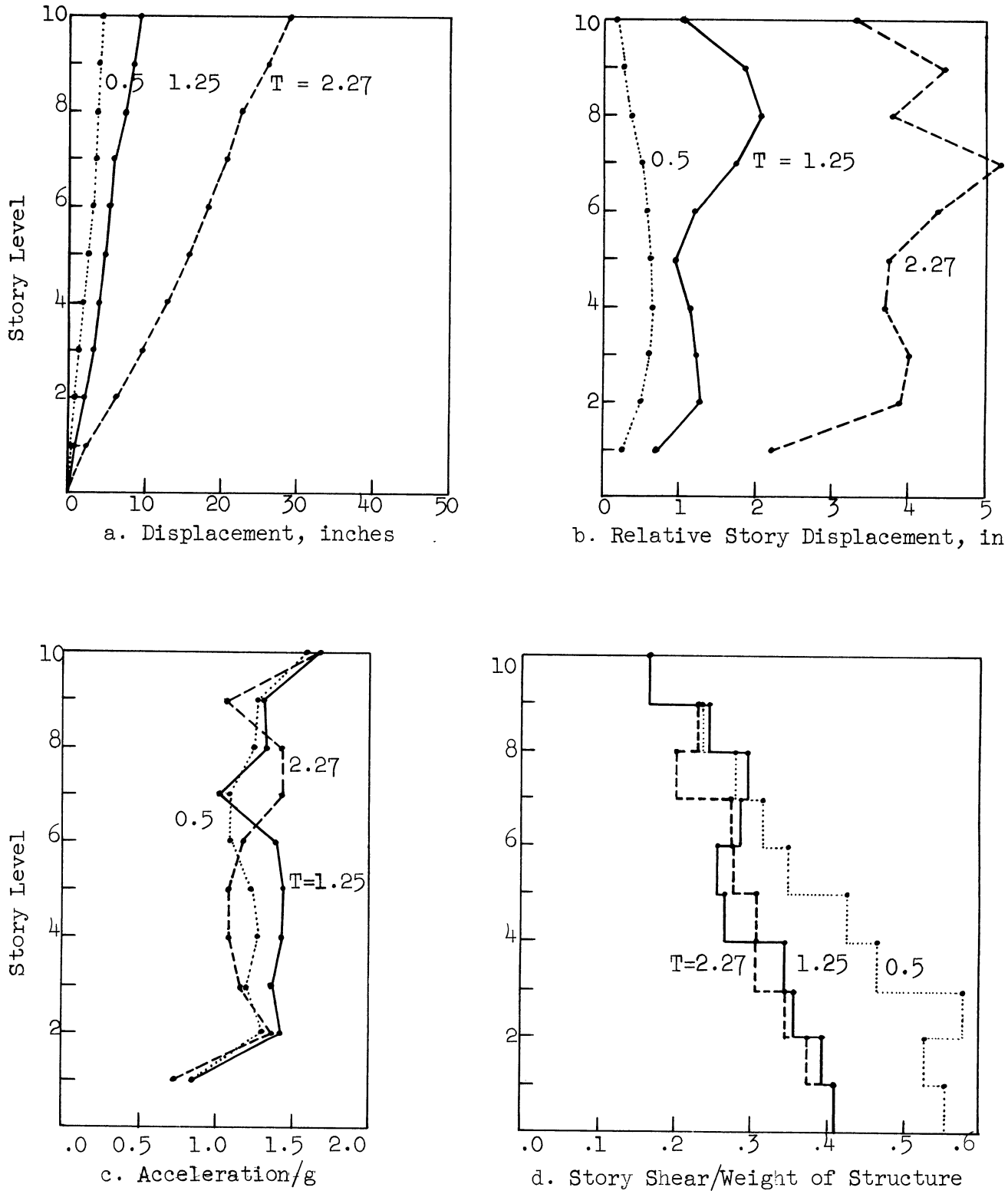

10-Story Ramberg-Osgood Models (r=10); El Centro 1940, N-S x 1.5

Figure 4.12. Effect of fundamental period of structure.

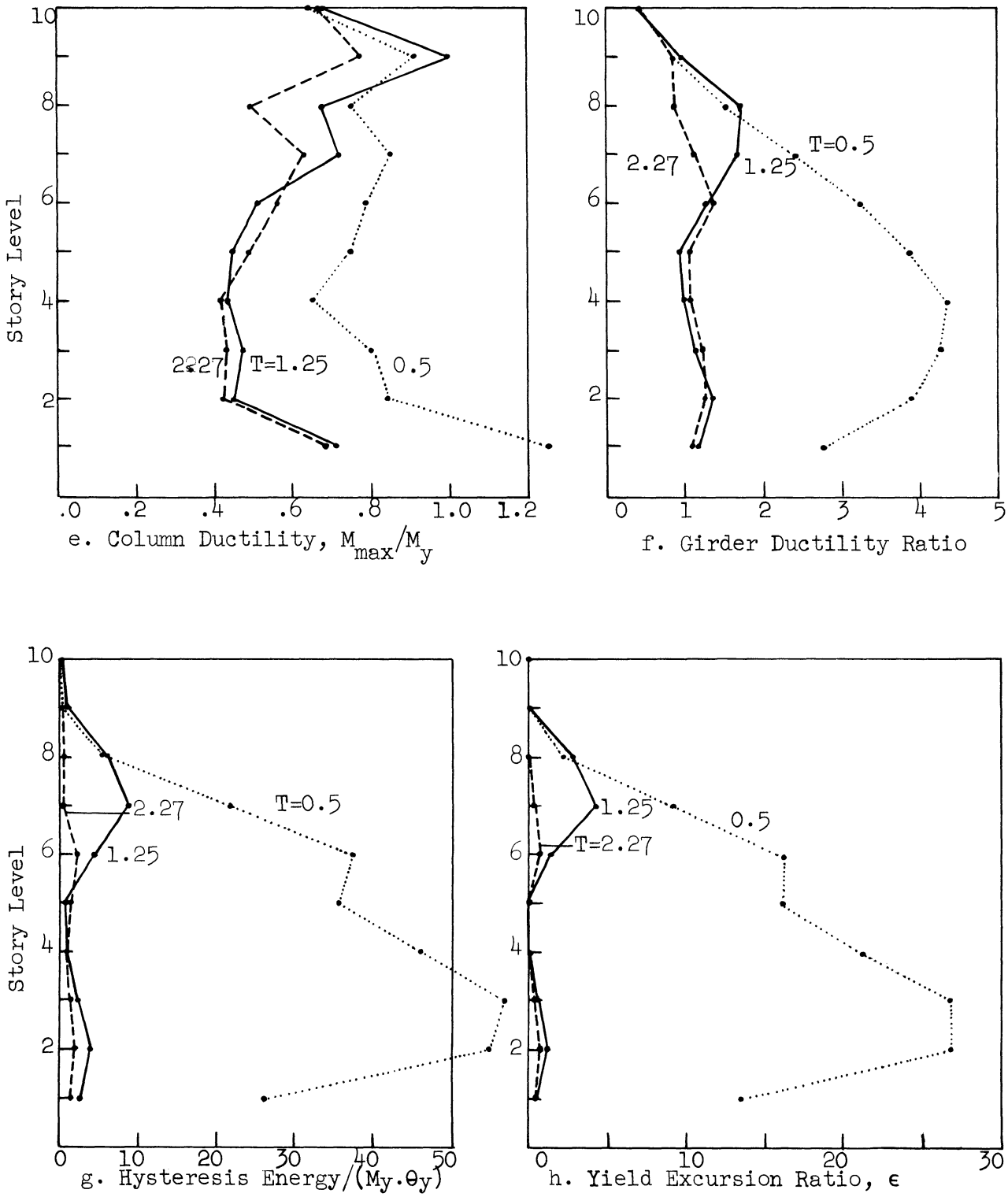

10-Story Ramberg-Osgood Models (r=10); El Centro 1940, N-S x 1.5

Figure 4.12. (Concluded)

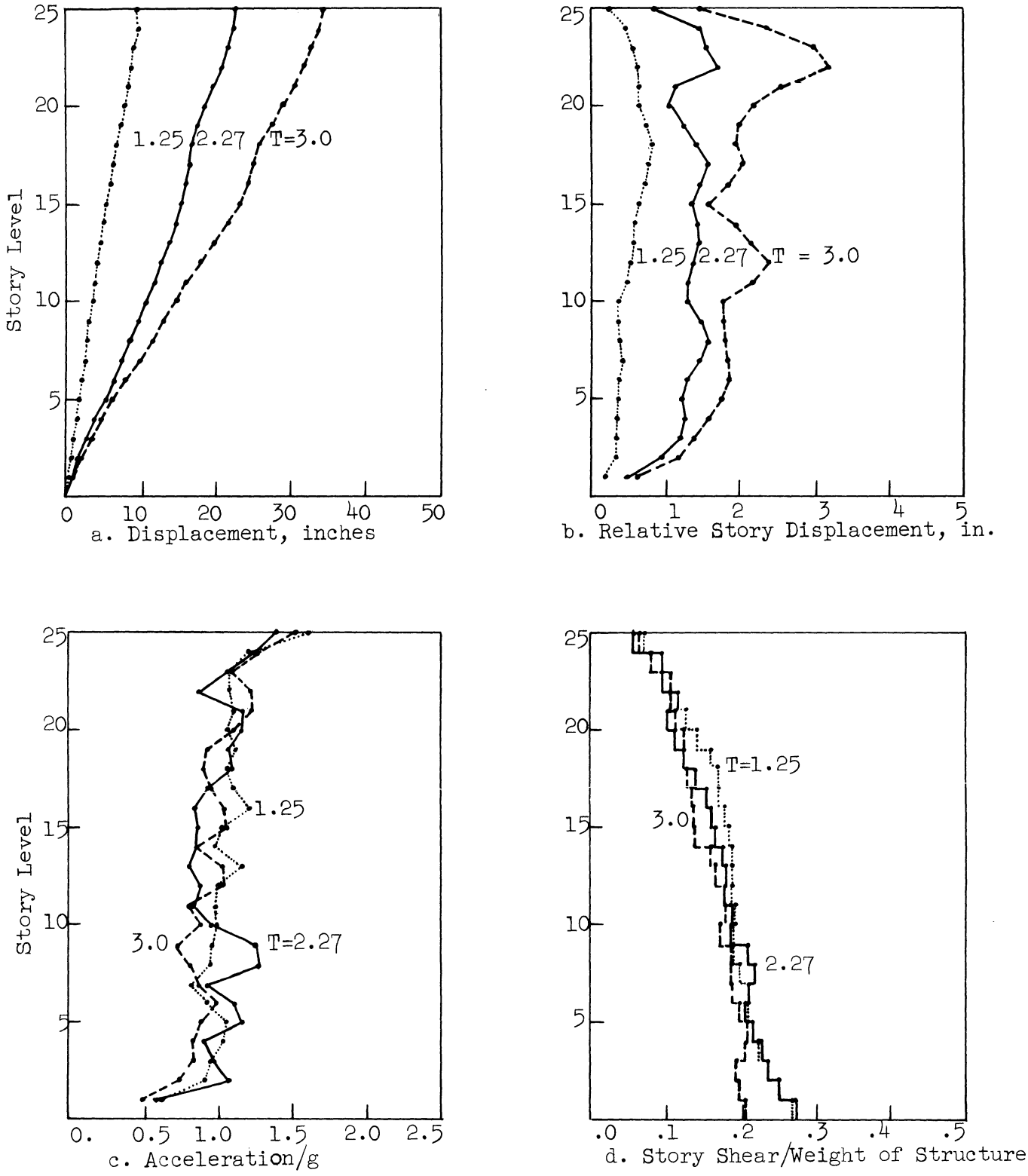

25-Story Ramberg-Osgood Models (r=10); El Centro 1940, N-S x 1.5

Figure 4.13. Effect of fundamental period of structure.

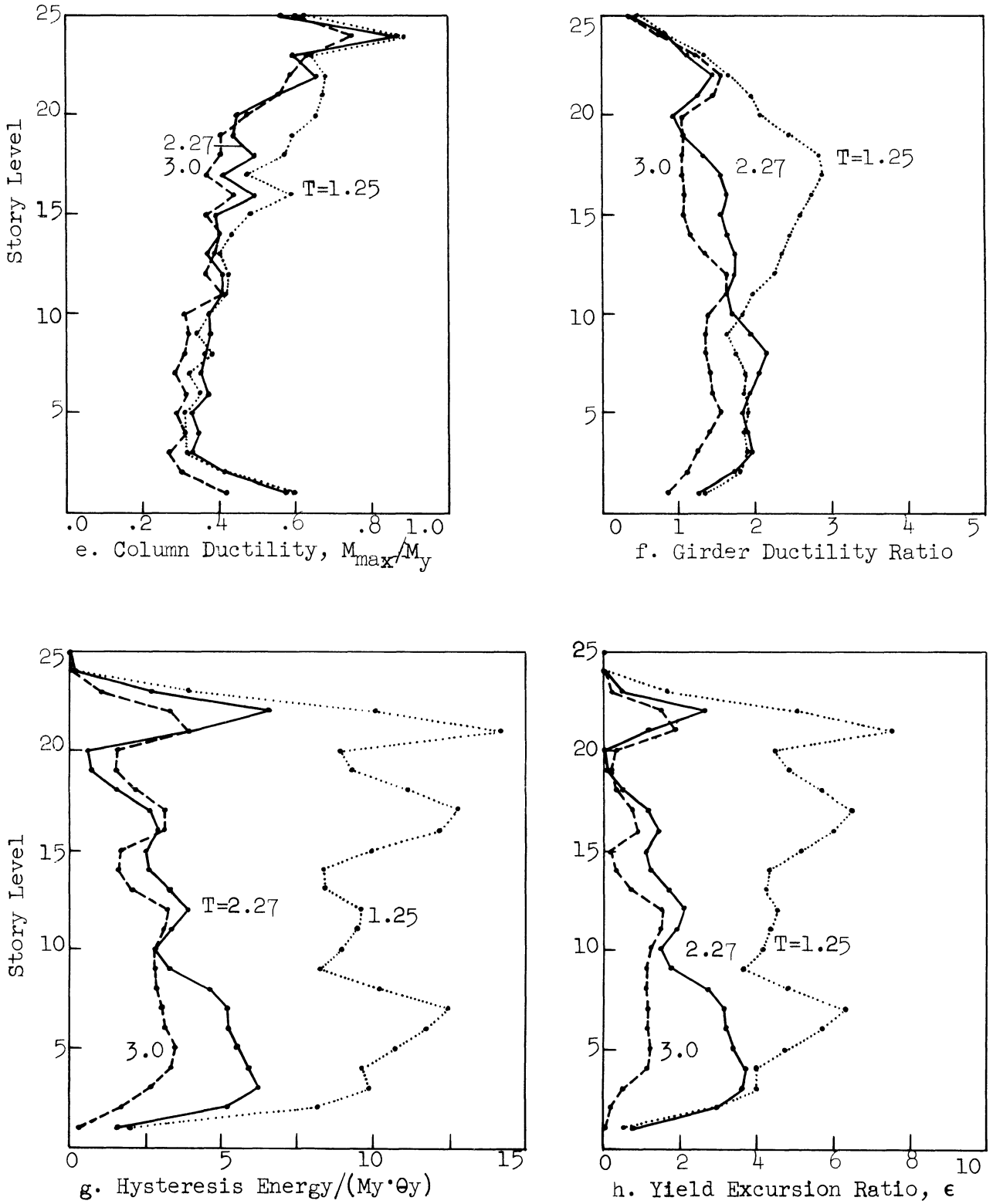

25-Story Ramberg-Osgood Models (r=10); El Centro 1940, N-S x 1.5

Figure 4.13 (Concluded)

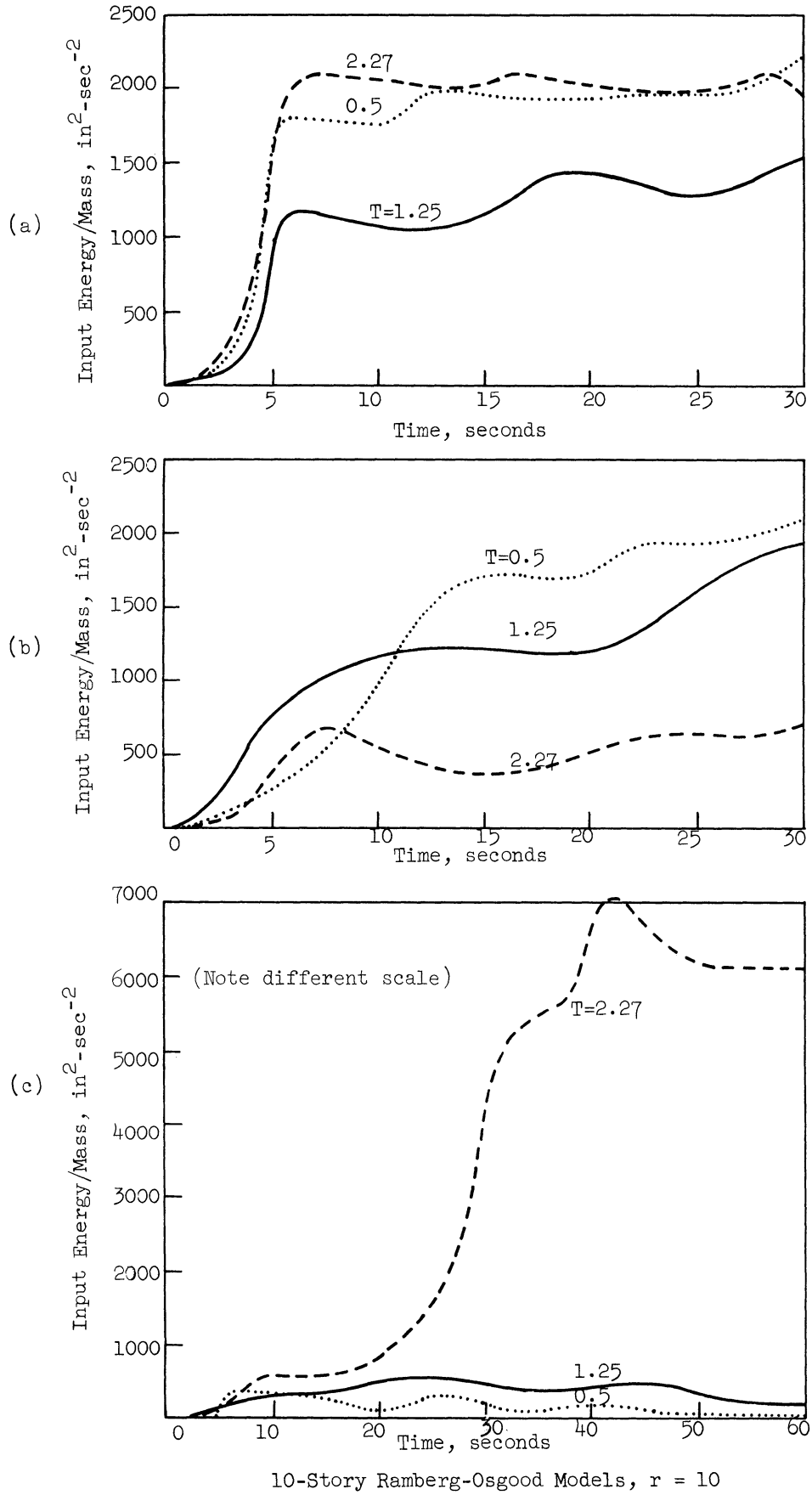

Figure 4.14. Input energy vs. time for the three accelerograms.

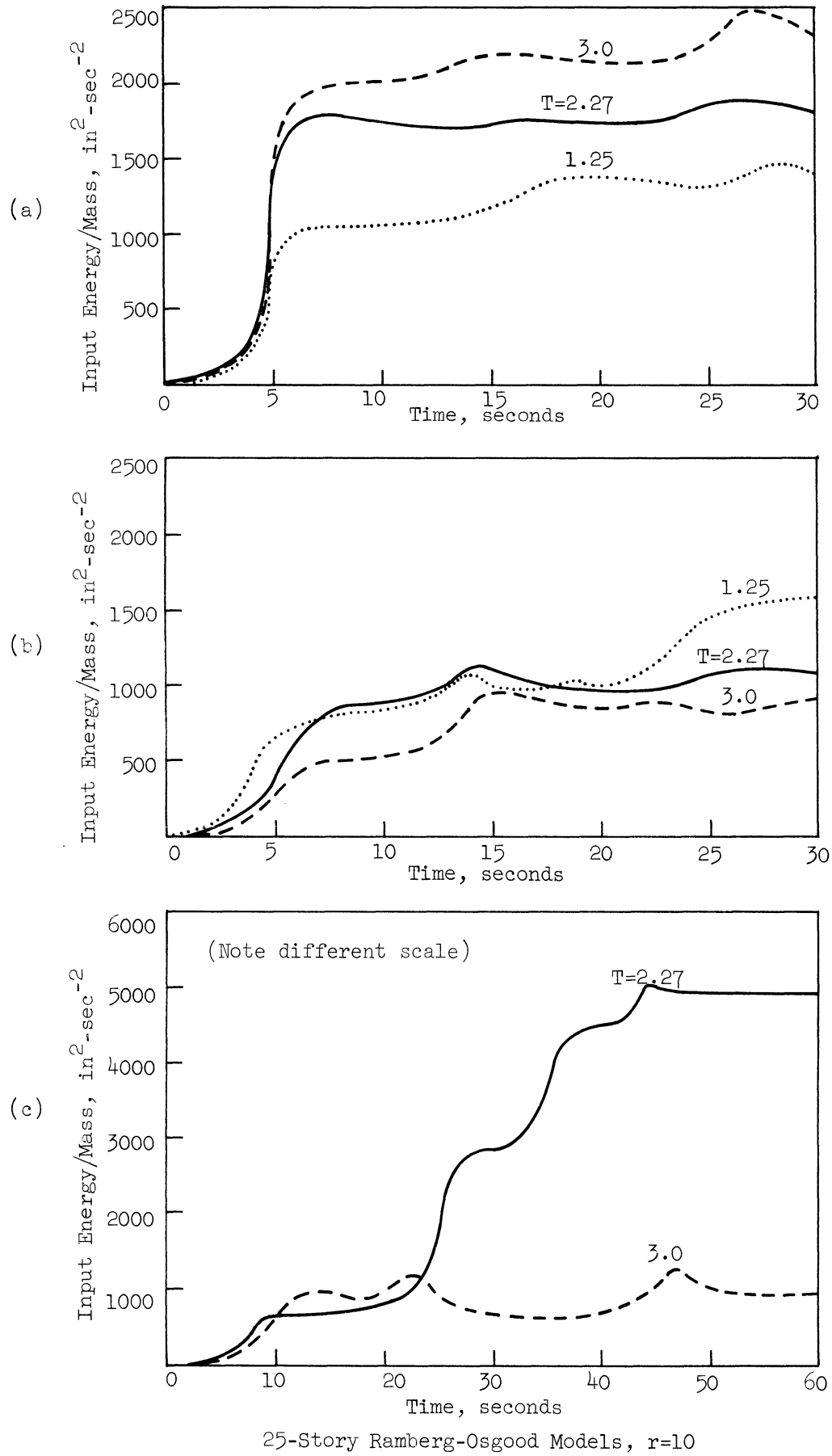

Figure 4.15. Input energy vs. time for the three accelerograms.

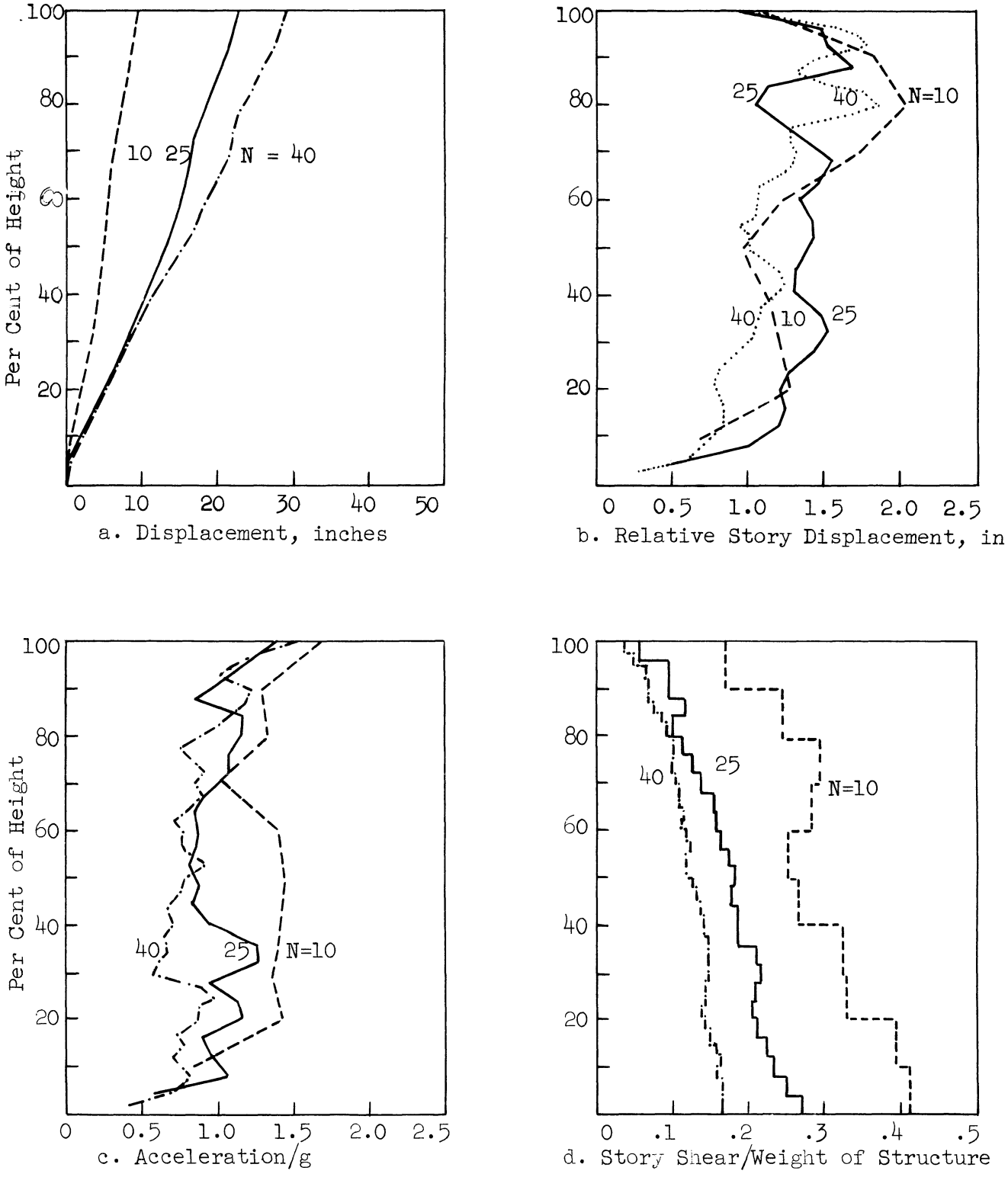

Standard Ramberg-Osgood Models (r=10); El Centro 1940, N-S x 1.5

N	10	25	40
T	1.25	2.27	3.0 sec.

Figure 4.16. Effect of height on the inelastic response.

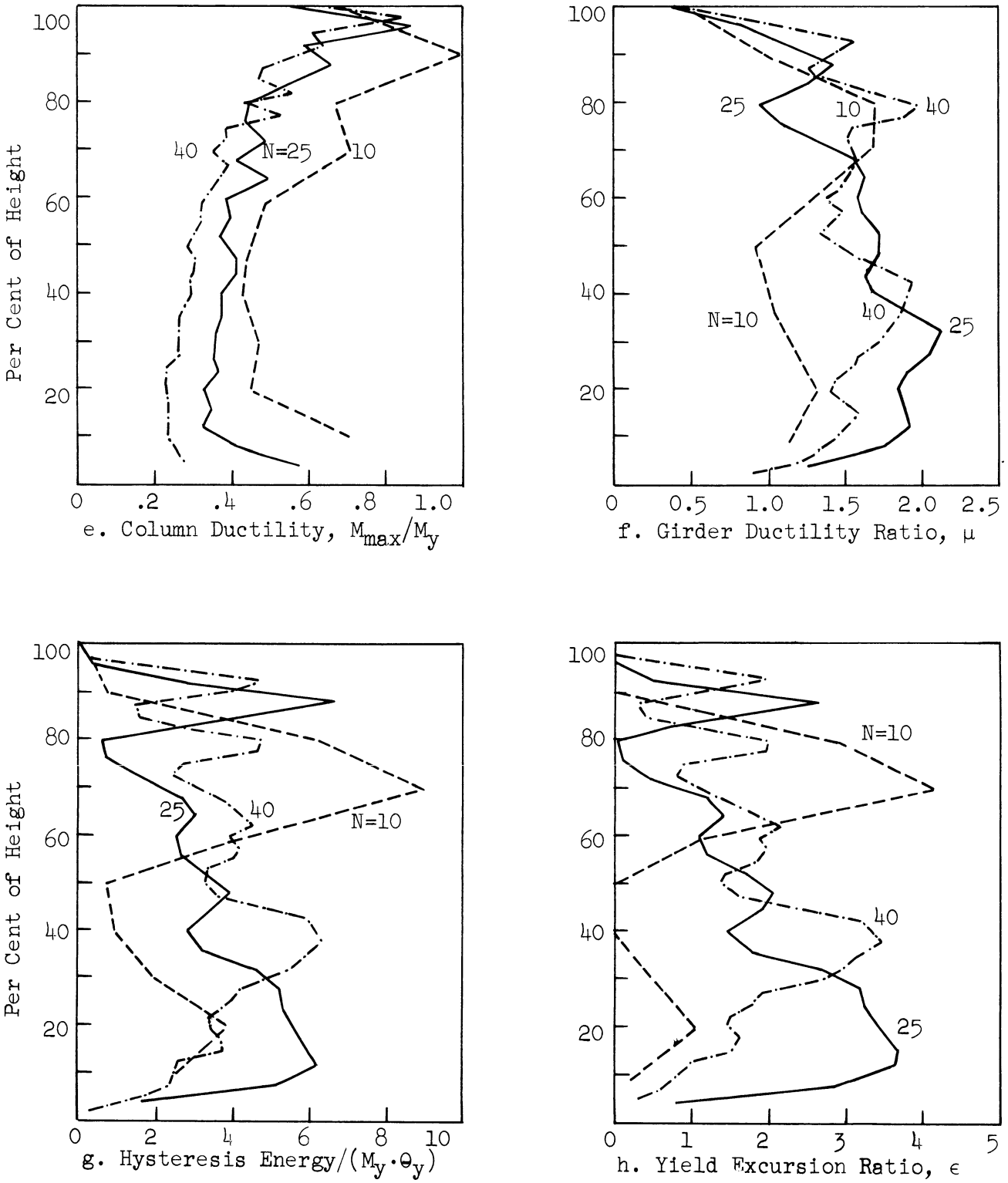

Standard Ramberg-Osgood Models (r = 10); El Centro 1940, N-S x 1.5.

N	10	25	40
T	1.25	2.27	3.0 sec.

Figure 4.16. (Concluded).

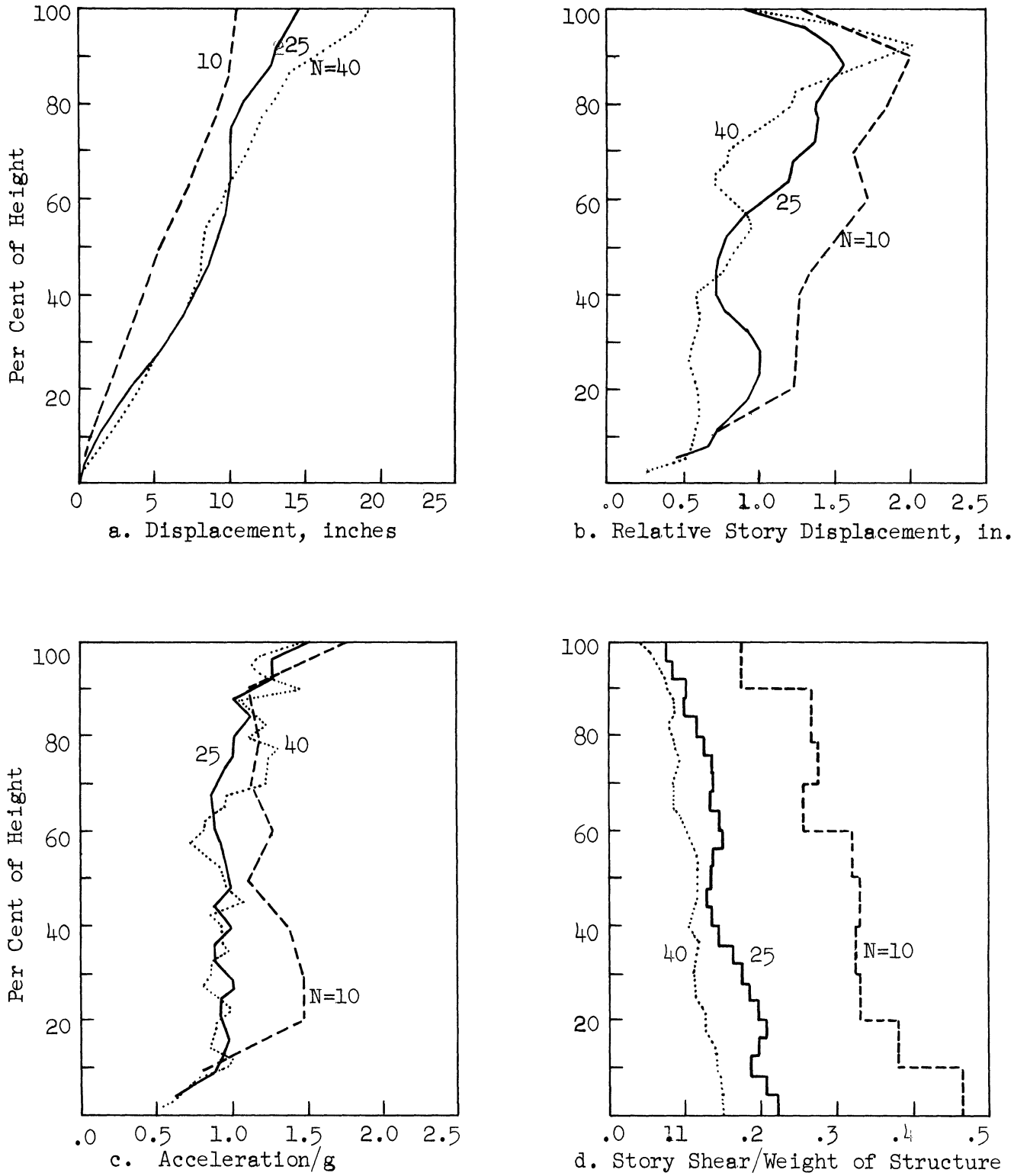

Standard Ramberg-Osgood Models (r=10); Taft 1952, S21°W x 3.0.

N	10	25	40
T	1.25	2.27	3.0 sec.

Figure 4.17. Effect of height on the inelastic response.

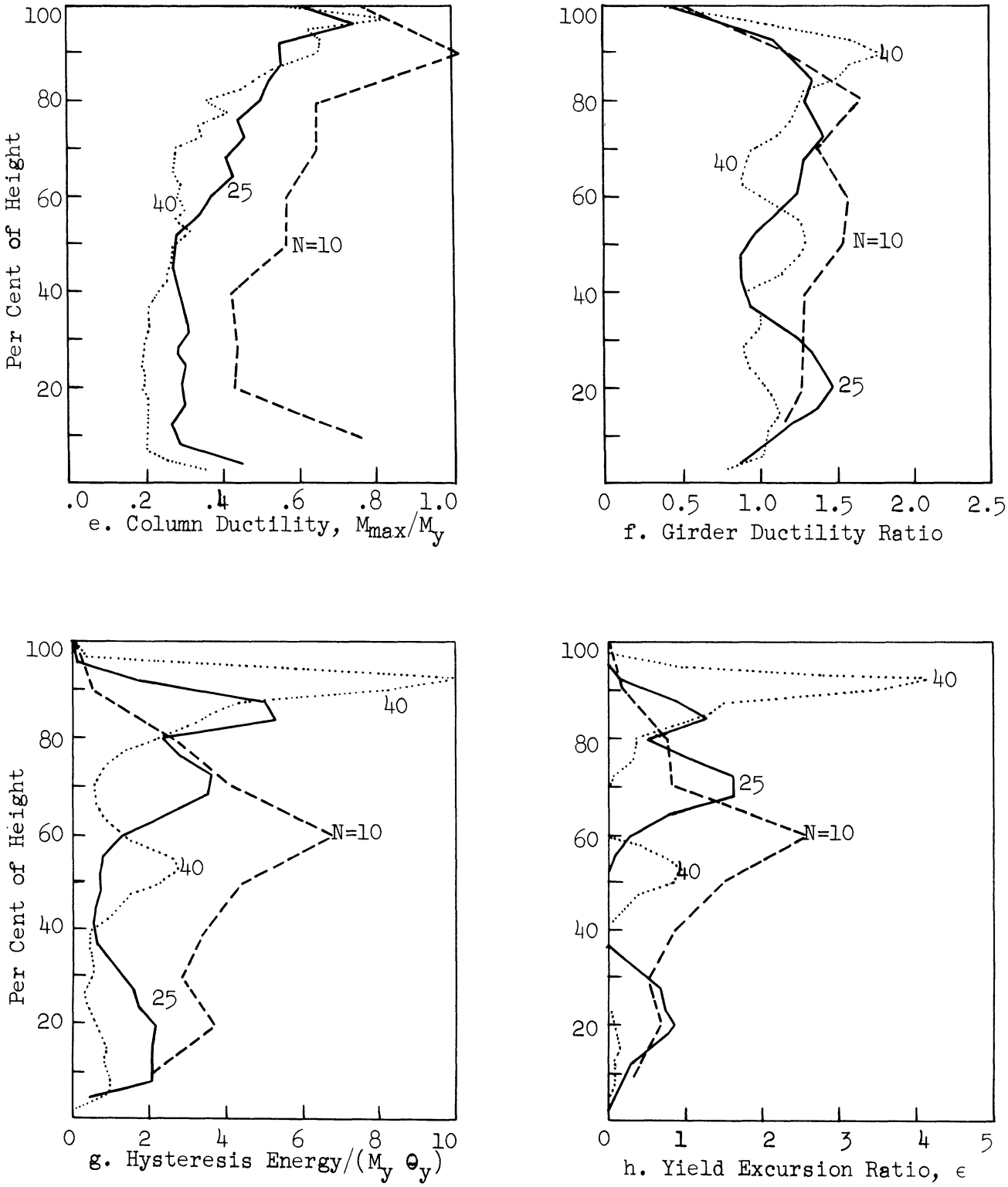

Standard Ramberg-Osgood Models (r=10); Taft 1952, S21°W x 3.0

N	10	25	40
T	1.25	2.27	3.0 sec.

Figure 4.17. (Concluded)

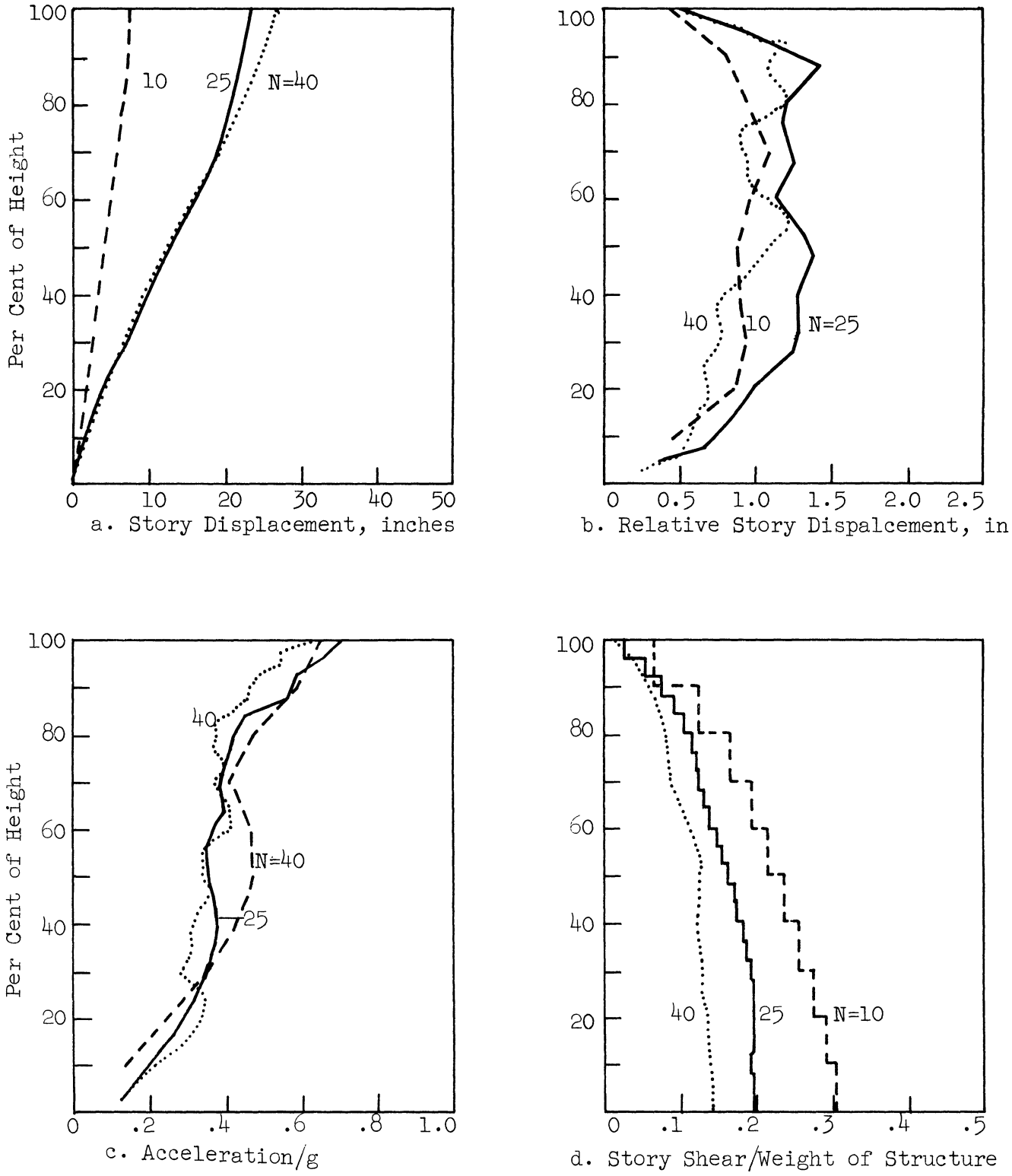

Standard Ramberg-Osgood Models (r=10); Alameda Park 1962, N10°-46'W x 2.4

N	10	25	40
T	1.25	2.27	3.0 sec.

Figure 4.18. Effect of height on the inelastic response.

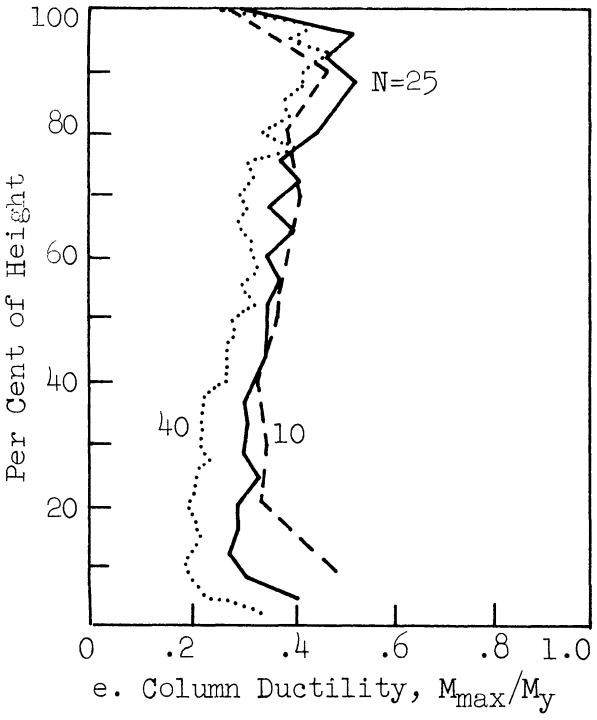

e. Column Ductility, M_{max}/M_y

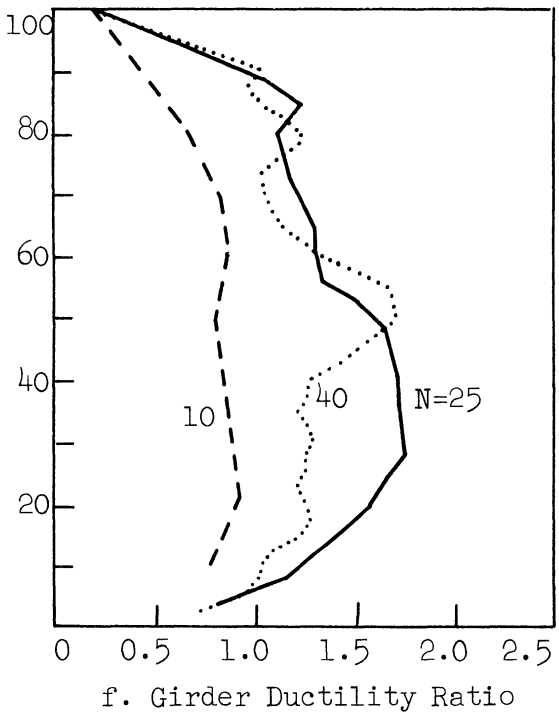

f. Girder Ductility Ratio

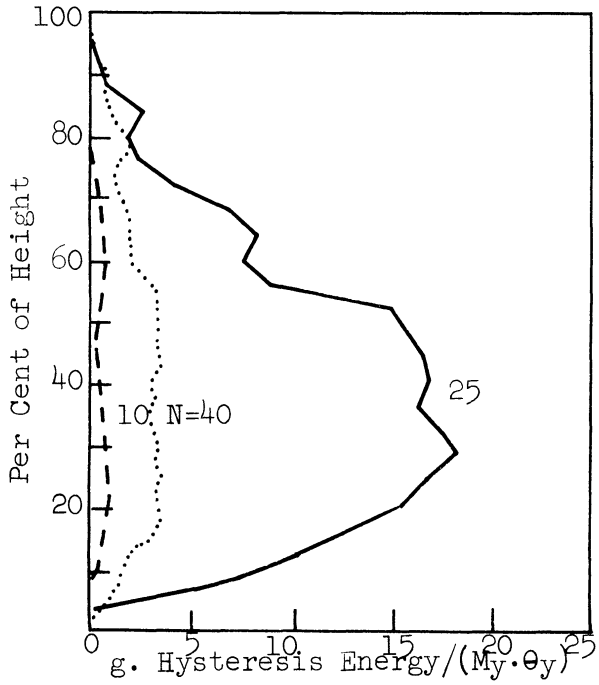

g. Hysteresis Energy/($M_y \cdot \theta_y$)

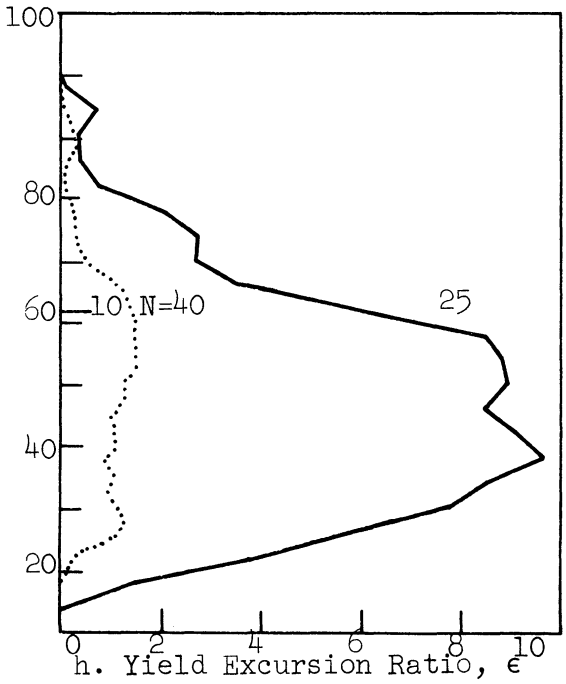

h. Yield Excursion Ratio, ϵ

Standard Ramberg-Osgood Models (r=10); Alameda Park 1962, N10°-46'W x 2.4

N	10	25	40
T	1.25	2.27	3.0 sec.

Figure 4.18. (Concluded).

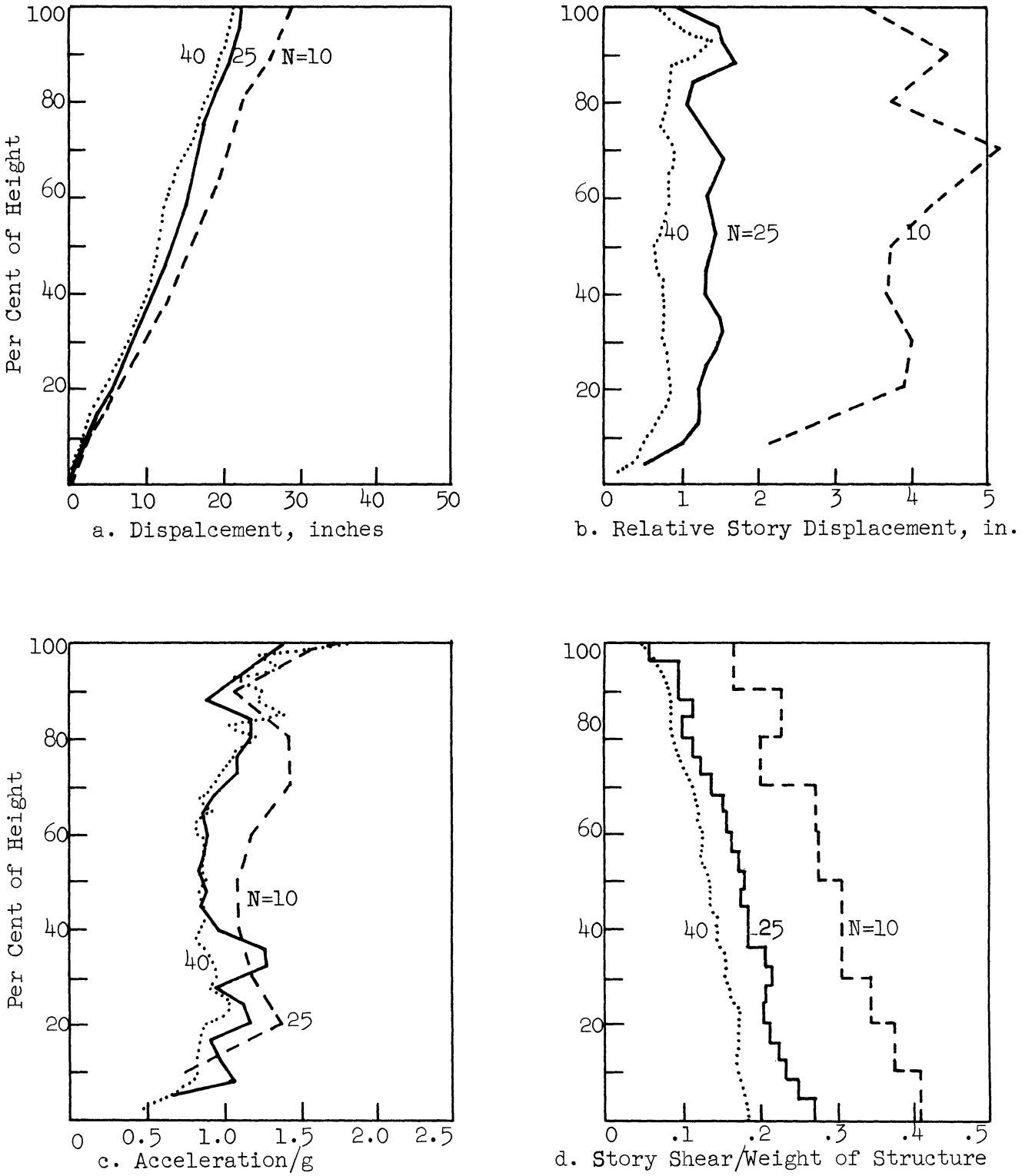

Ramberg-Osgood Models (r=10); T = 2.27 Seconds; El Centro 1940, N-S x 1.5

Figure 4.19. Effect of height on the inelastic response.

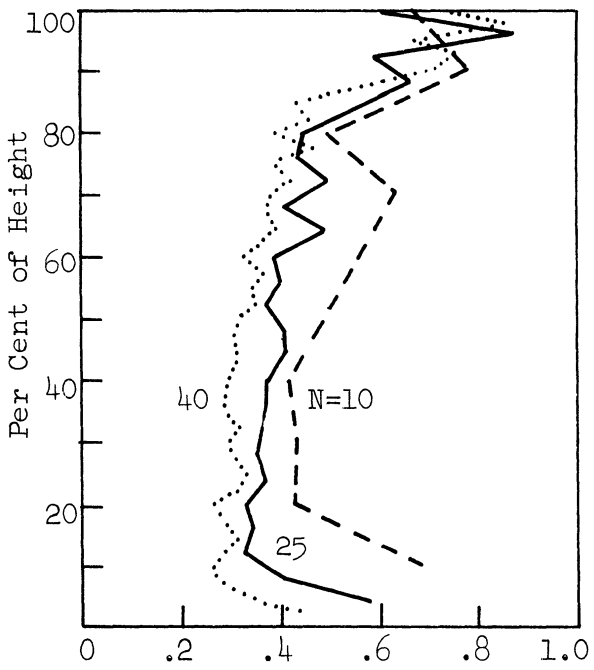

e. Column Ductility, M_{max}/M_y

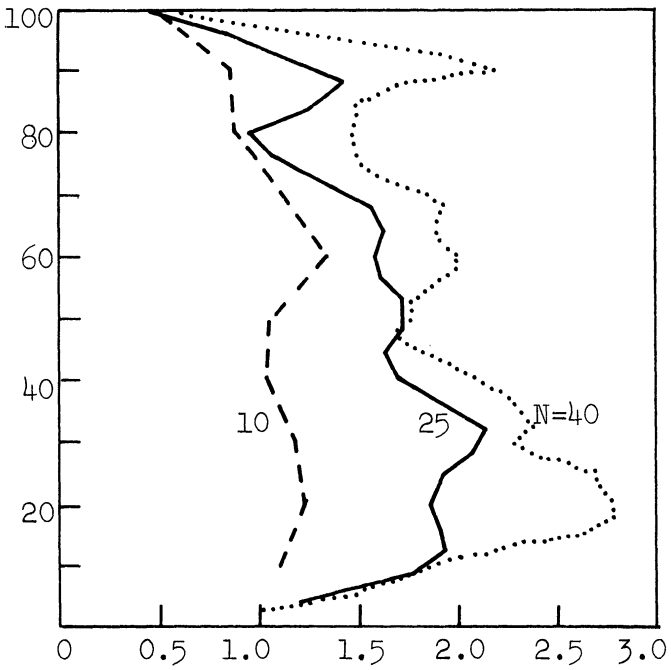

f. Girder Ductility Ratio

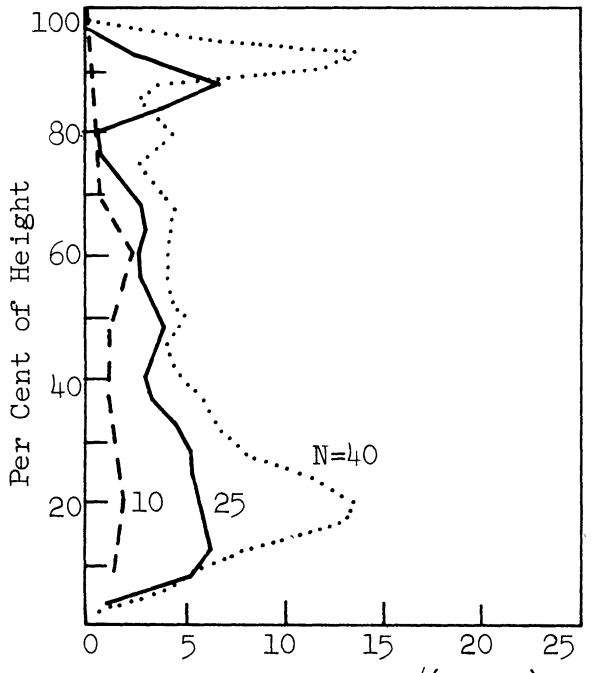

g. Hysteresis Energy/$(M_y \cdot \Theta_y)$

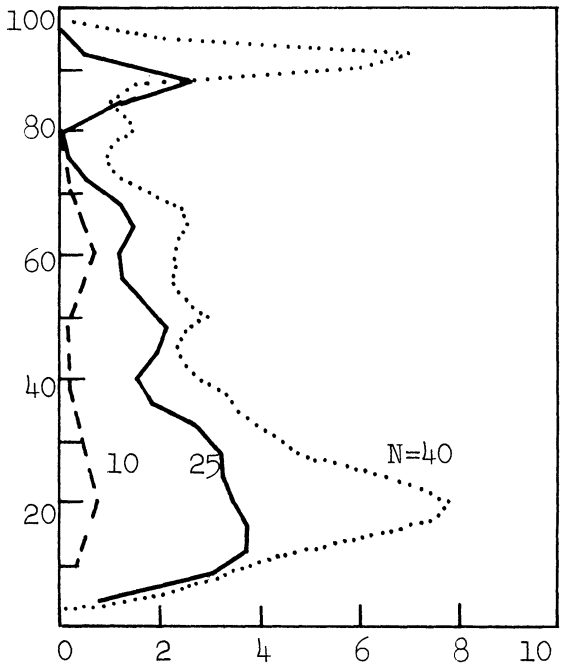

h. Yield Excursion Ratio, ϵ

Ramberg-Osgood Models (r=10); T=2.27 Seconds; El Centro 1940, N-S x 1.5

Figure 4.19. (Concluded)

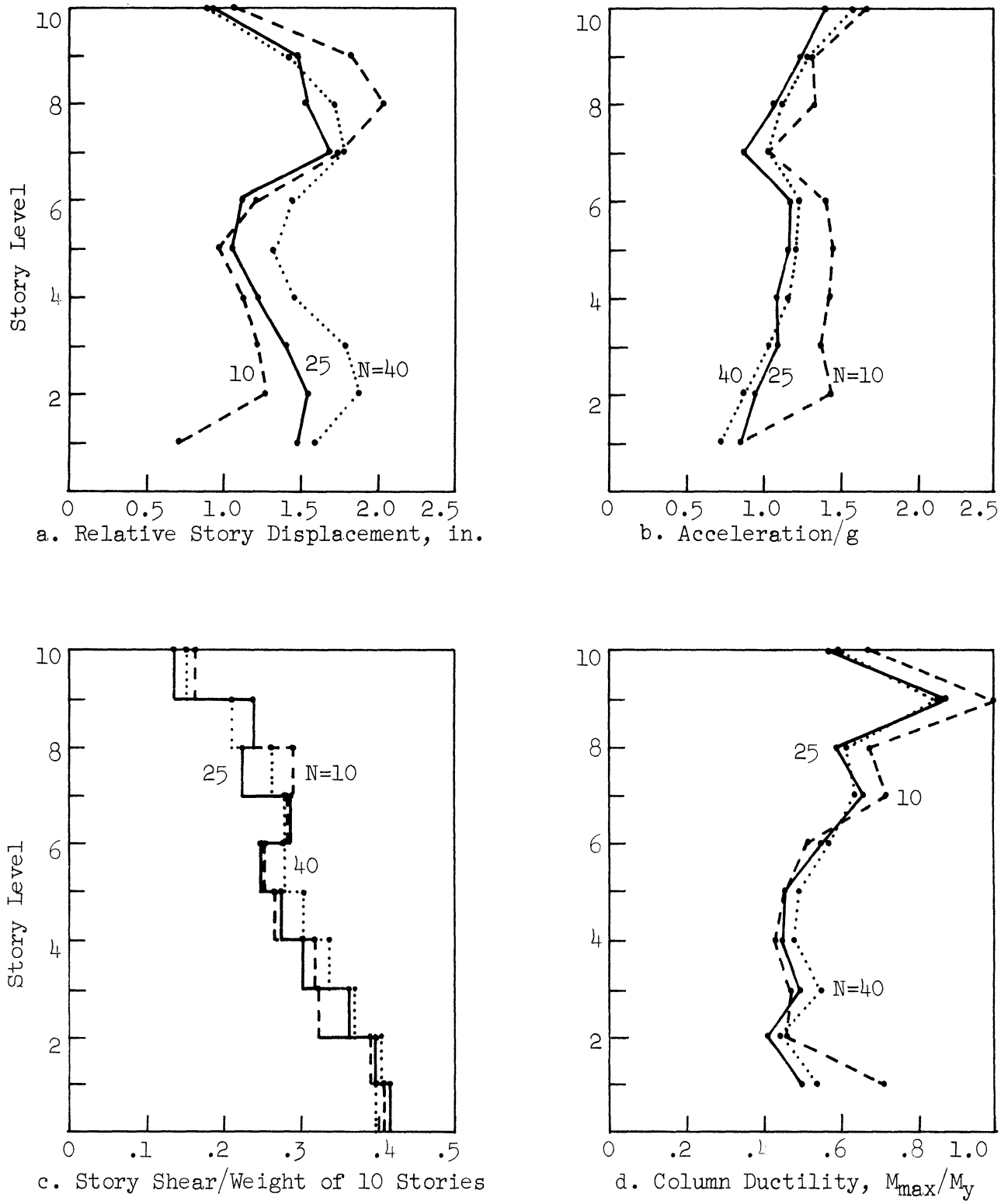

Standard Ramberg-Osgood Models (r=10); El Centro 1940, N-S x 1.5.

N	10	25	40
T	1.25	2.27	3.0 sec.

Figure 4.20. Response of top 10 stories.

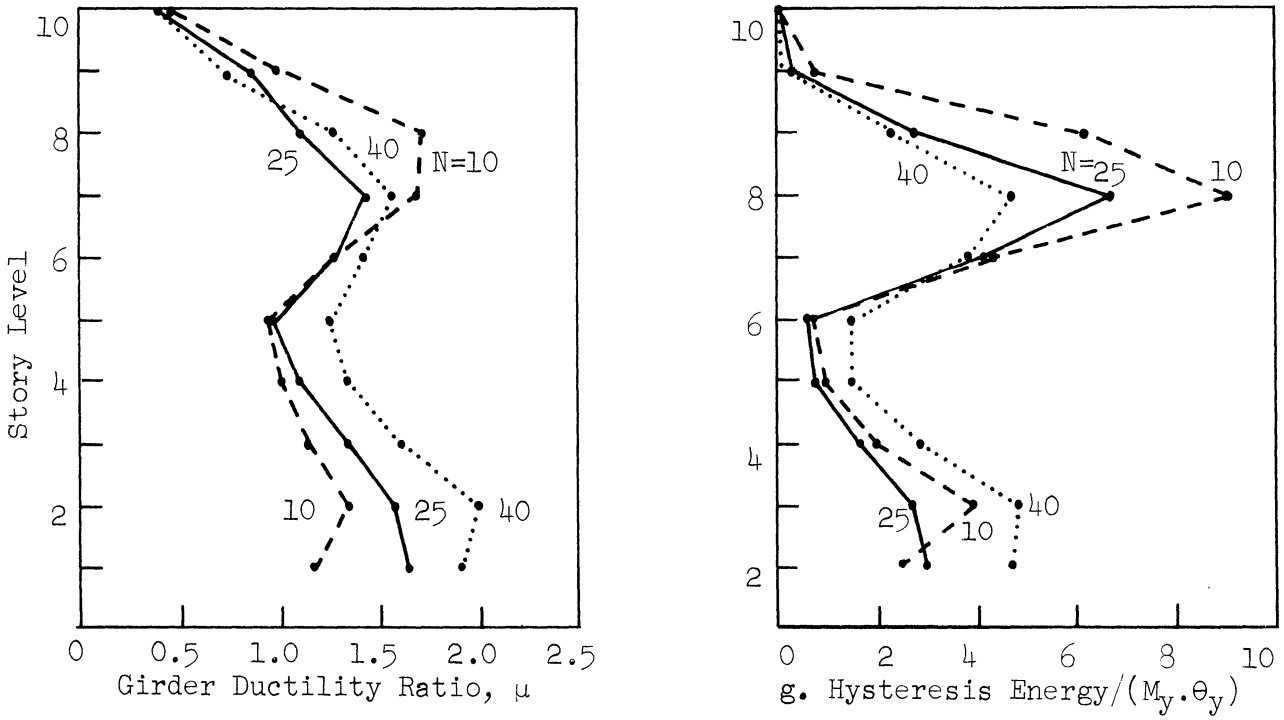

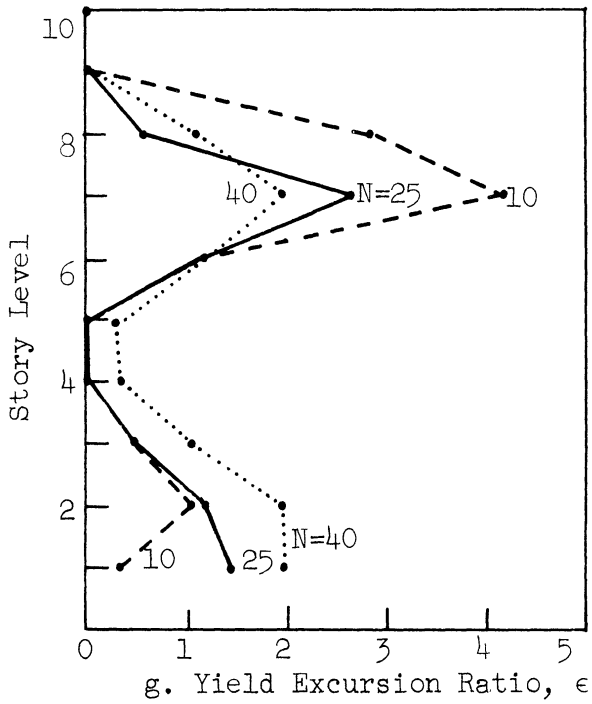

Standard Ramberg-Osgood Models (r=10); El Centro 1940, N-S x 1.5

N	10	25	40
T	1.25	2.27	3.0 sec.

Figure 4.20. (Concluded)

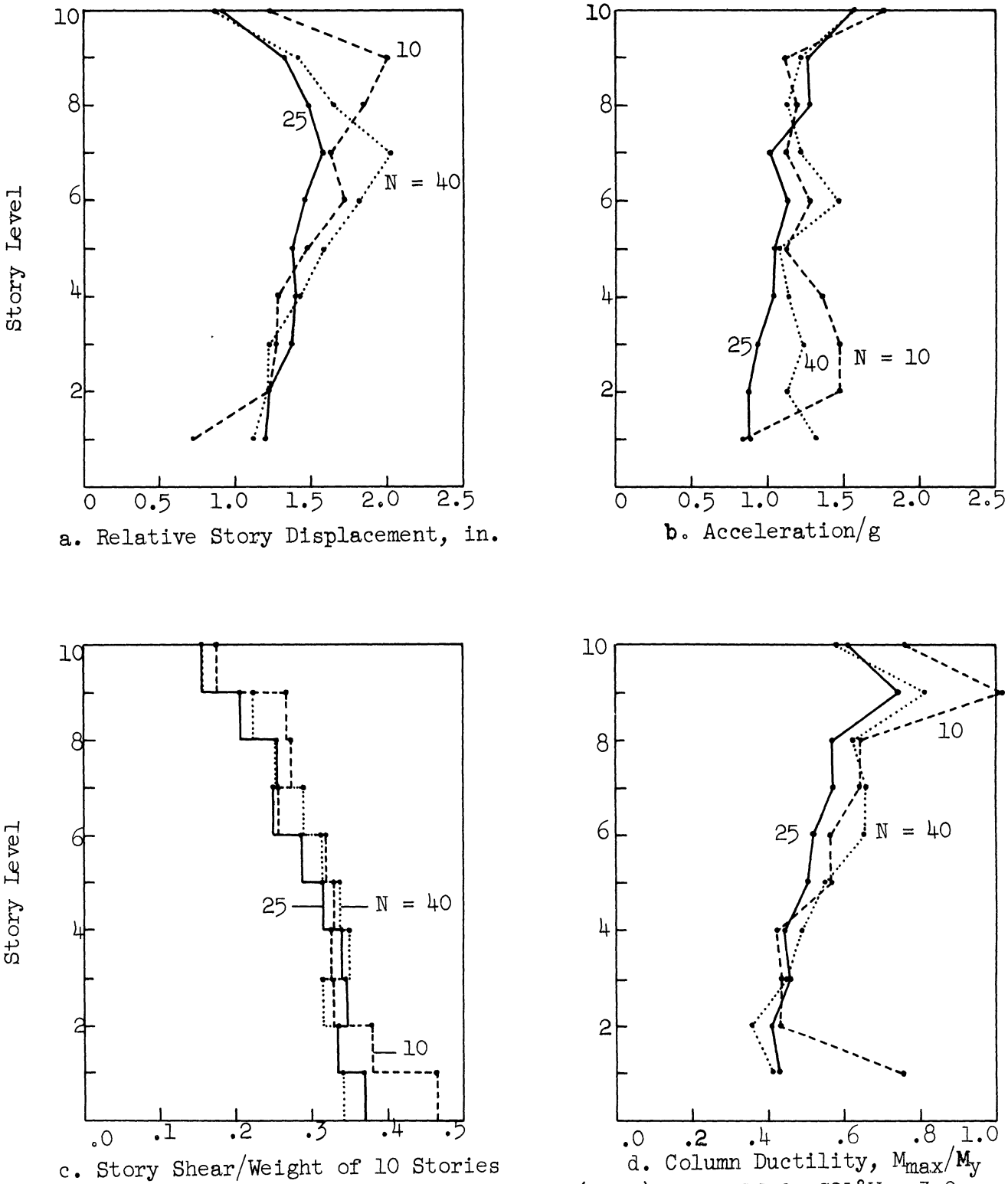

Standard Ramberg-Osgood Models (r=10); Taft 1952, S21°W x 3.0

N	10	25	40
T	1.25	2.27	3.0 sec.

Figure 4.21. Response of top 10 stories.

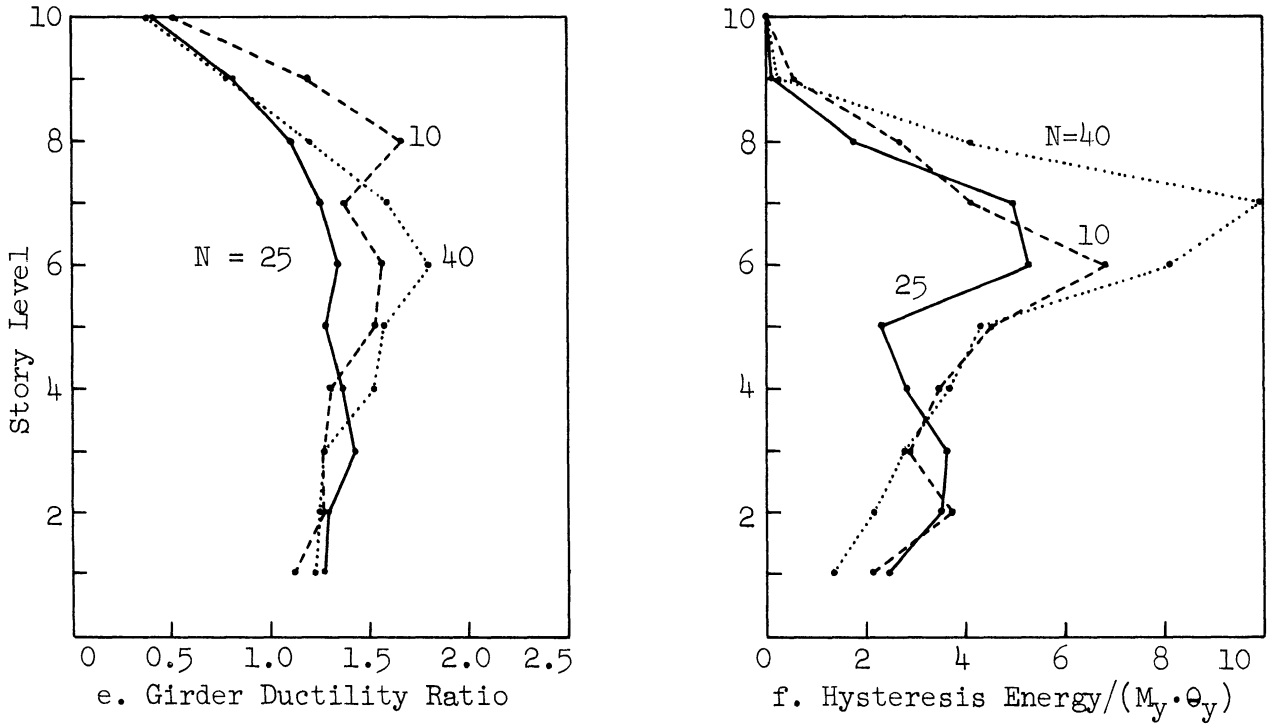

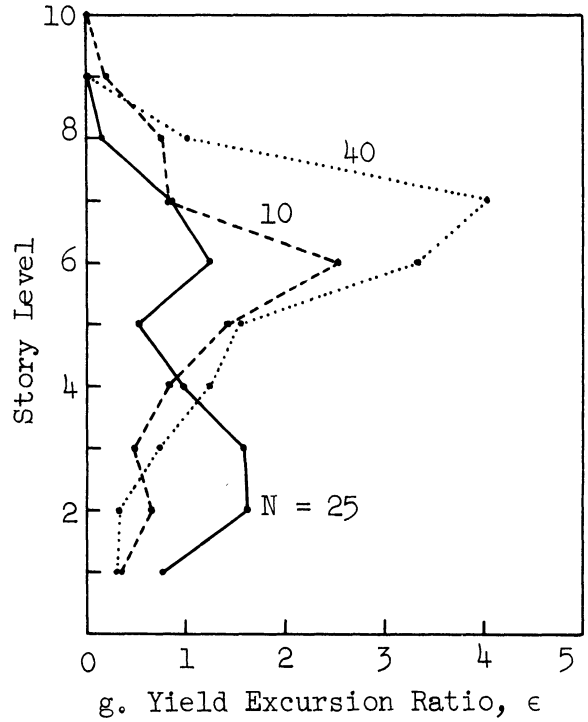

Standard Ramberg-Osgood Models (r=10); Taft 1952, S21°W x 3.0

N	10	25	40
T	1.25	2.27	3.0 sec.

Figure 4.21. (Concluded)

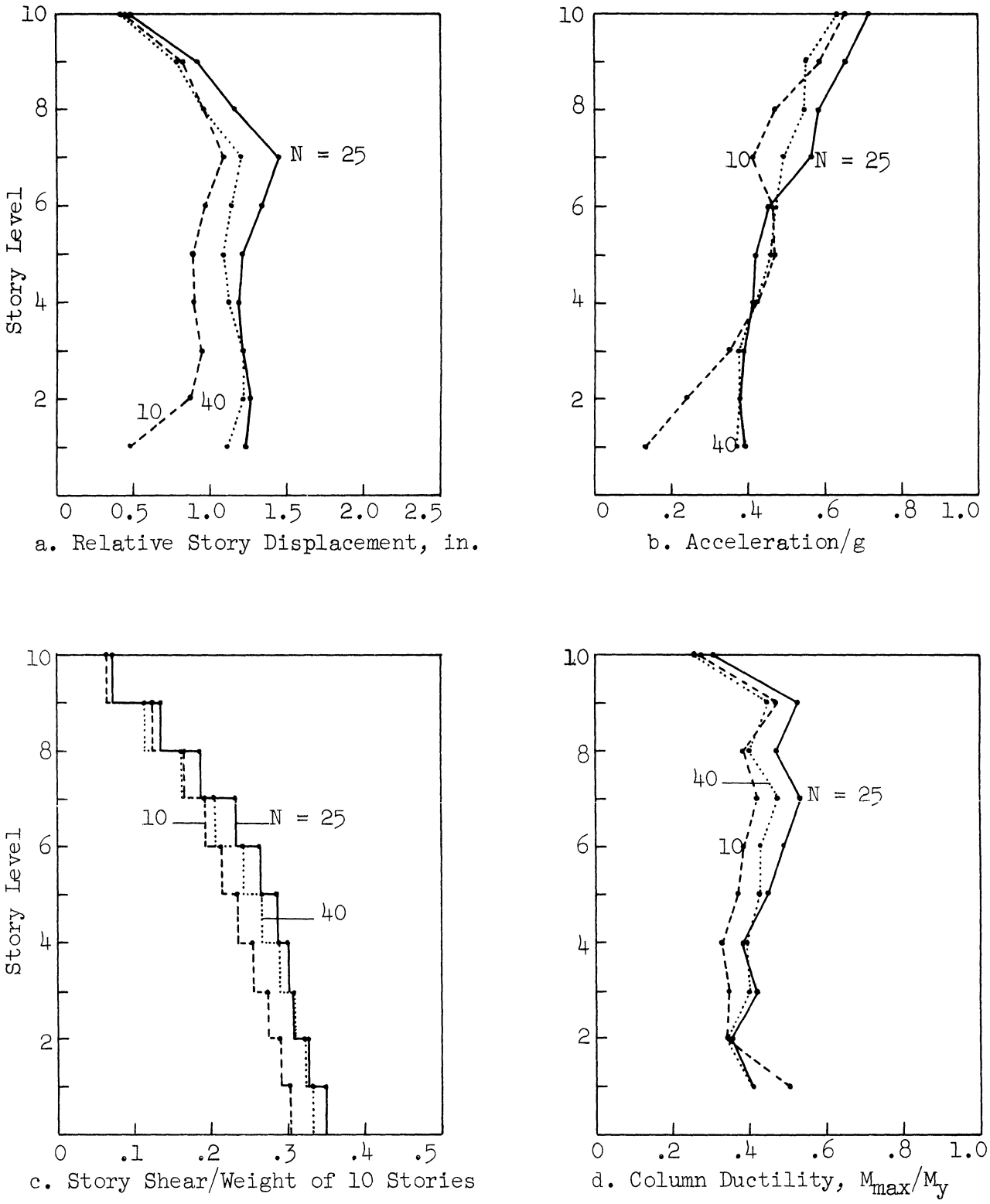

Standard Ramberg-Osgood Models (r=10); Alameda Park 1962, N10°-46'W x 2.4

N	10	25	40
T	1.25	2.27	3.0 sec

Figure 4.22. Response of top 10 stories.

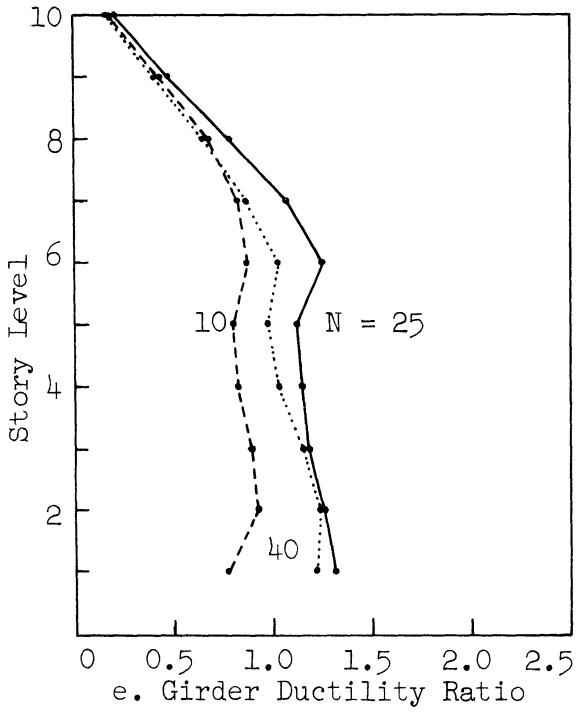

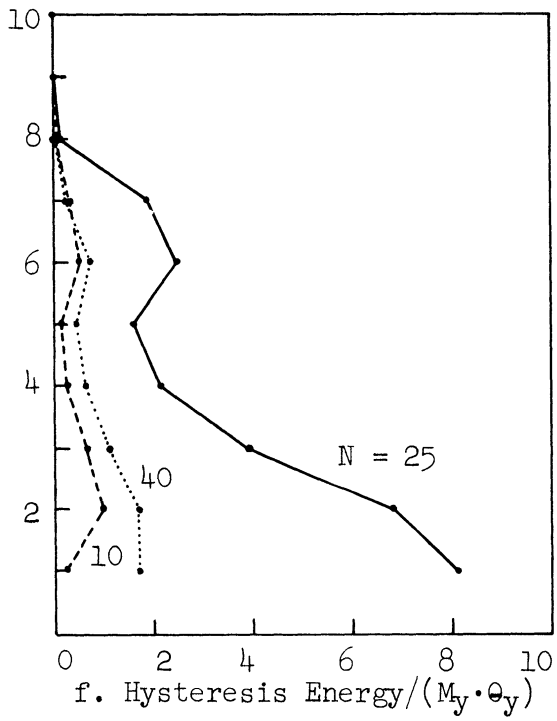

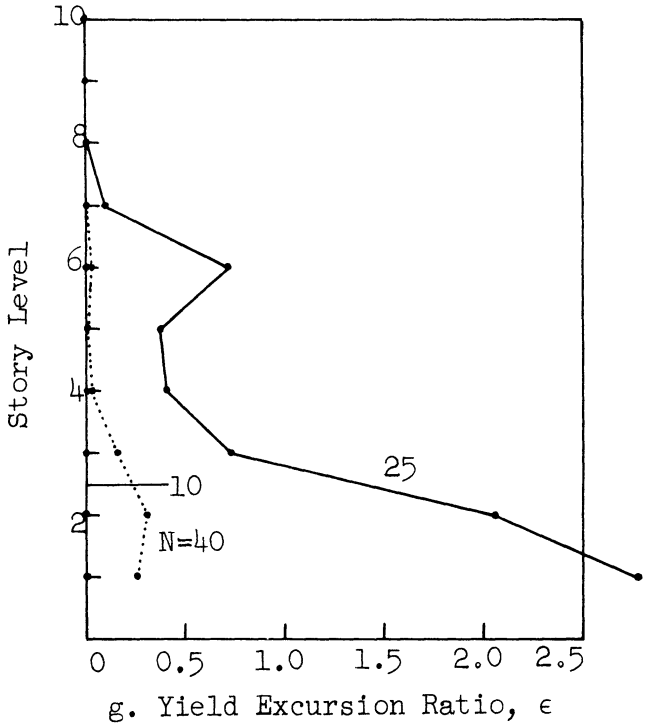

Standard Ramberg-Osgood Models (r=10); Alameda Park 1962, N10°-46'W x 2.4

N	10	25	40
T	1.25	2.27	3.0 sec

Figure 4.22. (Concluded)

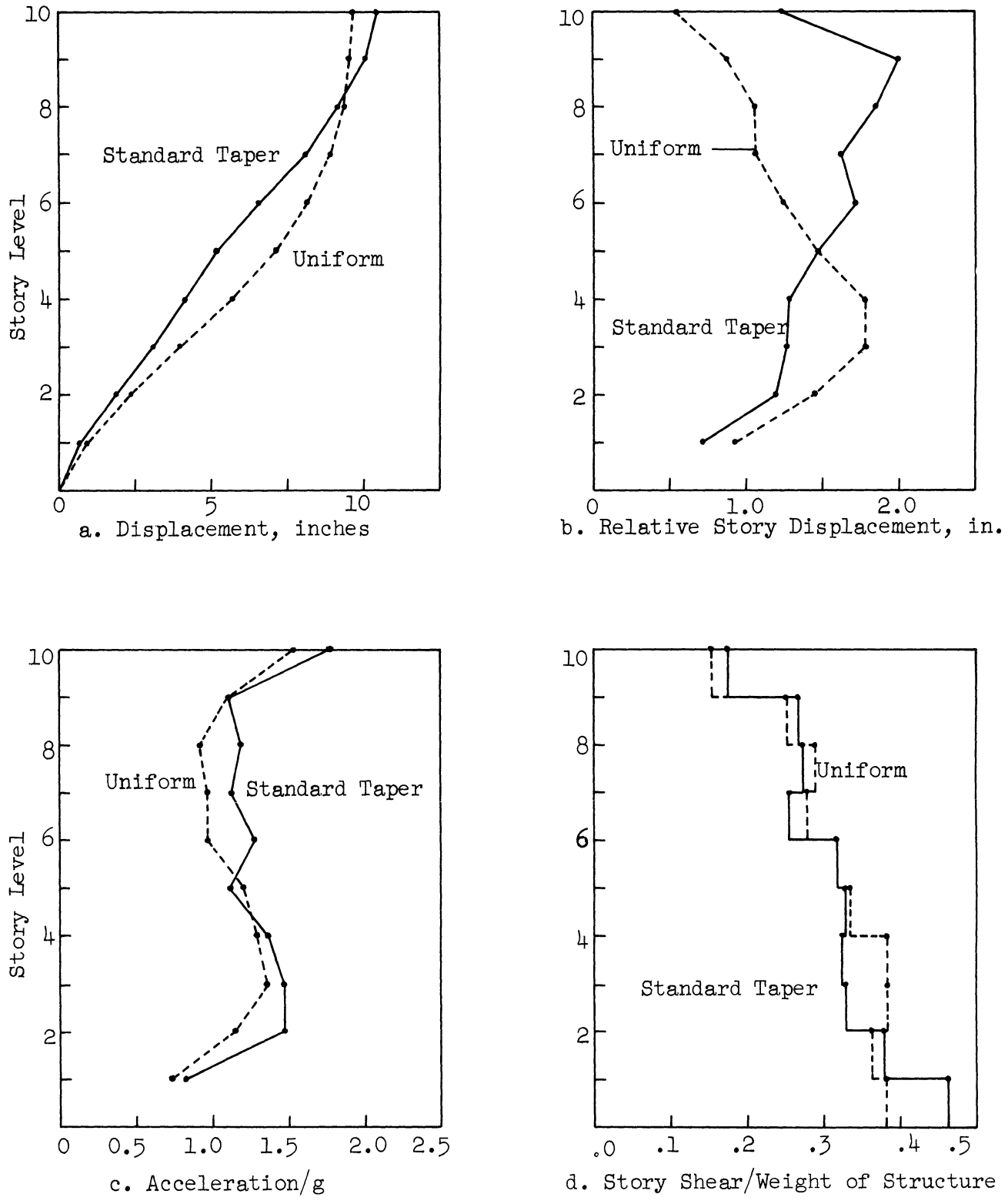

10-Story Ramberg-Osgood Models (r=10); Taft 1952, S21°W x 3.0

Figure 4.23. Effect of stiffness-strength taper.

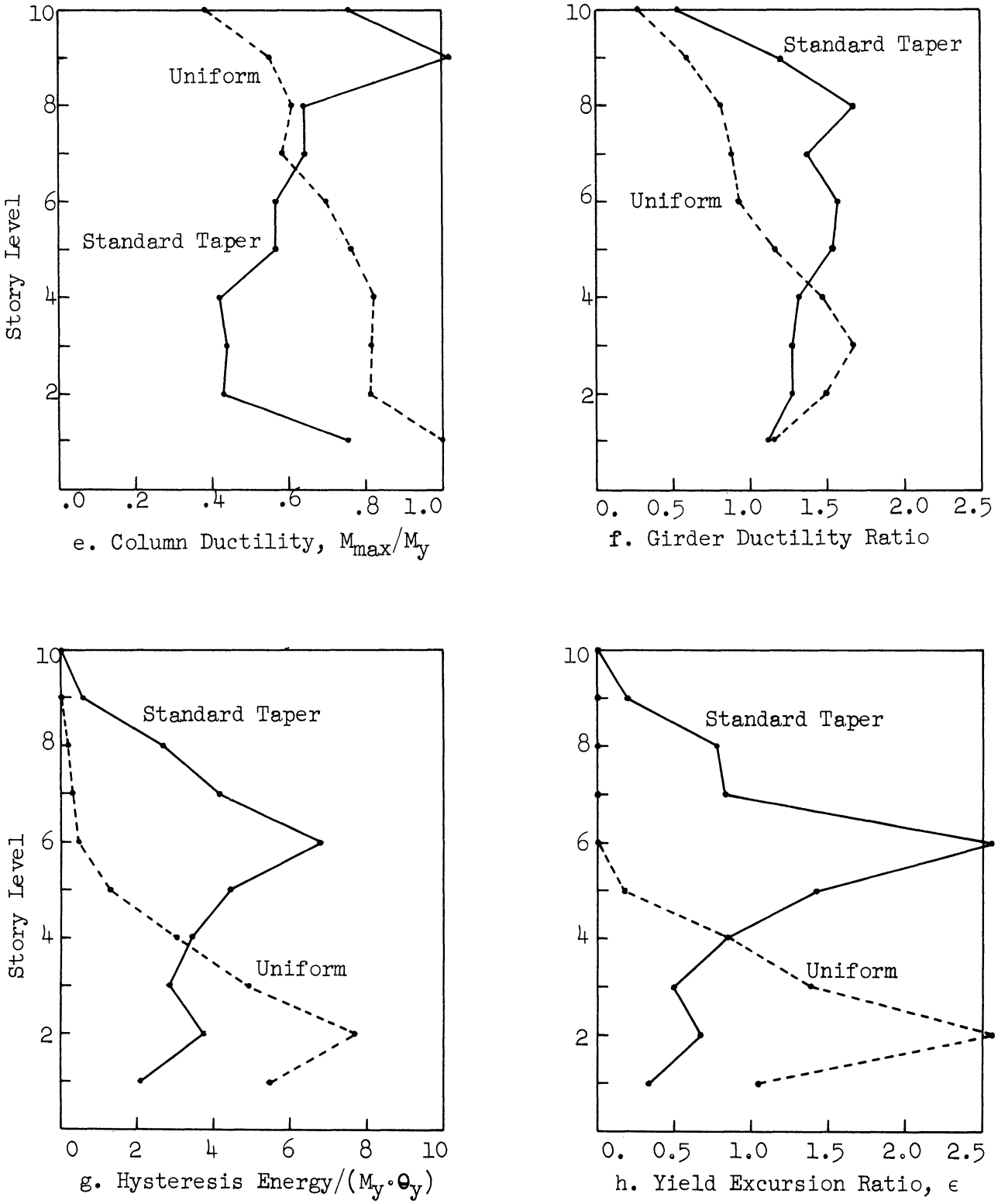

10-Story Ramberg-Osgood Models (r=10); Taft 1952, S21°W x 3.0

Figure 4.23. (Continued)

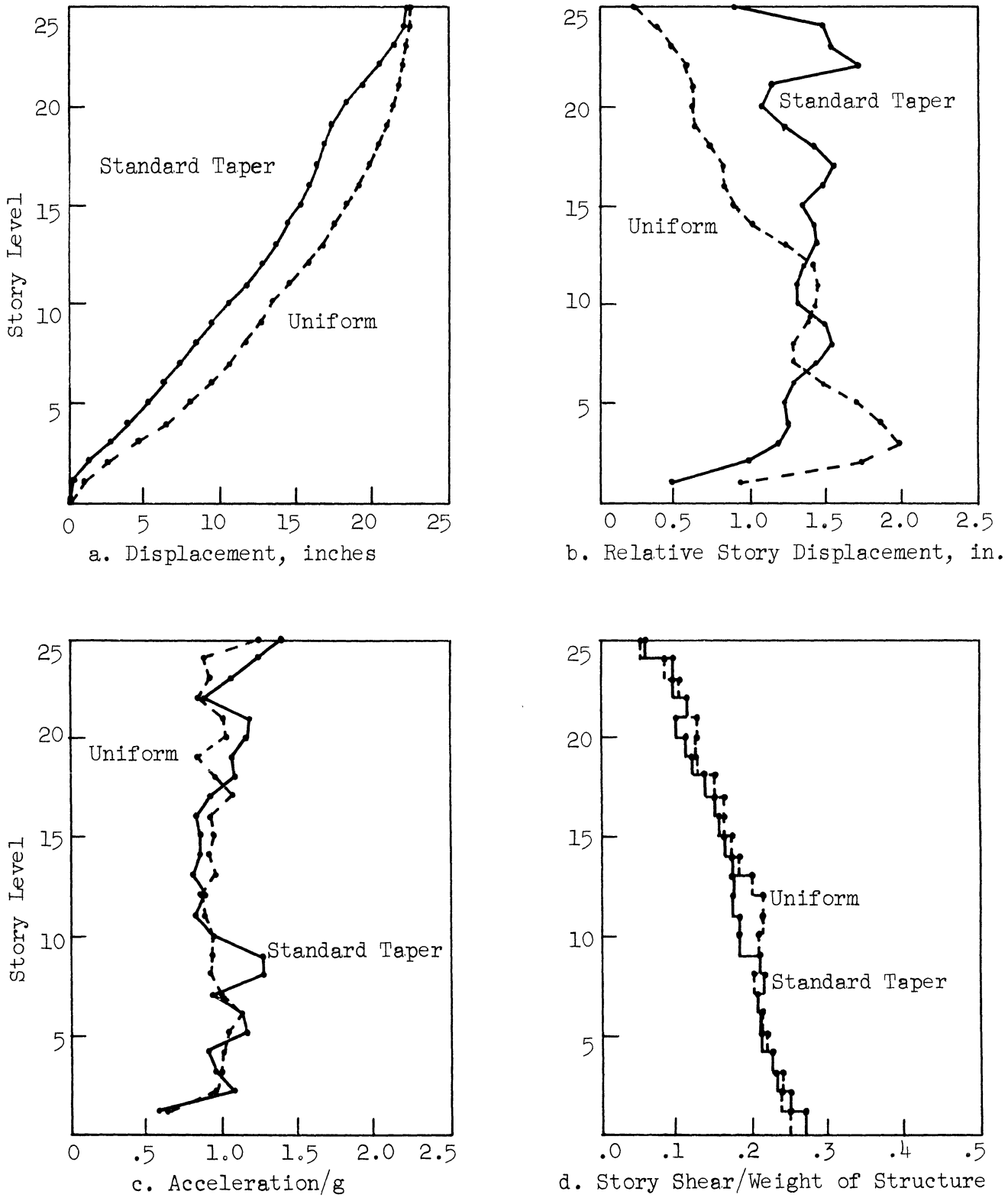

25-Story Ramberg-Osgood Models (r=10); El Centro 1940, N-S x 1.5

Figure 4.24. Effect of stiffness-strength taper.

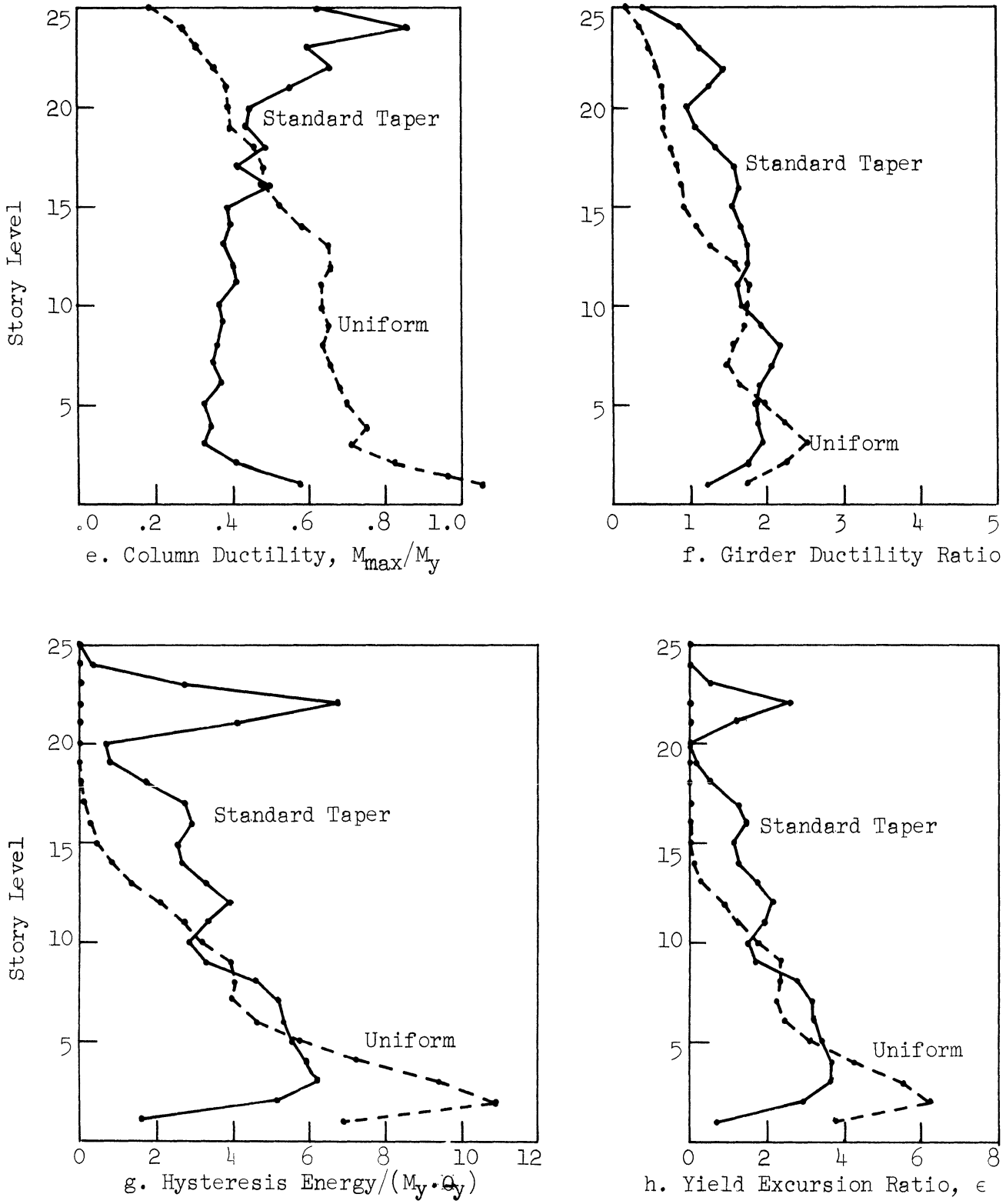

25-Story Ramberg-Osgood Models (r=10); El Centro 1940, N-S x 1.5

Figure 4.24. (Concluded)

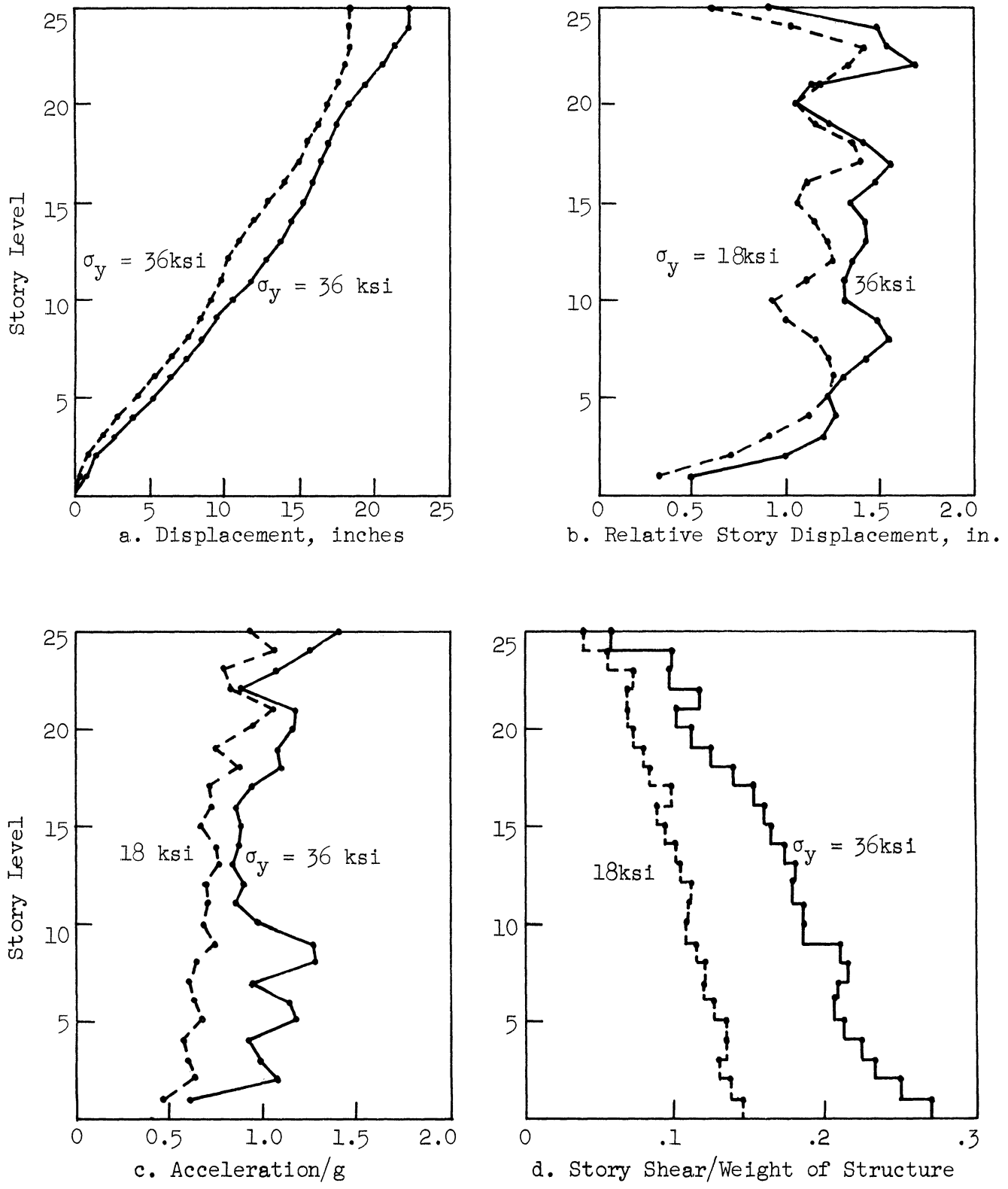

25-Story Ramberg-Osgood Models (r=10); T=2.27 Seconds; El Centro 1940, N-S x 1.5

Figure 4.25. Effect of strength on the inelastic response.

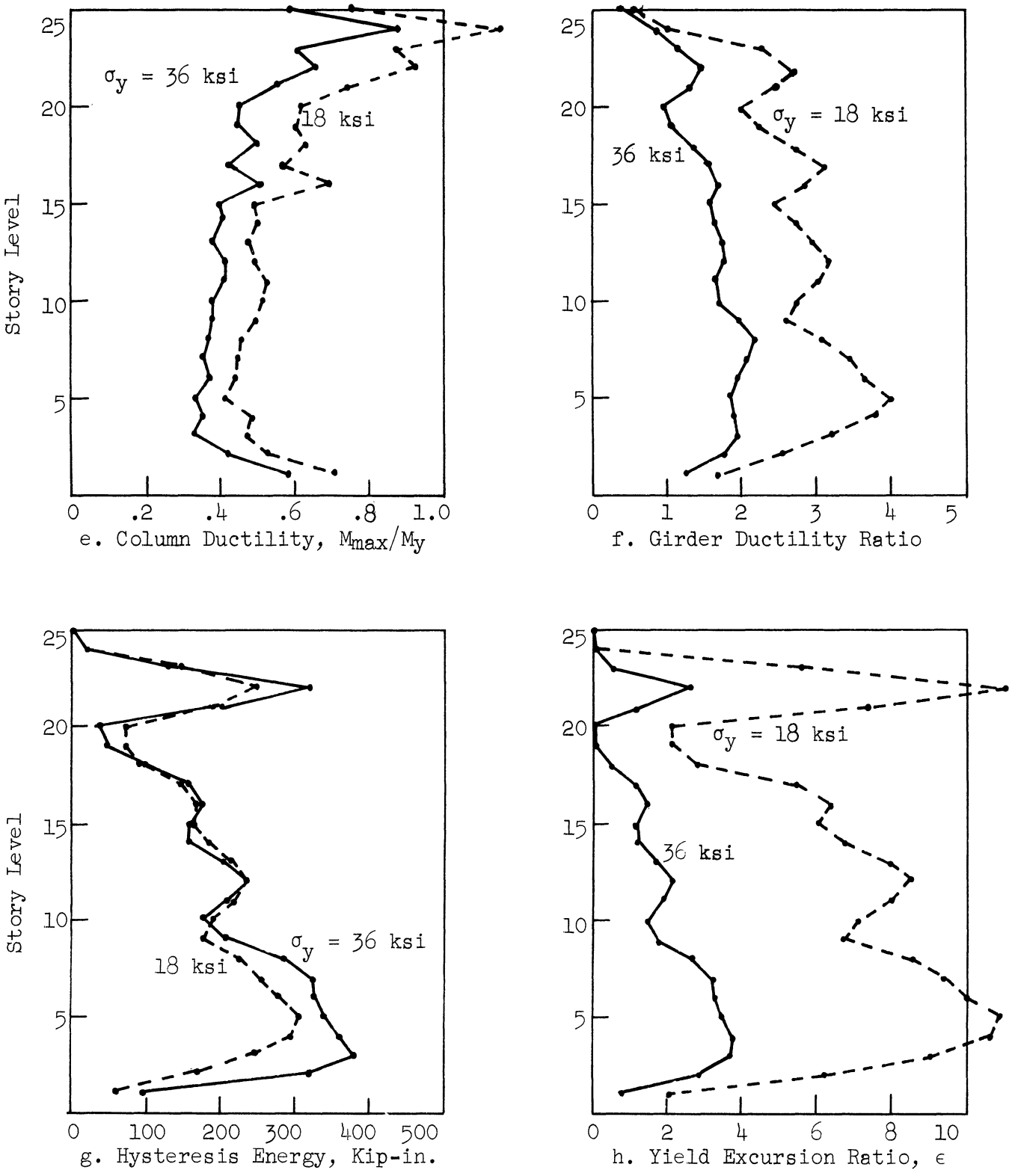

25-Story Ramberg-Osgood Models (r=10); T=2.27 Seconds; El Centro 1940, N-S x 1.5

Figure 4.25. (Continued)

CHAPTER 5

SOME ADDITIONAL CONSIDERATIONS

5.1 General

The program of investigation, as described in the foregoing chapters, was designed to lead to a better understanding of the inelastic behavior of multistory building frames, and to explore the significance of energy dissipation through ductile deformation of the girders. The schedule of analyses was also intended to evaluate the influence of other significant structural properties and characteristics of earthquake motion upon the resulting inelastic response. Damping and secondary effects such as the P-Δ effect and the effect of shear and axial strains in the frame members, were not included in the analysis in order to maintain simplicity of the procedure and convenience in interpreting results. It is the purpose of this chapter to describe the additional research which was undertaken to estimate the nature and order of magnitude of the influence of some of these factors.

The overturning effect of gravity loads acting through the sidesway displacements (commonly called the P-Δ effect) and the effect of axial deformation of columns are some of the factors which have generally been ignored in the past dynamic analyses of multistory structures. Their influence upon the structural response is believed to be of secondary significance and their inclusion, especially in the nonlinear dynamic analysis, increases the complexity of the procedure considerably. But the first of these, the P-Δ effect, has been a matter of recent concern in some of the static[21,22] and dynamic[23] studies which lead to stability questions.

The effect of axial deformation of columns on the elastic modal periods and mode shapes of an 18-story structure was evaluated by Rubinstein.[24] The increase in the fundamental period was computed to be of the order of ten percent which decreased rapidly in the higher modes. The method of analysis, as described in Chapter 2, was modified to include these two factors so that their separate as well as combined influence upon the inelastic behavior of the 10- and 25-story models could be studied.

Very little information is available, at present, about the true nature and amount of structural and nonstructural damping in buildings. However, it is believed that the structural damping is of a very small magnitude in steel framed structures and the major part of the total damping is provided by the nonstructural elements. These elements are being minimized in the modern trend of building taller and lighter structures. The result is that the nonstructural energy dissipative power of modern tall buildings is much less than for the traditional types of buildings.

The big question of which form and how much damping is reasonable to introduce into these structures for a dynamic analysis must be answered. Some attempts to answer this question[18,19] have been made in recent years. These results indicate that the coefficient of damping in a multistory structure may range from 0.5 to 5 percent of critical. Nielsen's[18] representation of damping in steel framed buildings by interfloor dashpots was used in this study to evaluate the effect of introducing a small amount of viscous damping on the

inelastic response of a 10-story model. In this study the amount of damping was varied from 1 to 5 percent of critical in the fundamental mode.

5.2 Sidesway Effect of Gravity Loads, the P-Δ Effect

5.2.1 Procedure

To illustrate the P-Δ effect in frames, let a single story symmetrical portal be considered, which is shown in Figure 5.1. Let Δ be the lateral displacement of the floor. If the static load on each column is P , then there will be a sidesway moment equal to P·Δ in each column due to the loads P acting through the sidesway Δ . This sidesway moment requires an additional shear, V' , in each column which is given by

$$V' = \frac{P \cdot \Delta}{H} \tag{5.1}$$

where H is the story height.

Let M^1 and M^2 be the end moments in each column. The net shear V in each column will be

$$V = \frac{M^1 + M^2}{H} + V' \tag{5.2}$$

From Equations (5.1) and (5.2) the expression for V becomes

$$V = (M^1 + M^2 + P \cdot \Delta)/H \tag{5.3}$$

The restoring force, Q , on the floor mass becomes

$$Q = -\frac{2}{H}(M^1 + M^2 + P \cdot \Delta) \tag{5.4}$$

Thus, the effect of the P·Δ moment is to modify the column shears which in turn affect the restoring force on the floor mass as given in Equations (5.3) and (5.4).

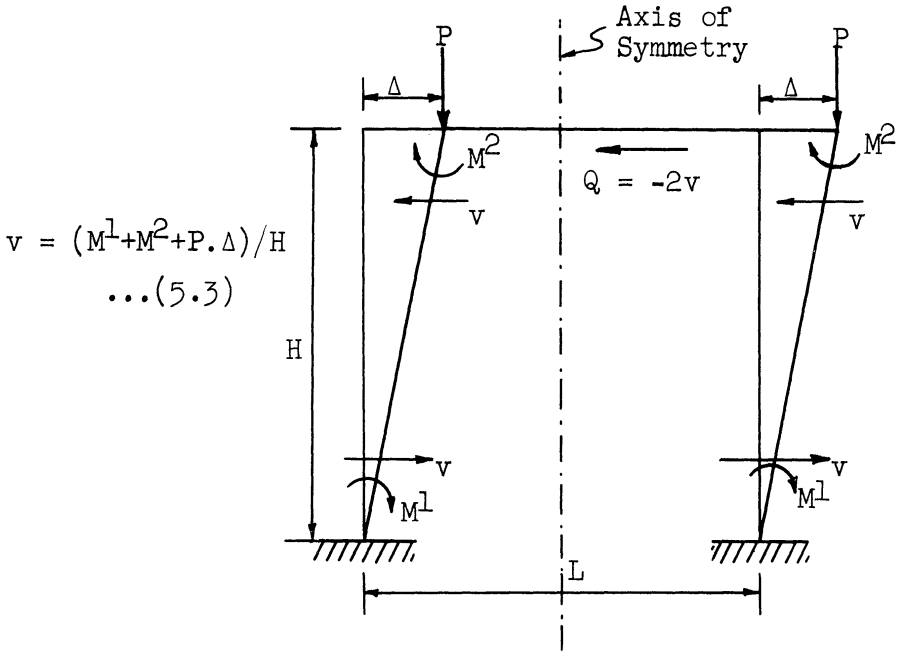

Fig. 5.1. P-Δ Effect in single story frame.

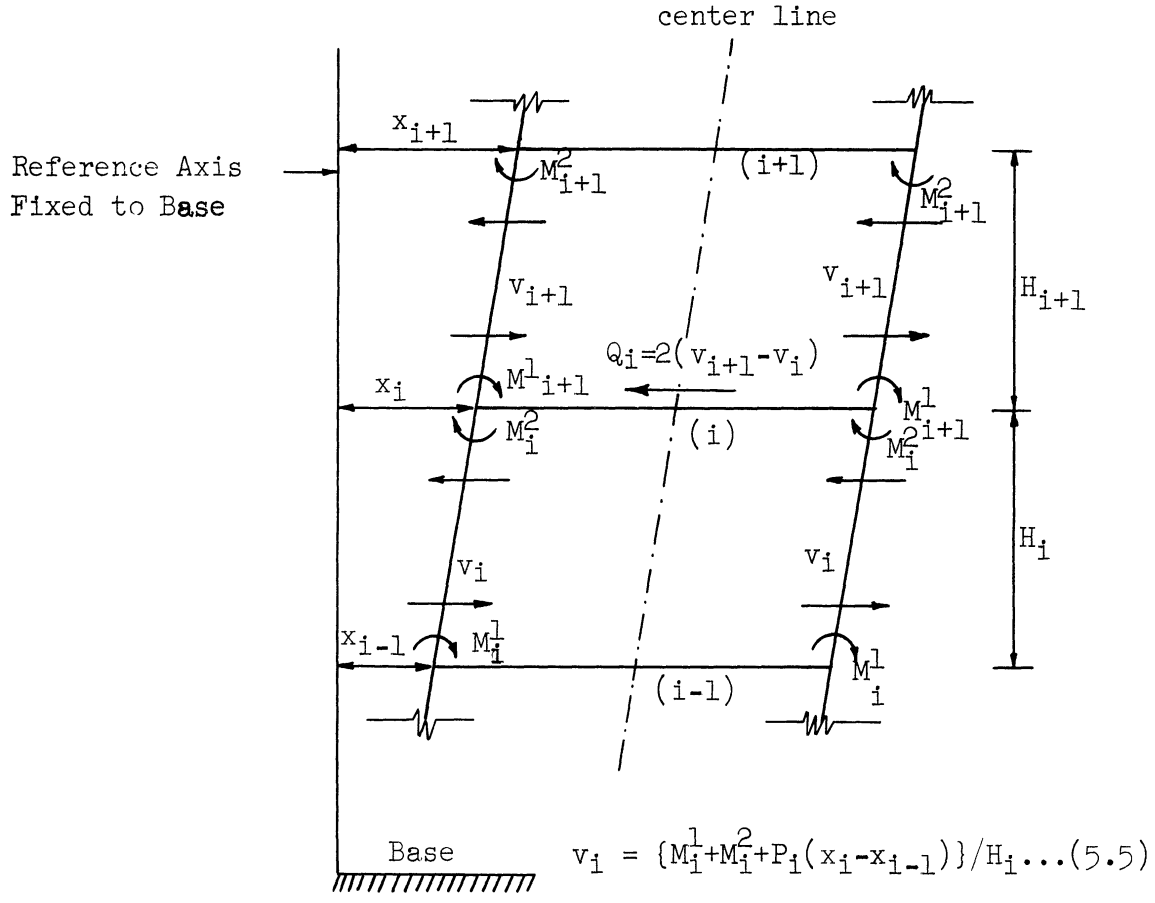

Figure 5.2. P-Δ Effect in multi-story frame.

It may be noted that the girder shears will introduce tension in one column and compression in the other, which are equal because the frame is symmetrical about its centerline. These equal tension and compression forces in the columns will produce equal and opposite sidesway moments with the result of no net change in the story shear. Hence, for the purpose of computing the P-Δ effect in a symmetrical frame it is only necessary to consider the static dead loads carried by the columns.

To illustrate the P-Δ effect in multistory structures, let the i-th story of a single-bay frame be shown in Figure 5.2. The net shear in each column of this story is given by

$$V_i = \{M_i^1 + M_i^2 + P_i(x_i - x_{i-1})\}/H_i \qquad (5.5)$$

where suffix i denotes the story number and $(x_i - x_{i-1})$ is the lateral displacement of the i-th floor relative to the (i-1)-th floor. Shear in the columns of the (i+1)-th story is given, in the same manner, by

$$V_{i+1} = \{M_{i+1}^1 + M_{i+1}^2 + P_{i+1}(x_{i+1} - x_i)\}/H_{i+1} \qquad (5.6)$$

The net restoring force, Q_i, on the i-th floor mass is given by

$$Q_i = 2(V_{i+1} - V_i) \qquad (5.7)$$

The modification required to include the P-Δ effect in the analysis, therefore, appears in the addition of the last term in Equation (5.5) and (5.6). The column shears and the restoring forces on story masses were computed from Equations (5.5) and (5.7) in each sub-step of the Runge-Kutta procedure for solving the differential equations of

motion,

$$m_i \ddot{x}_i + Q_i = - m_i \ddot{y} \qquad (2.1)$$

It may be noted further that the effect of axial column loads on their stiffness was not considered either in the original analysis or in the modification of the procedure to include the P-Δ effect.

5.2.2 Results

With this modified analysis the effect of P-Δ was evaluated in the 10-story elastic frame subjected to the Taft 1952, S21°W componen with acceleration ordinates multiplied by the factor of 3, as was done before. A comparison of some significant response parameters with earlier results (where P-Δ was ignored) is shown in Figure 5.3. The maximum floor displacements have increased by about 10 percent due to the P-Δ effect whereas the maximum absolute floor accelerations are generally less, indicating that the system has become softer due to the P-Δ effect. The column moments and the ductile deformation of girders are larger when P-Δ is included.

Next, the standard 10-story frame with Ramberg-Osgood girders (r = 10) was analyzed for the same Taft accelerogram. A comparison of the results with and without the P-Δ effect is presented in Figure 5.4. Contrary to intuition, the floor displacements are less with P-Δ effect included. But the difference in the lower stories is so small that it is not even seen in the figure, while in the upper half of the frame the difference is of the order of one percent or less. The other three response parameters show a mixed trend of being less

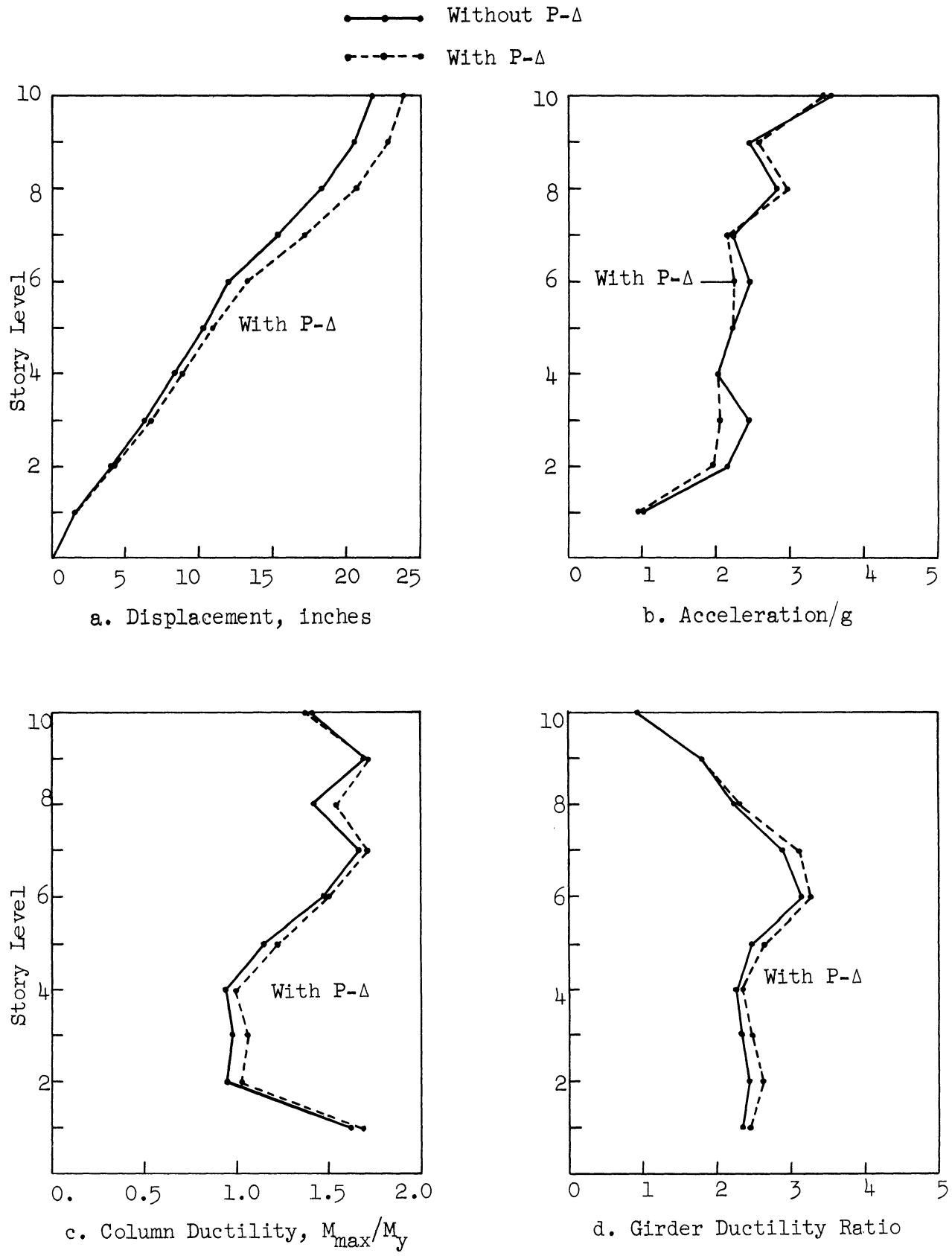

10-Story Elastic Model, T = 1.25 Sec; Taft 1952, S21°W x 3.0

Figure 5.3. Effect of P-Δ on the elastic response.

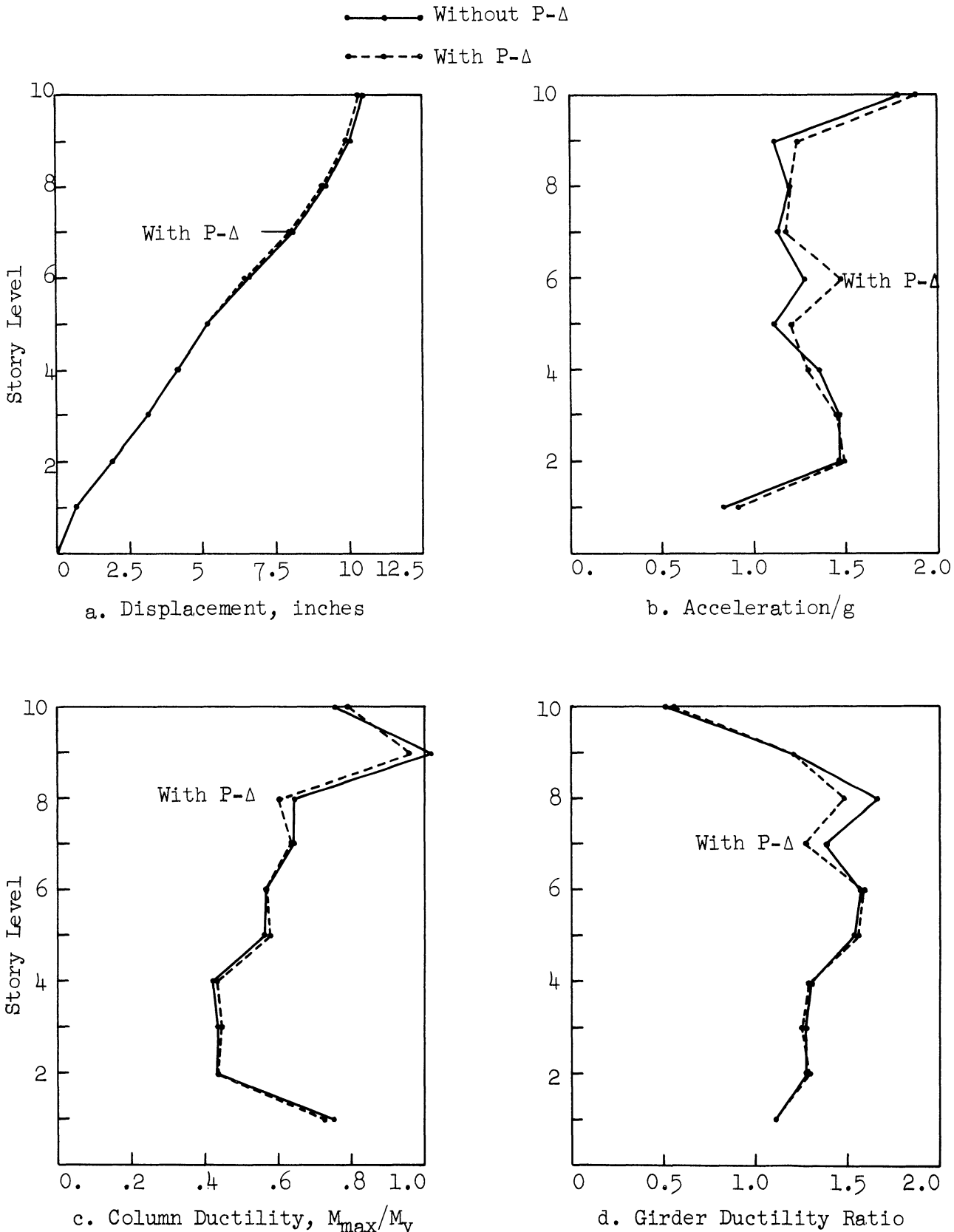

10-Story Standard R-0 Model, r = 10, T = 1.25; Taft 1952, S21°W x 3.0

Figure 5.4. Effect of P-Δ on the inelastic response.

in some stories and more in the others. A comparison of Figures 5.3 and 5.4 shows that the effect of P-Δ is more pronounced in the elastic frame than in the inelastic model.

A comparison of the energy versus time curves for the elastic and the Ramberg-Osgood models with and without the P-Δ effect is shown in Figure 5.5. A similar comparison of the displacement versus time curves for the 10-th story mass is presented in Figure 5.6. The response curves with P-Δ included tend to oscillate about those without P-Δ . But the fluctuations in the elastic case are more than in the inelastic frame. In Figure 5.6(a), a slight increase in the period of lateral vibration can also be seen due to the P-Δ effect, which is much less pronounced in the inelastic response. A close examination of the input energy curves of Figures 5.5(a) and (b) also shows that the increase or decrease in energy due to the P-Δ is similarly distributed with time for the elastic and the inelastic cases. Similar observation can be made in Figures 5.6(a) and (b) for the lateral displacements.

The 10- and 25-story standard Ramberg-Osgood frames were analyzed for the El Centro 1940, N-S component by 1.5. The comparison of these results with the corresponding earlier results without the P-Δ effect is presented in Figures 5.7 and 5.8, respectively. The change in the maximum response parameters due to the P-Δ effect is generally of the order of one percent or so and shows a mixed trend of increase and decrease.

On the basis of these results it appears that in typical multistory frames the P-Δ effect influences the elastic response by as much as 10 percent, whereas its effect on the inelastic response is

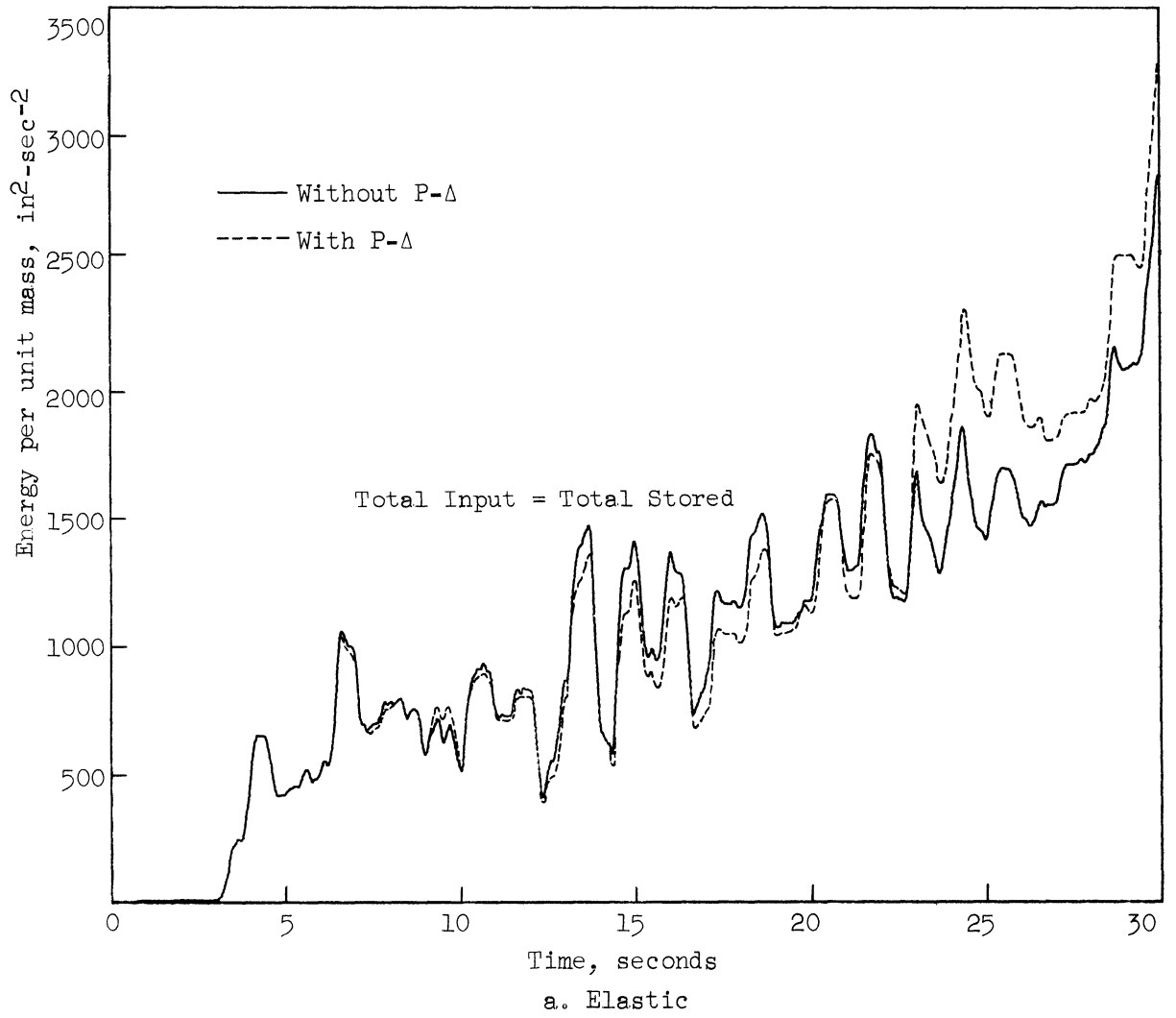

a. Elastic

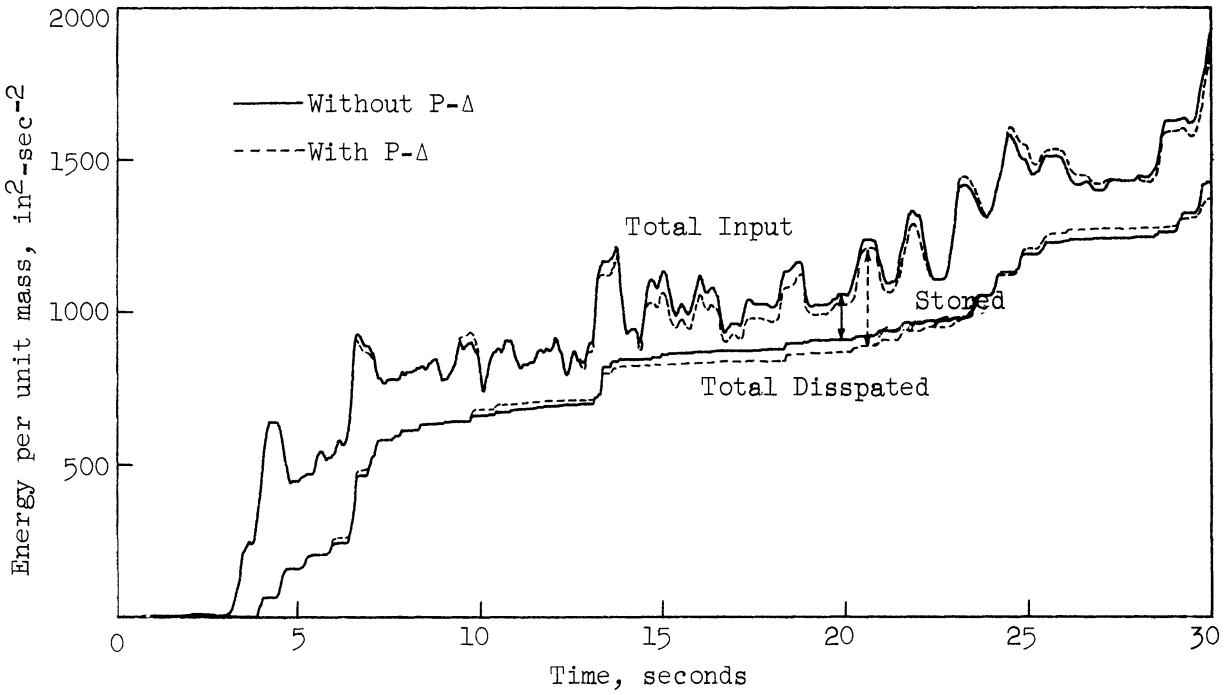

b. Ramberg-Osgood (r=10)

10-Story Model, T=1.25; Taft 1952, S21°W x 3.0

Figure 5.5. Effect of P-Δ on input and dissipated energy.

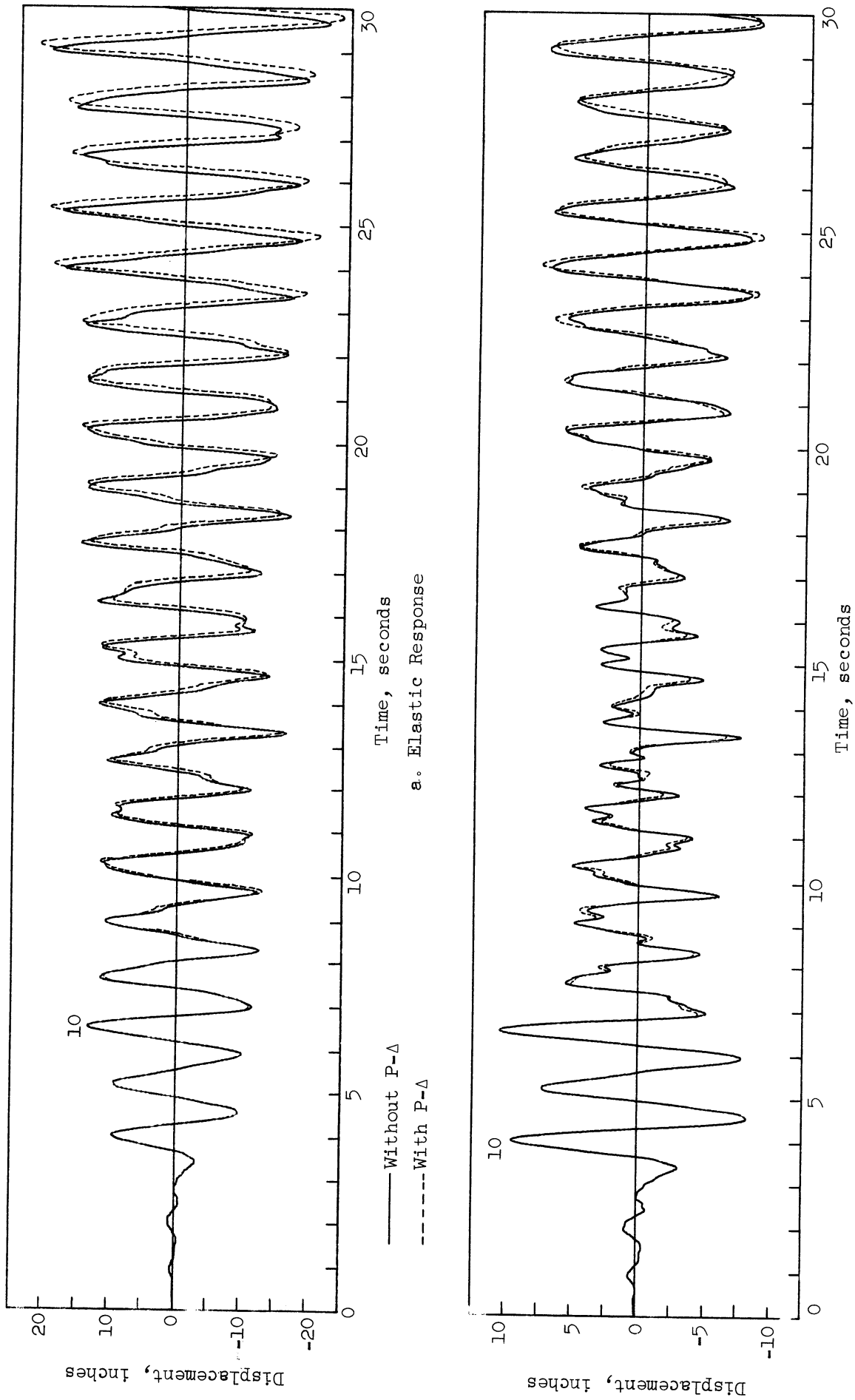

Figure 5.6. Effect of P-Δ on lateral response; 10-story model, T=1.25; Taft 1952, S21°W x 3.0.

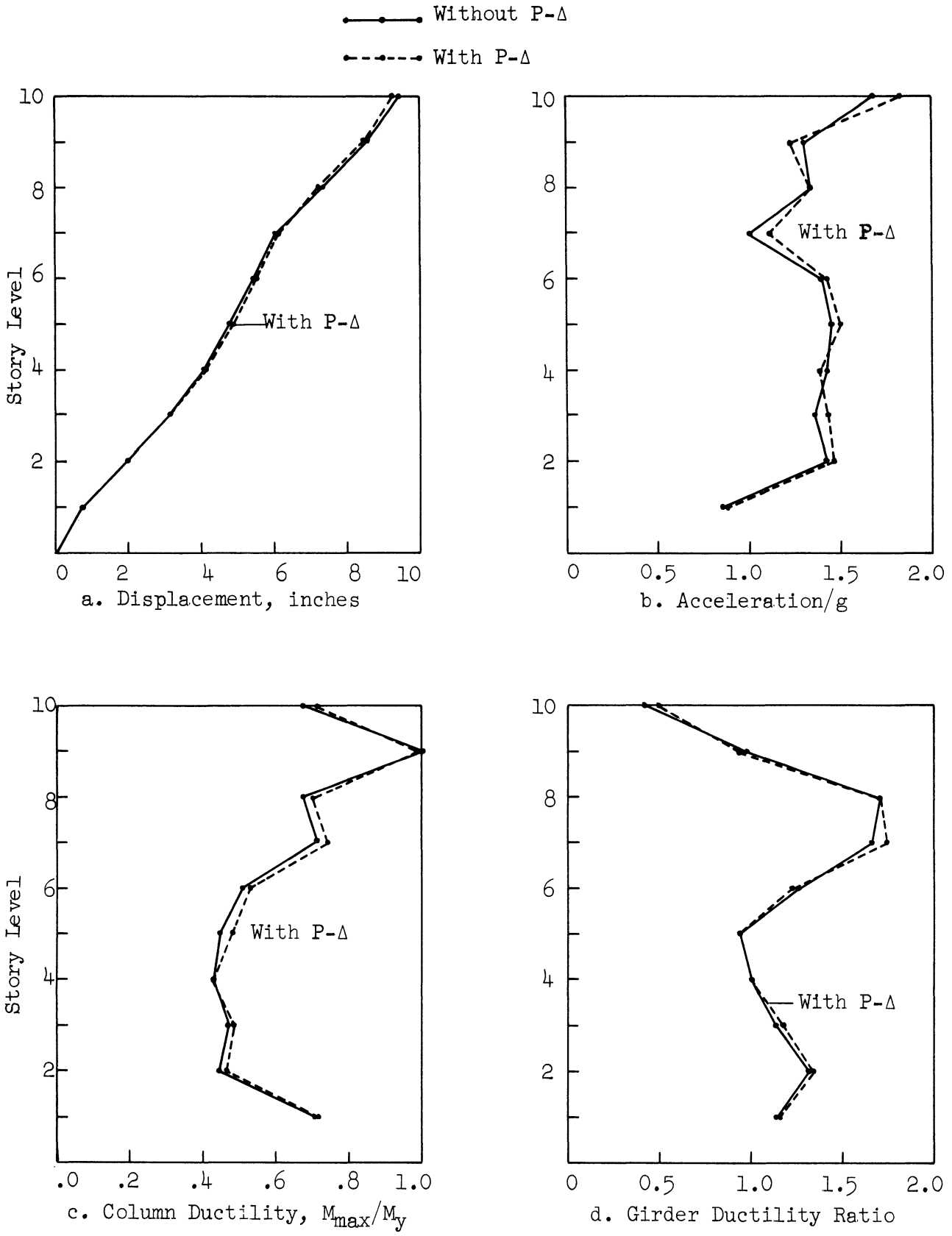

10-Story Standard R-0 Model, r = 10, T = 1.25; El Centro 1940, N-S x 1.5

Figure 5.7. Effect of P-Δ on the inelastic response.

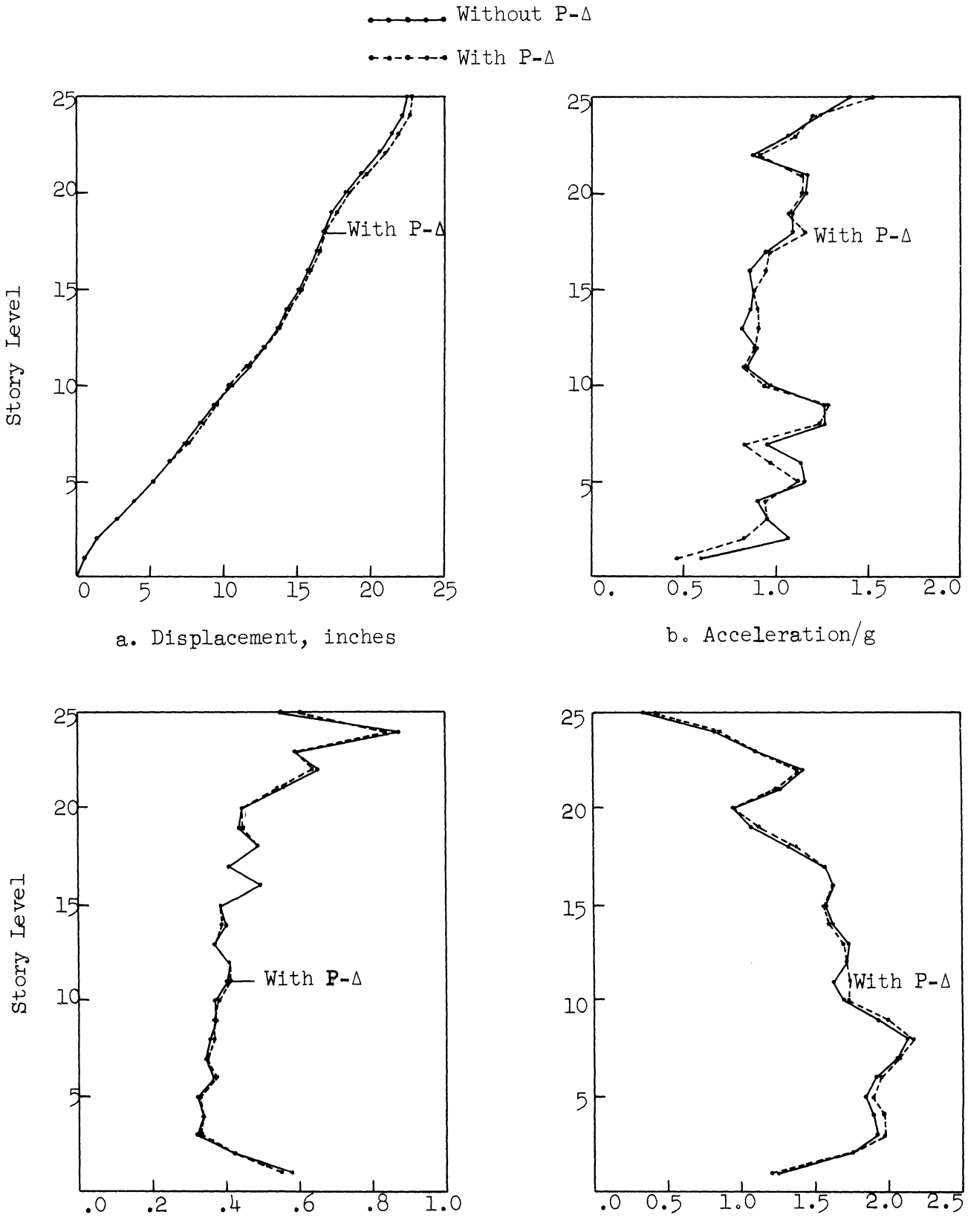

a. Displacement, inches

b. Acceleration/g

c. Column Ductility, M_{max}/M_y

d. Girder Ductility Ratio

25-Story Standard R-0 Model, r = 10, T = 2.27; El Centro 1940, N-S x 1.5

Figure 5.8. Effect of P-Δ on the inelastic response.

less significant, being of the order of one percent or so. Also, the magnitude of the change seems to be unaffected by the height of the structure or the type of the earthquake.

5.3 Axial Deformation of Columns

5.3.1 Procedure

During lateral vibration of multistory frames axial forces are induced in columns which give rise to vertical displacements of the girder ends. The effect of the axial deformation of columns is generally ignored in dynamic analyses of multistory structures. In other words, the columns are assumed to be infinitely rigid against axial loads. This approach was used during the first phase of this investigation and now the axial deformations of the columns will be considered in order to evaluate their influence upon the inelastic response.

In Step (2) of the analysis, which was described in Section 2.3, the incremental joint rotations, $\Delta\theta$'s , are computed from the known values of the Δx's . Including the vertical deformation of the joints increases the size of the stiffness matrix so that the stiffness matrix equation of the structure takes the form

$$\begin{Bmatrix} \Delta Q \\ -- \\ \Delta M \\ \\ \Delta V \end{Bmatrix} = \left[\begin{array}{c:cc} K_{xx} & K_{x\theta} & K_{xy} \\ \hdashline K_{\theta x} & K_{\theta\theta} & K_{\theta y} \\ K_{yx} & K_{y\theta} & K_{yy} \end{array}\right] \begin{Bmatrix} \Delta x \\ -- \\ \Delta\theta \\ \\ \Delta Y \end{Bmatrix} \tag{5.8}$$

In the computation of lateral response of the frame the vector

$$\begin{Bmatrix} \Delta M \\ \\ \Delta V \end{Bmatrix} = \{0\} \tag{5.9}$$

so that the second sub-matrix equation of Equation (5.8) can be written as

$$\{0\} = \begin{bmatrix} K_{\theta x} \\ K_{yx} \end{bmatrix} \{\Delta x\} + \begin{bmatrix} K_{\theta\theta} & K_{\theta y} \\ K_{y\theta} & K_{yy} \end{bmatrix} \begin{Bmatrix} \Delta\theta \\ \Delta y \end{Bmatrix}$$

This can also be rewritten as

$$- \begin{bmatrix} K_{\theta x} \\ K_{yx} \end{bmatrix} \{\Delta x\} = \begin{bmatrix} K_{\theta\theta} & K_{\theta y} \\ K_{y\theta} & K_{yy} \end{bmatrix} \begin{Bmatrix} \Delta\theta \\ \Delta y \end{Bmatrix} \qquad (5.10)$$

This matrix equation has to be solved in Step (2) of the computational procedure for the incremental joint rotations and vertical displacements, $\Delta\theta$'s and Δy's , respectively. For a symmetrical single-bay frame of N stories (as considered in this investigation) Equation (5.10) represents a set of $2N$ simultaneous linear equations of equilibrium. All the sub-matrices in this equation are of order $N \times N$. Also, it turns out that the sub-matrices $K_{\theta\theta}$ and K_{yy} are symmetrical tri-diagonal matrices and $K_{\theta y}$ $(= K_{y\theta})$ is a diagonal matrix. The sub-matrix $K_{\theta x}$ is also a tri-diagonal matrix involving the stiffness coefficients of the columns only, while K_{yx} is a null matrix.

The $2N \times 2N$ stiffness matrix on the right hand side of Equation (5.10) can be transformed into a symmetrical pentadiagonal form by rearranging the rows and columns. The entire Equation (5.10), transformed in this manner, was solved by a recursion scheme which turned out to be very efficient.

The rotations and the vertical displacements at the two ends of each girder are equal in magnitude because of the symmetry of the

frame. Therefore, the girders can still be treated as antisymmetrical in bending. This is shown in Figure 5.9. The Ramberg-Osgood M-θ relations (2.13) and (2.14) are still valid in the following modified form:

$$\frac{\theta'}{\theta_y} = \frac{M}{M_y}\left\{1 + \frac{3}{r+2}\left|\frac{M}{M_y}\right|^{r-1}\right\} \qquad (2.13a)$$

$$\frac{\theta'-\theta'_o}{2\theta_y} = \frac{M-M_o}{2M_y}\left\{1 + \frac{3}{r+2}\left|\frac{M-M_o}{2M_y}\right|^{r-1}\right\} \qquad (2.14a)$$

where,

$$\theta' = \theta - (2y)/L \qquad (5.11)$$

θ is the total joint rotation taken positive if clockwise and y is the vertical displacement at the left end of the girder, considered positive upwards. The incremental joint rotations, θ's, as obtained from the solution of the matrix Equation (5.10) are modified by making use of Equation (5.11) in incremental form as

$$\Delta\theta' = \Delta\theta - (2\cdot\Delta y)/L \qquad (5.12)$$

These $\Delta\theta$'s are the increments in the θ''s satisfying the Ramberg-Osgood hysteresis behavior defined by Equations (2.13a) and (2.14a).

These are the modifications which were needed to make the analysis include the effect of axial deformation of columns. It may be noted that the computation of stiffness sub-matrices $K_{\theta y}$, $K_{y\theta}$ and K_{yy} in Equation (5.10) requires the areas of the column sections in addition to the flexural stiffness properties of the columns and girders. The areas, A, for the 14 WF sections from the Handbook of Steel Sections

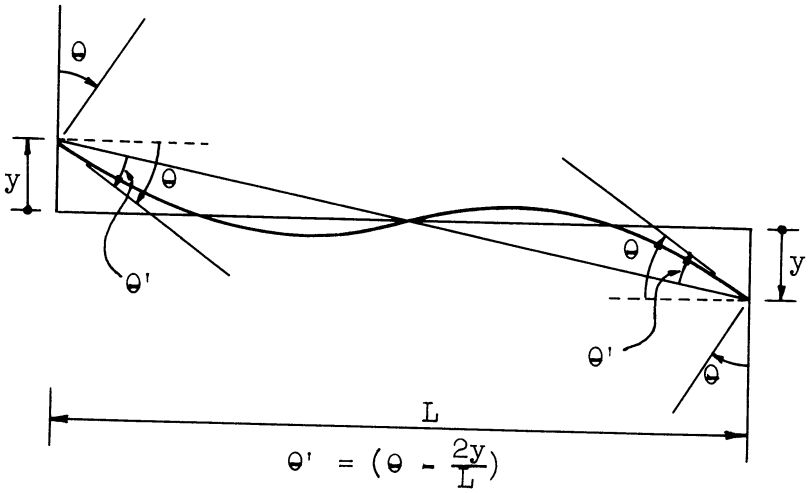

Figure 5.9. Girder bending with vertical joint displacements.

were plotted against their moment of inertia, I_x , values on a log-log graph. A straight line was then fitted through these points, whose equation is

$$A = 50 \text{ in.}^2 \left(\frac{I_x}{2100 \text{ in.}^4} \right)^{.836} \qquad (5.13)$$

This empirical equation was used to derive the areas of the column sections from their I_x values, which for the standard 40-story frame were tabulated in Table 3.1. The lengths of the columns equal to the depths of the girders at the connections were treated as rigid stubs in axial deformation also, as was done before in flexure. The deformable length of columns in the i-th story was, therefore, taken equal to $(H_i - d_i)$, where H_i is the height of the story from center to center of the girders, and d_i is the depth of the girder in the i-th story.

5.3.2 Results

The effect of the axial deformation of columns was first evaluated on the 10-story standard Ramberg-Osgood frame subjected to the Taft 1952 accelerogram. The results of this analysis are presented in Figure 11, where a comparison is also made with the corresponding response parameters previously determined without this effect. The story displacements have increased by about three percent whereas the column moments and girder ductility ratios are less by as much as 10 to 20 percent. As is commonly understood, the effect of axial deformation of columns is to make the system softer. This tendency can be clearly seen in these results.

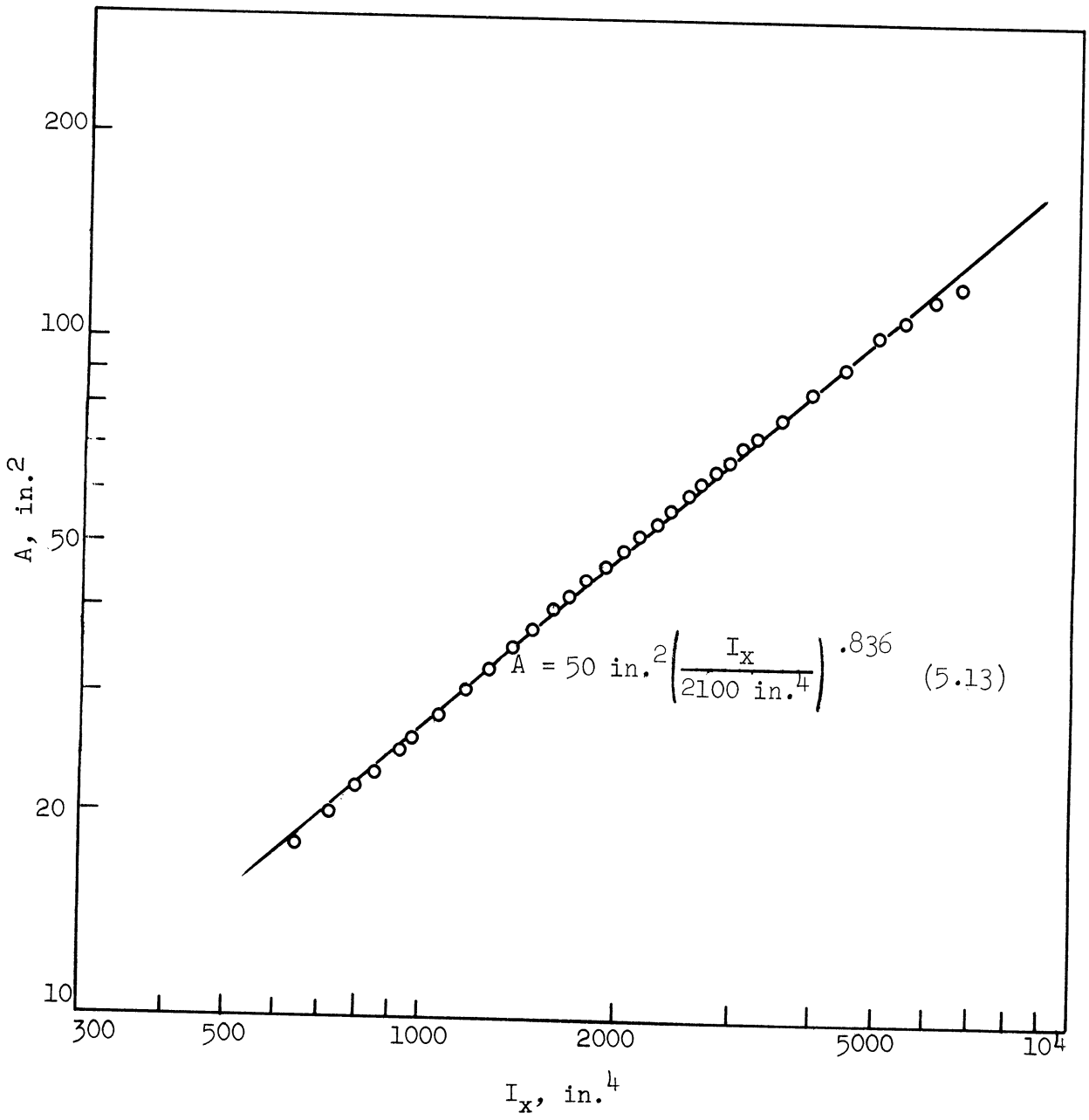

Figure 5.10. Area vs. moment of inertia for 14WF sections.

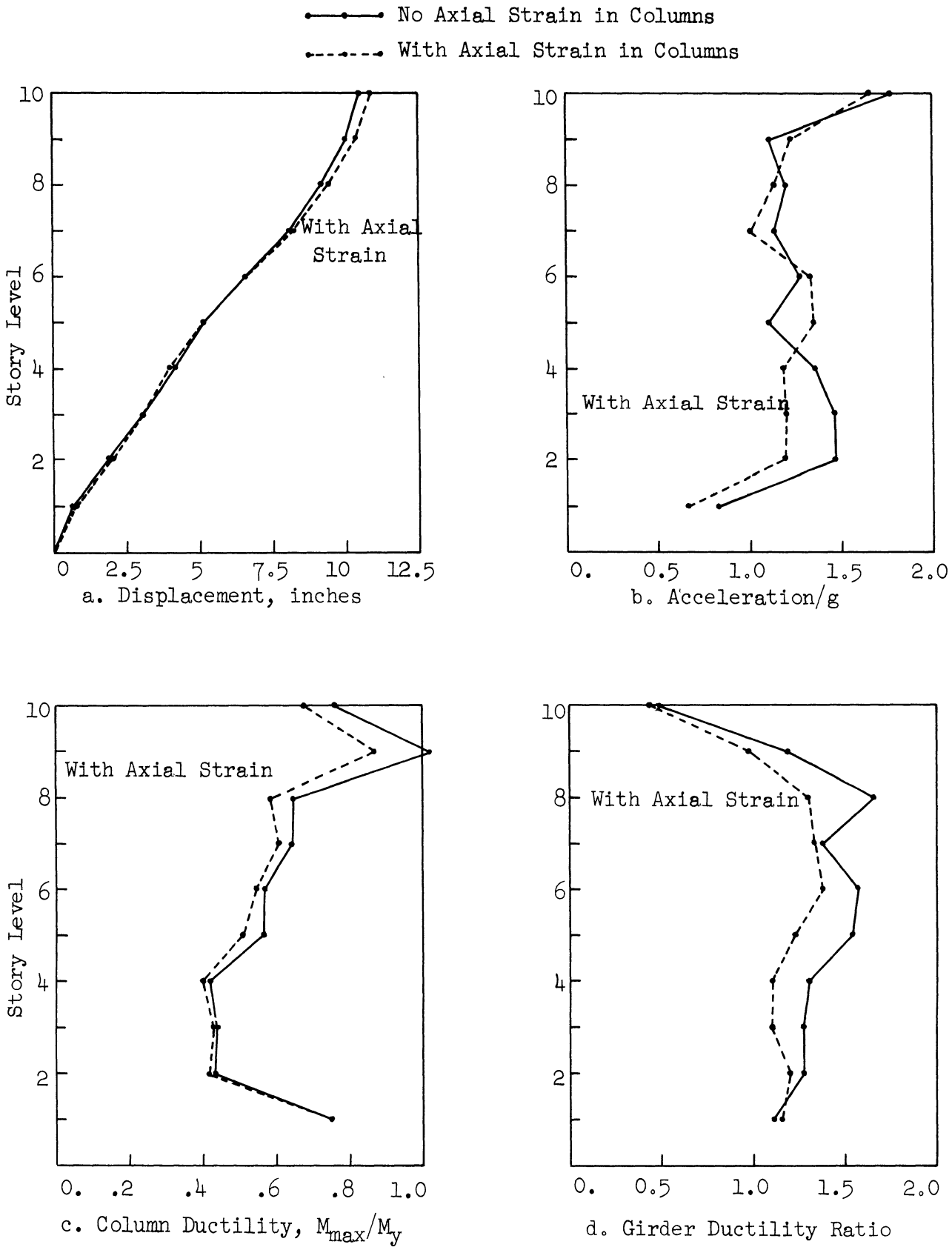

10-Story Standard R-0 Model, r = 10, T = 1.25; Taft 1952, S21°W x 3.0

Figure 5.11. Effect of axial deformation of columns on the inelastic response.

In Figure 5.12 are shown the maximum vertical displacements of the joints and the maximum compressive forces in the columns as obtained from the above analysis. The maximum vertical displacement of the top floor joint is 0.226 inch and the maximum total column load (static + dynamic) in the bottom story is 783.7 kips which is about three and one half times greater than the static load in that column. It appears, therefore, that a dynamic magnification of this order can be expected in the column loads of multistory buildings when subjected to severe earthquakes, such as the one considered here.

The influence of the axial deformations on the inelastic response of this 10-story model seems to be much larger than that of the P-Δ effect, as can be seen from Figures 5.11 and 5.4 . What happens if the two effects are taken together? The 10-story frame was again analyzed for the same Taft accelerogram, but this time including the P-Δ as well as the axial deformation of columns in the analysis. The results are shown in Figure 5.13 and compared with the results when neither of these two effects were considered. The results show a predominance of the axial strain effect in the combined influence of the two effects. This again confirms the insignificant influence of the P-Δ effect on the inelastic response of multistory frames.

It is logical to believe, from the analysis as well as the results (Figure 5.11), that the effect of axial deformation of columns is to make the structure softer by reducing its lateral stiffness. The elastic modal periods of this 10-story frame were computed by including the effect of vertical joint displacements. This involves determination of the lateral stiffness matrix, K'_{xx} , from Equations (5.8) and (5.9).

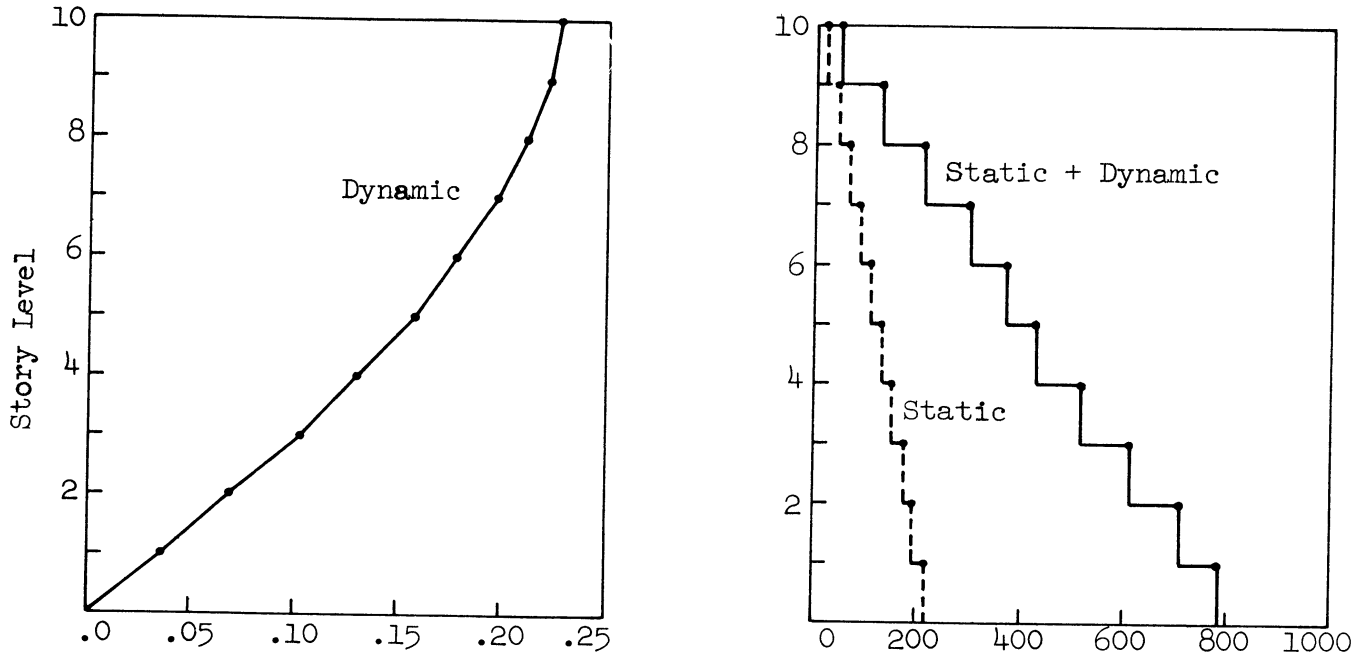

a. Vertical Displacement, inches

b. Column Load, kips

10-Story Standard R-0 Model, r = 10, T = 1.25; Taft 1952, S21°W x 3.0

Figure 5.12. Max. vertical joint displacements and column loads.

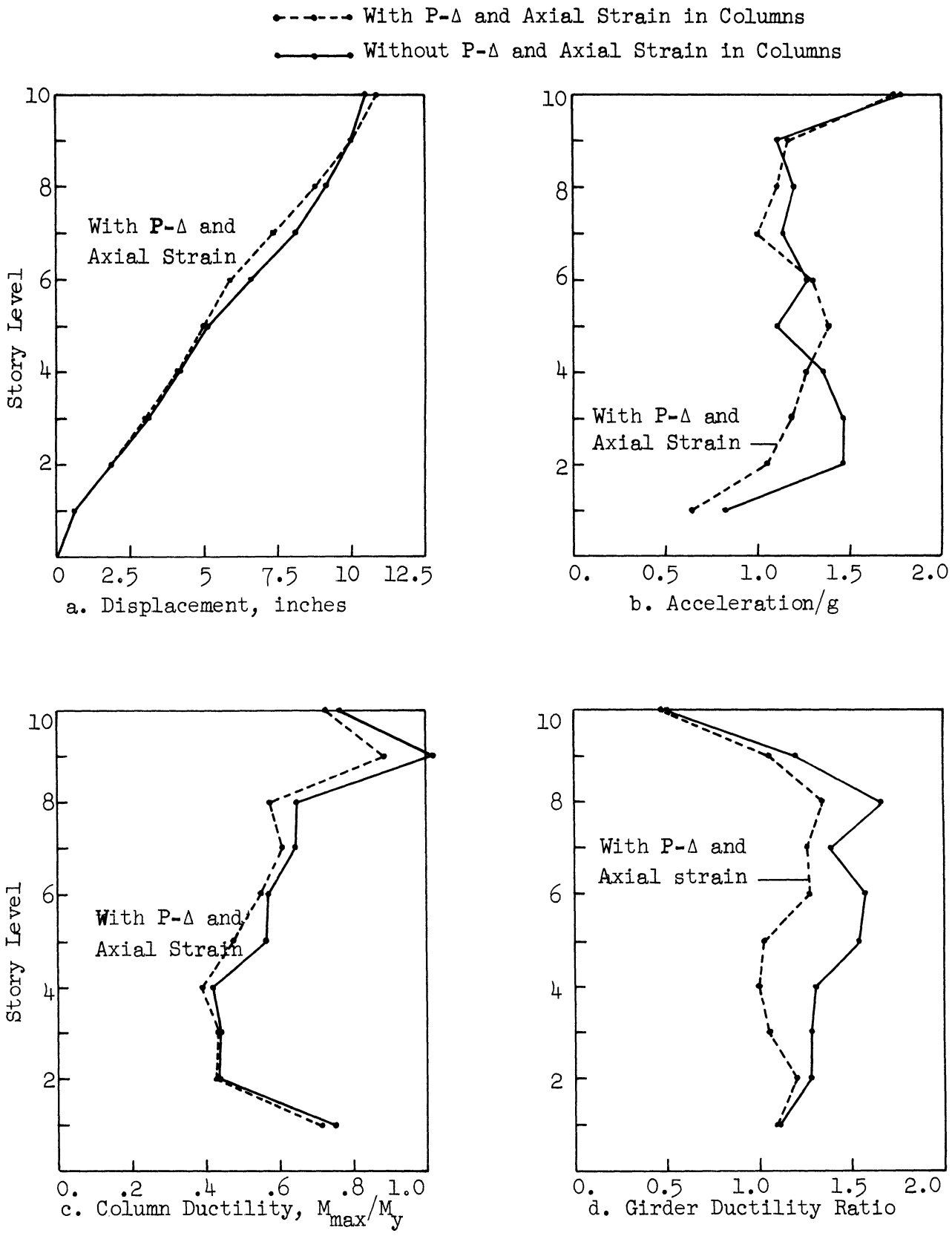

10-Story Standard R-0 Model, r = 10, T = 1.25; Taft 1952, S21°W x 3.0

Figure 5.13. Combined effect of P-Δ and axial deformation of columns on the inelastic response.

The expression for K'_{xx} can be written as

$$[K'_{xx}] = [K_{xx}] - [K_{x\theta} \mid K_{xy}] \left[\begin{array}{c|c} K_{\theta\theta} & K_{\theta y} \\ \hline K_{y\theta} & K_{yy} \end{array}\right]^{-1} \left[\begin{array}{c} K_{\theta x} \\ \hline K_{yx} \end{array}\right] \qquad (5.14)$$

If the matrix inversion involved in Equation (5.14) is performed on the full $2N \times 2N$ matrix, errors may develop because of the large difference in the order of the flexural and axial deformation stiffness values. This was pointed out by Rubinstein.[24] To avoid this difficulty the inversion was performed by partitioning the matrix as shown in Equation (5.14). Inversion by this technique involves inverting smaller $N \times N$ matrices each having elements of the same order of magnitude.

The fundamental period of the frame computed by using the stiffness matrix K'_{xx} from Equation (5.14) was 1.45 seconds as compared with the previous value of 1.25 seconds. Thus, the axial deformation of columns increased the elastic fundamental period of the 10-story frame by 16 percent. It would be interesting to see if this period change could predict the change in the response that was caused by including the axial deformation of the columns. Thus, the stiffness of the 10-story model neglecting the axial deformation of the columns was proportionately reduced to make its elastic fundamental period equal to 1.45 seconds.

This was done to simulate the effect of axial deformation of columns on the elastic stiffness of the frame. The new10-story Ramberg-Osgood model, with $T = 1.45$ seconds but the M_y -values of the members remaining unchanged, was analyzed by the old procedure of Chapter 2 for the same Taft accelerogram. The results are shown in

Figure 5.14 through 5.16 along with their comparison with the results previously shown in Figure 5.11. A study of the Figure 5.14 shows that change in the inelastic response caused by this period change is about twice what was caused by permitting the axial deformation of columns in the original structure. But the trend of these two changes on the response results is similar although their magnitudes are different. Figure 5.15 shows the energy-time curves from these three analyses, while the displacement-time curves of the 10-th story-mass are shown in Figure 5.16. These response parameters have quite different time variations. These results seem to indicate that the effect of axial deformation of columns on the inelastic response of a structure may not be predicted by an equivalent change in its elastic stiffness.

5.4 Damping

5.4.1 Procedure

A good representation of damping for our multistory models having equal floor weights appeared to be interfloor viscous dashpots of equal magnitude in each story as shown in Figure 5.17. This representation has the additional advantage of simplifying the analysis. The value of the damping force per unit velocity, S, was determined to provide a specified percentage of critical damping, β, in the elastic fundamental mode of the 10-story frame. The determination of β involves the dominant complex eigenvalues of an unsymmetrical matrix which is obtained from the mass, damping and the stiffness matrices of the structure. The method, which was earlier used by Berg,[7] was employed for this purpose. For our models the mass matrix is a diagonal matrix and the damping matrix, D, for the dampers, as shown in Figure 5.17, takes the form,

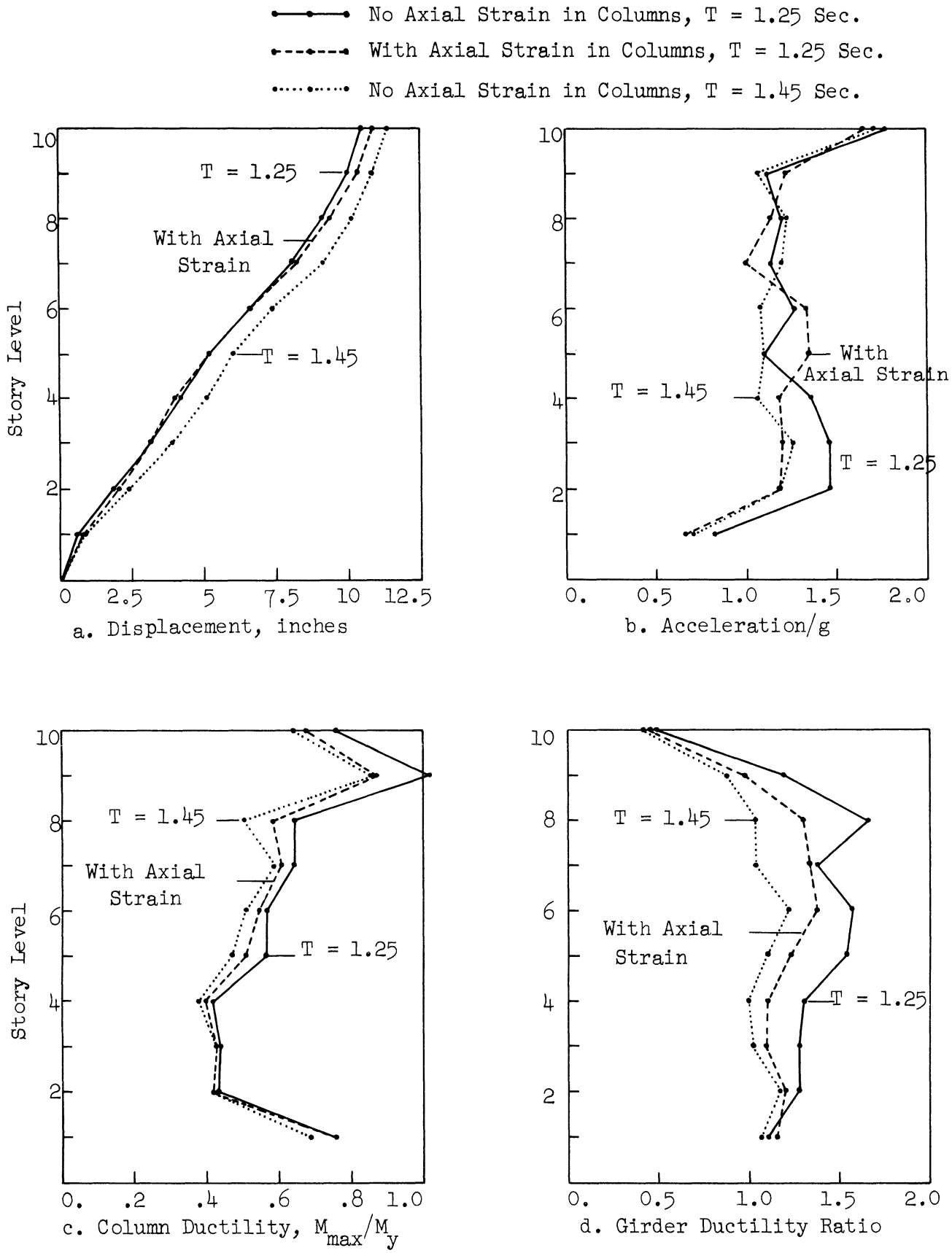

10-Story Ramberg-Osgood Model, r = 10; Taft 1952, S21°W x 3.0

Figure 5.14. Effect of period change equivalent to axial deformation of columns on the inelastic response.

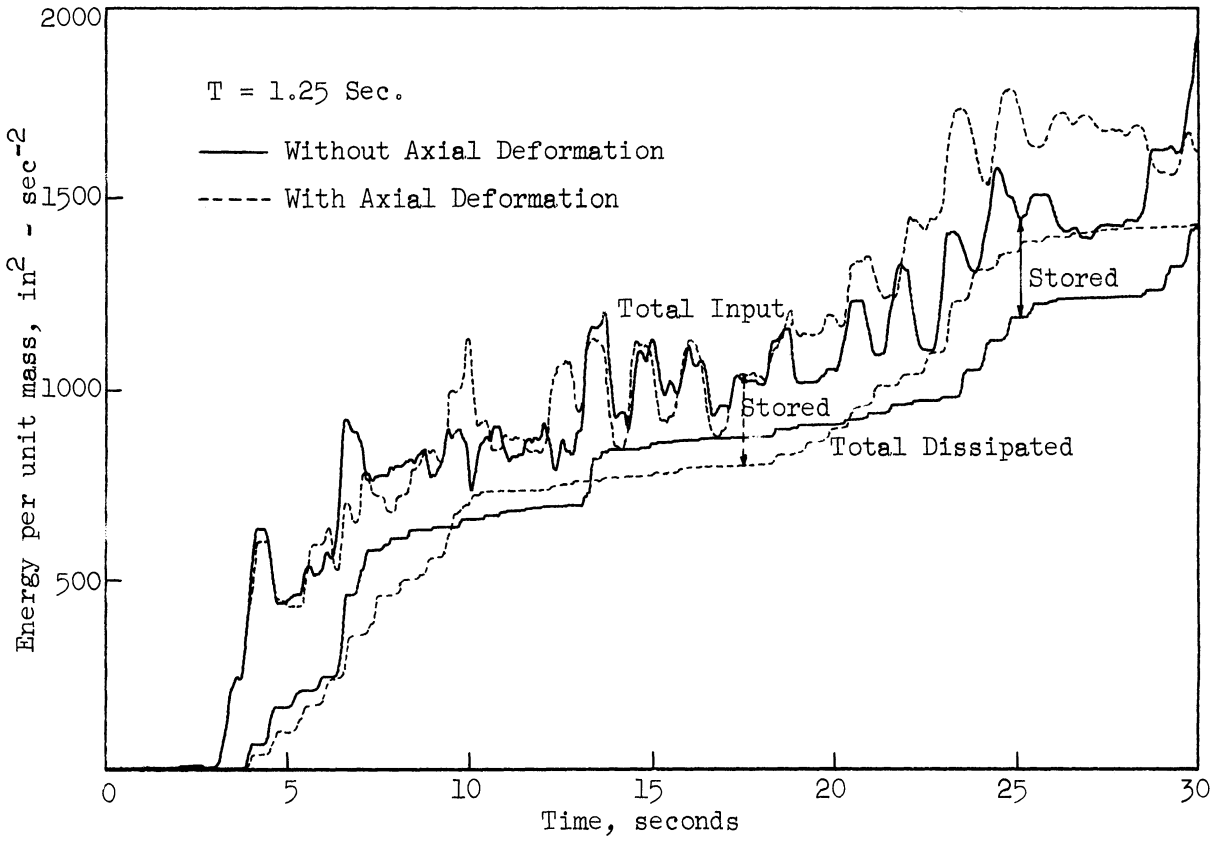

a. Axial Deformation of Columns

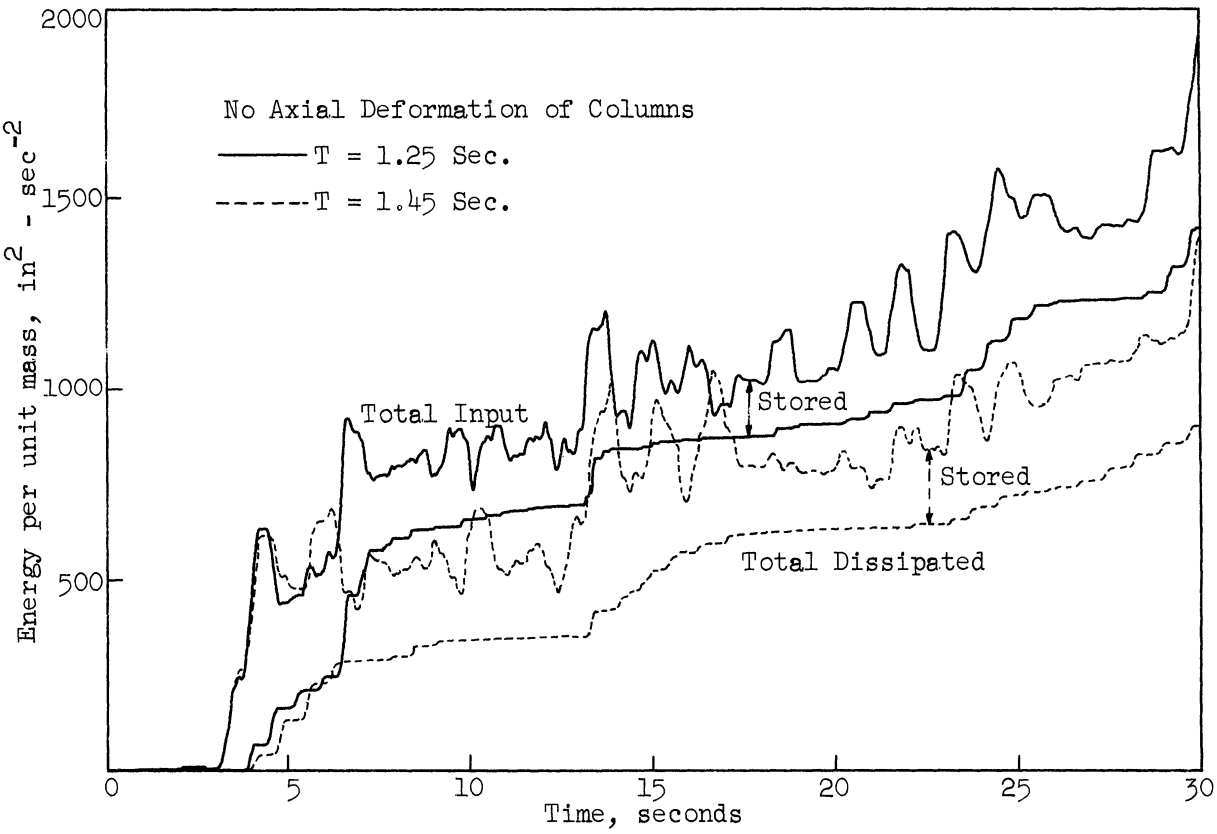

b. Equivalent Change in Elastic Fundamental Period

10-Story Ramberg-Osgood Model, r = 10; Taft 1952, S21°W x 3.0

Figure 5.15. Effect of column axial deformation on inelastic response.

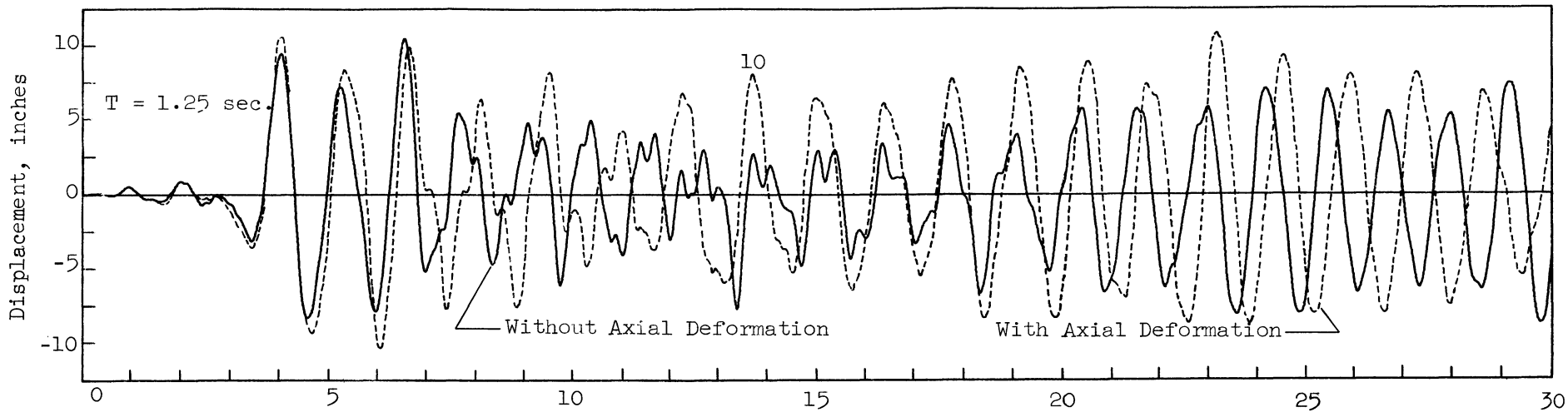

a. Axial Deformation of Columns

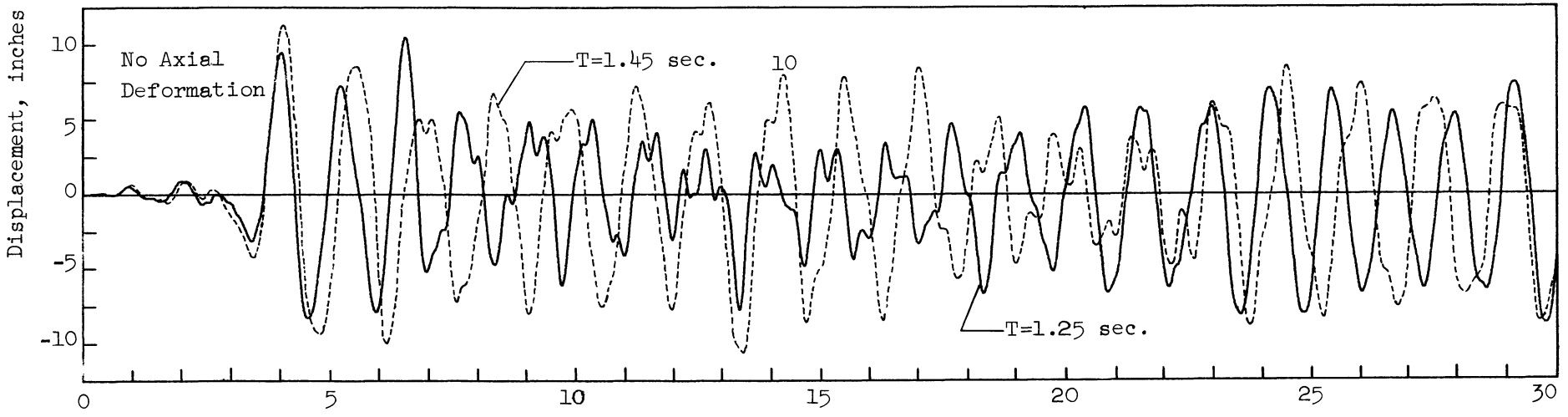

b. Equivalent Change in Elastic Fundamental Period

Figure 5.16. Effect of column axial deformation on lateral response; N=10, r=10; Taft 1952, S21°W x 3.0.

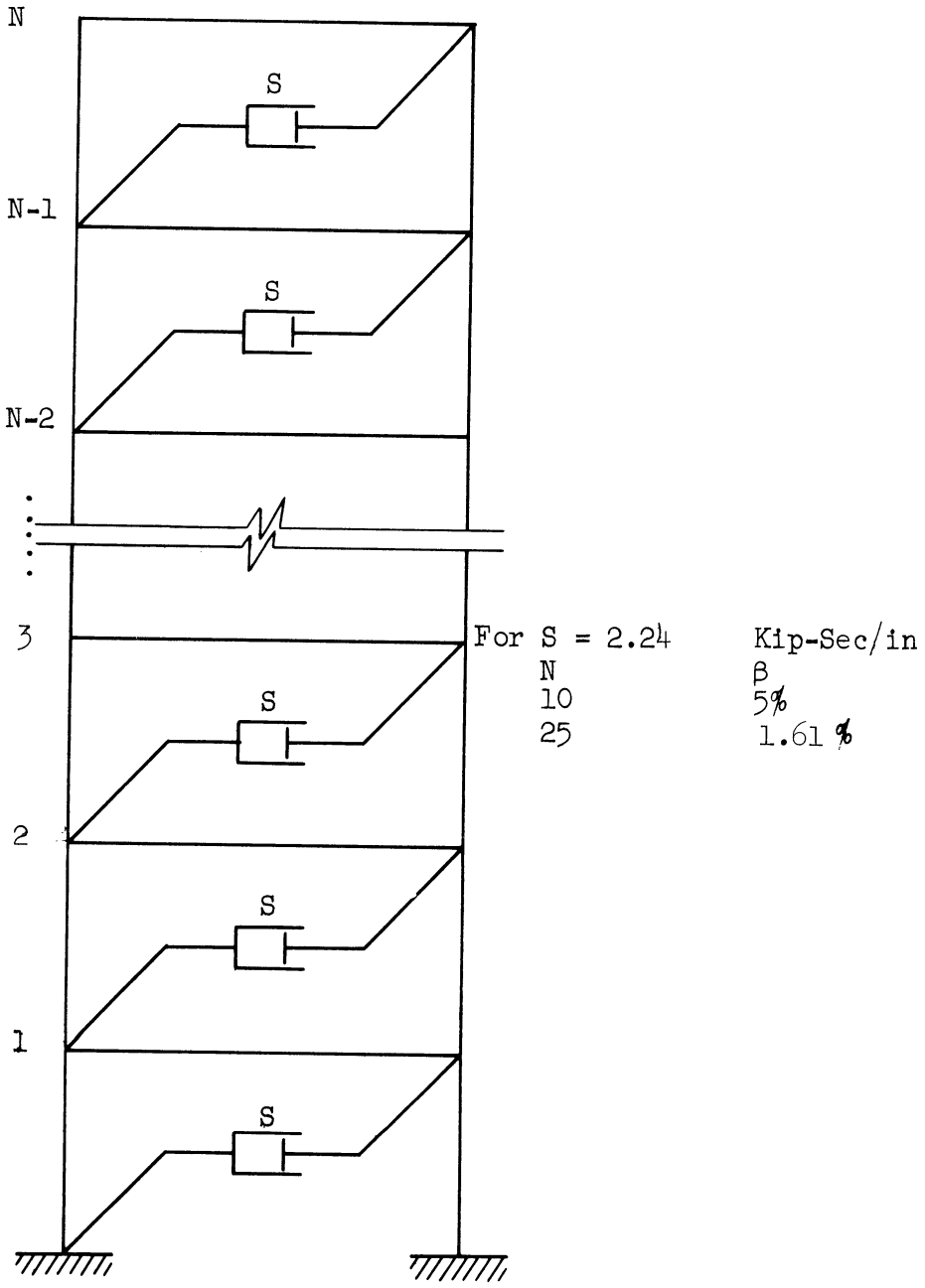

Figure 5.17. Interfloor viscous damping.

$$[D] = \begin{bmatrix} 2S & -S & & & & 0 \\ -S & 2S & -S & & & \\ & -S & 2S & & & \\ & & & 2S & -S & \\ 0 & & & -S & S & \end{bmatrix}_{N \times N} \qquad (5.15)$$

The value of S for $\beta = 5$ percent of critical damping in the fundamental mode of the 10-story frame was computed to be 2.24 kip-sec/in. This same damping force gives 1.61 percent of critical damping in the fundamental mode of the 25-story frame. For a different value of β, S could be computed by simple linear proportioning.

To incorporate this form of damping in the analysis of the structural response, the differential equations similar to Equation (2.1) are

$$[m]\{\ddot{x}\} + [D]\{\dot{x}\} + \{Q\} = - [m]\ddot{y} \qquad (5.16)$$

These equations of motion were then solved by using the Runge-Kutta procedure as before, with the other elements in the analysis remaining unchanged.

5.4.2 Results

Analyses with interfloor viscous damping were performed on the 10-story standard Ramberg-Osgood frame subjected to the Taft 1952, S21°W x 3.0 accelerogram. The damping force was varied to give values of β = 1, 2, 3 1/2, and 5 percent. The results are presented in Figures 5.18 through 5.22.

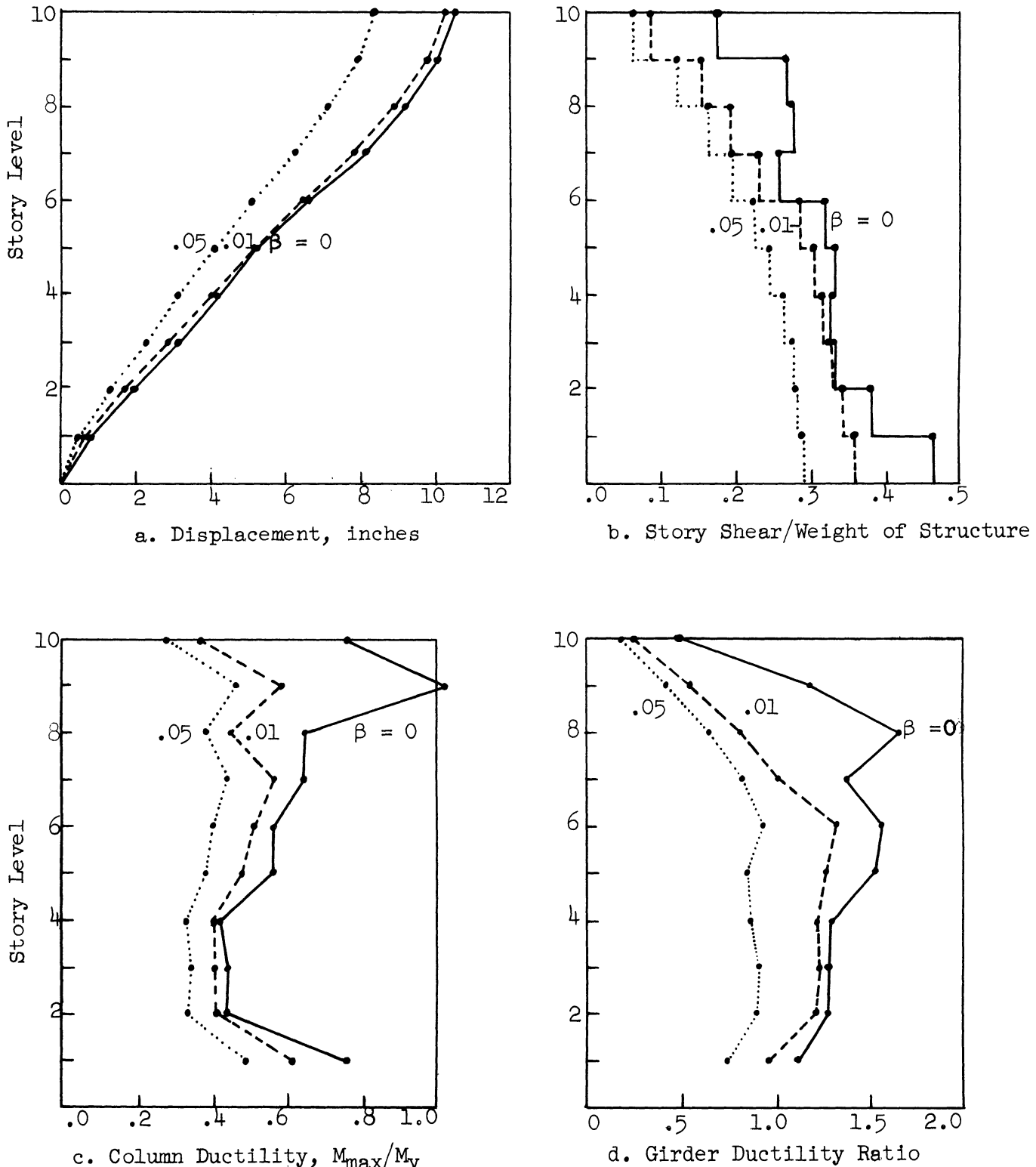

10-Story Standard R-0 Model, r = 10, T = 1.25; Taft 1952, S21°W x 3.0

Figure 5.18. Effect of damping on the inelastic response.

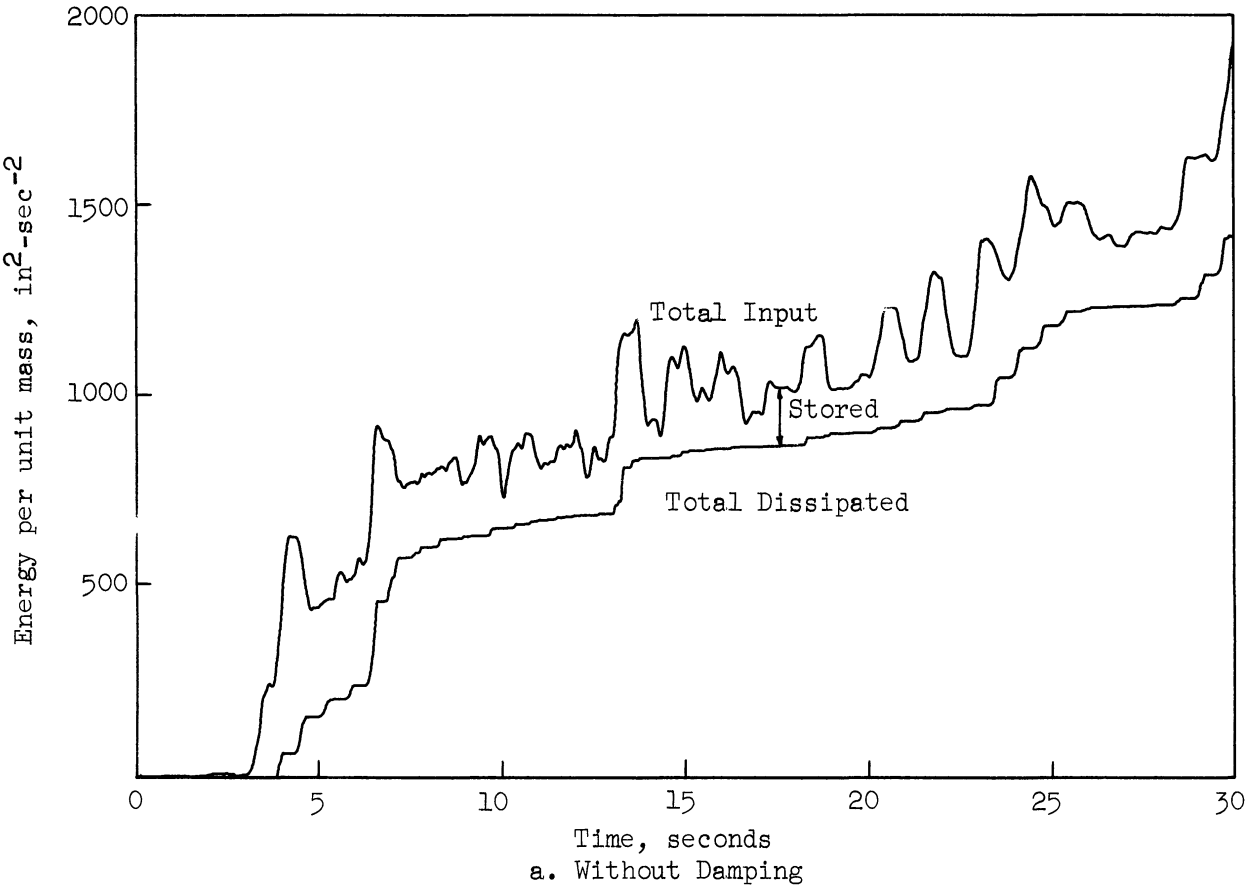

a. Without Damping

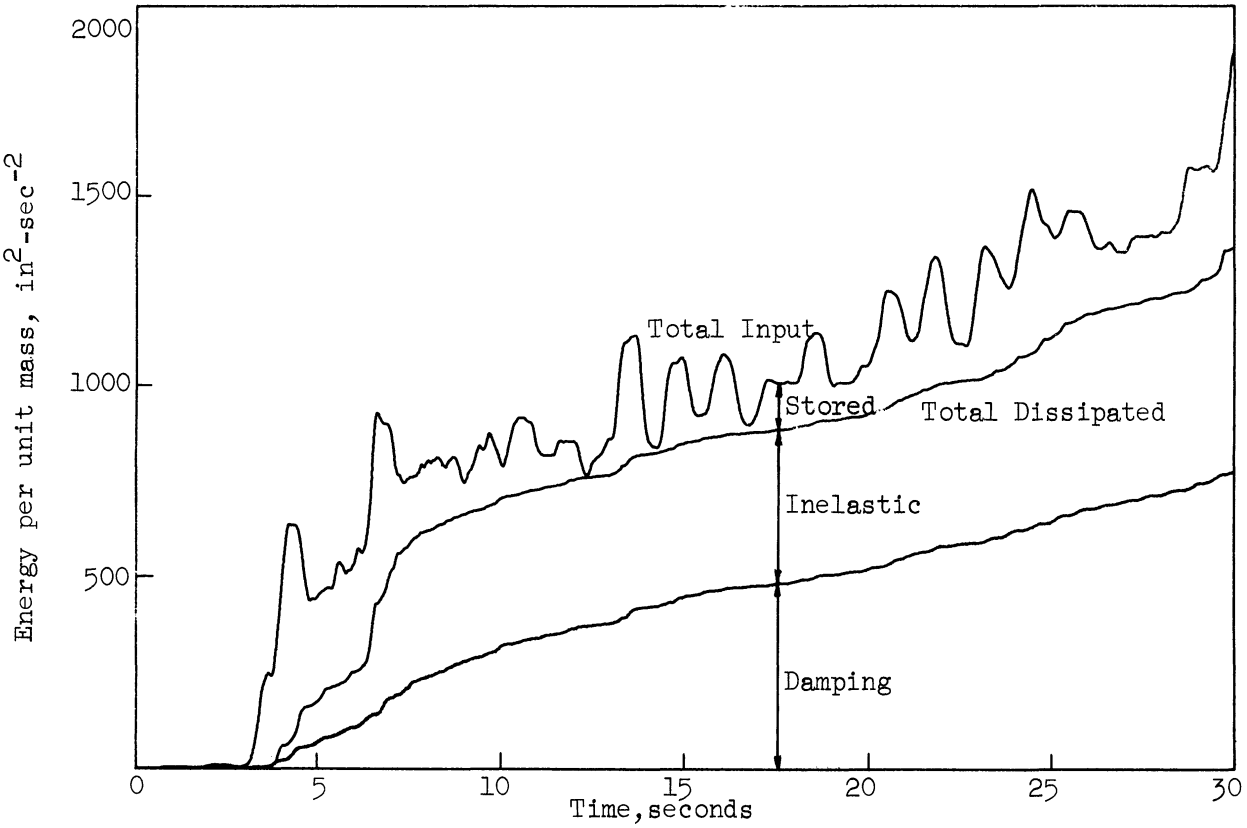

b. With Damping, β = 1%

10-Story Ramberg-Osgood Model, r=10, T=1.25; Taft 1952, S21°W x 3.0

Figure 5.19. Effect of damping on input and dissipated energy.

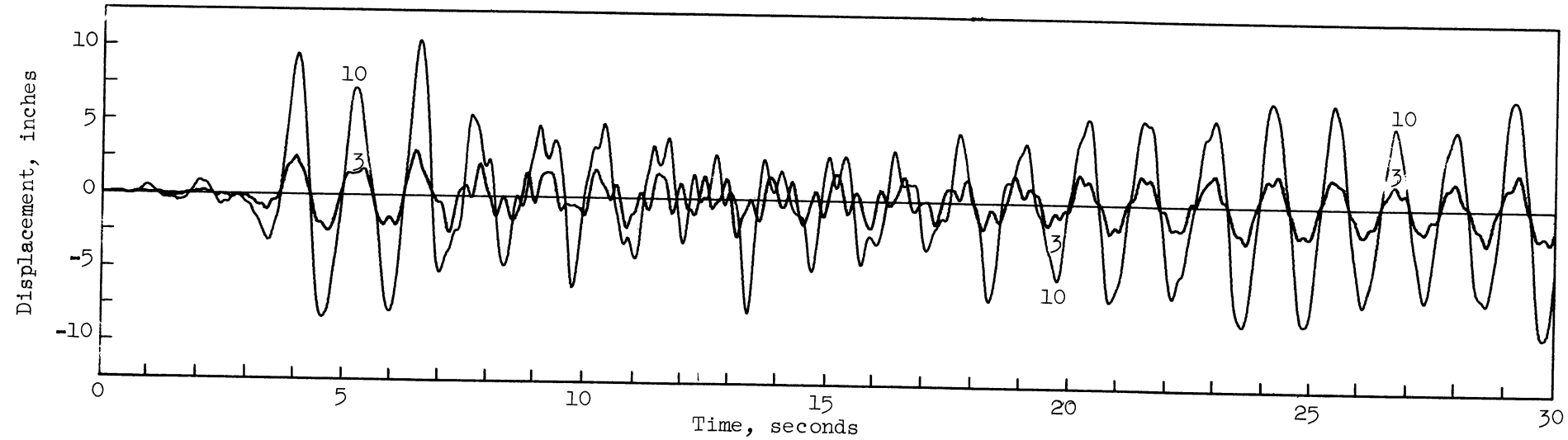

a. Without Damping

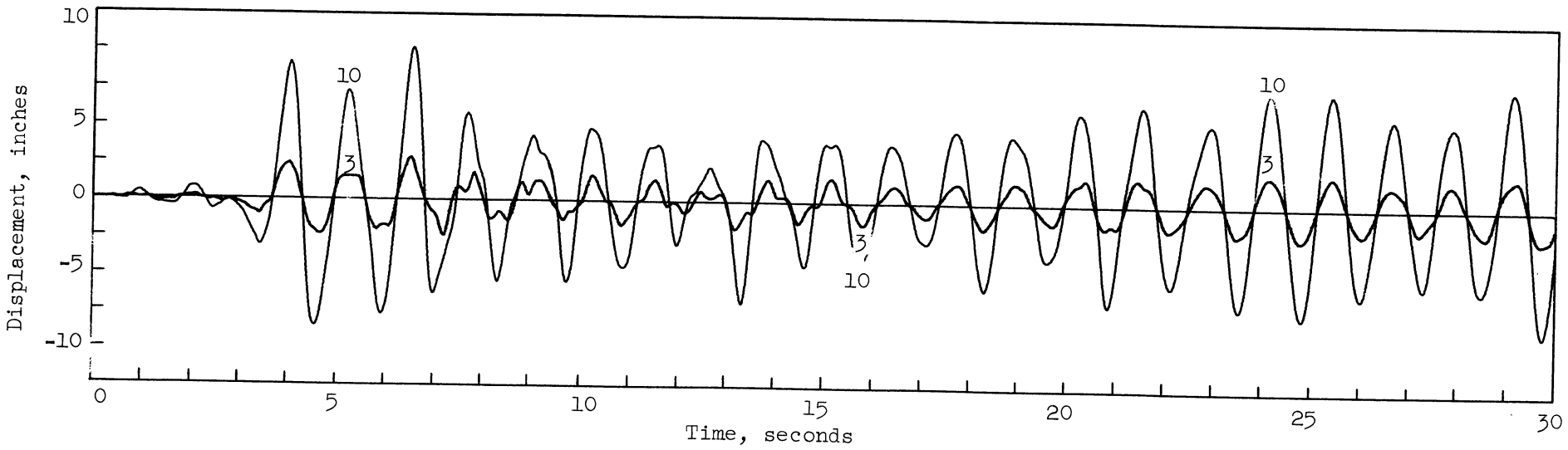

b. With Damping, β = 1%

10-Story Ramberg-Osgood Model, r = 10, T = 1.25; Taft 1952, S21°W x 3.0

Figure 5.20. Effect of damping on the lateral displacements.

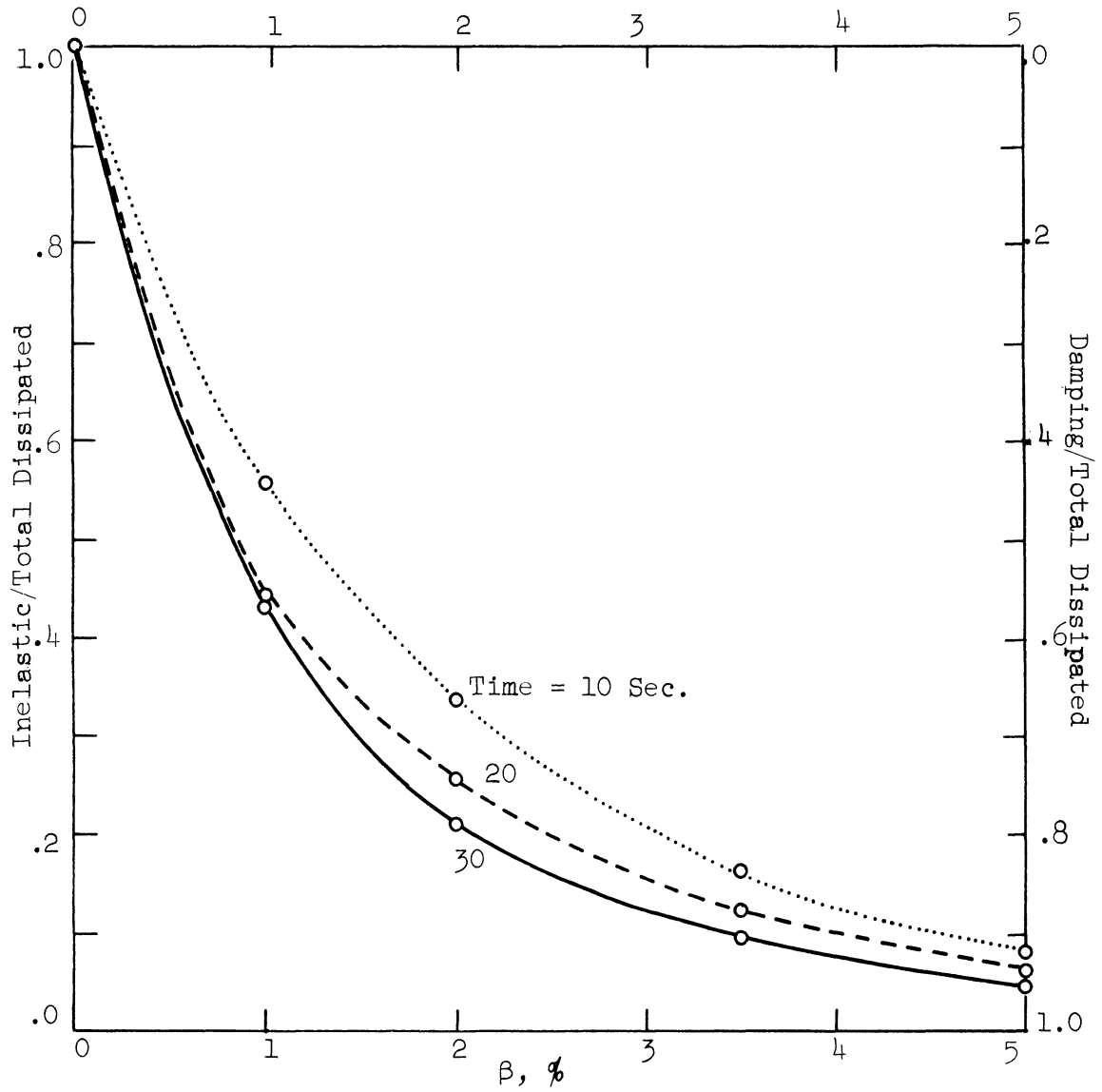

10-Story Standard R-0 Model; r=10, T=1.25; Taft 1952, S21°W x 3.0

Figure 5.21. Effect of earthquake duration on energy dissipation.

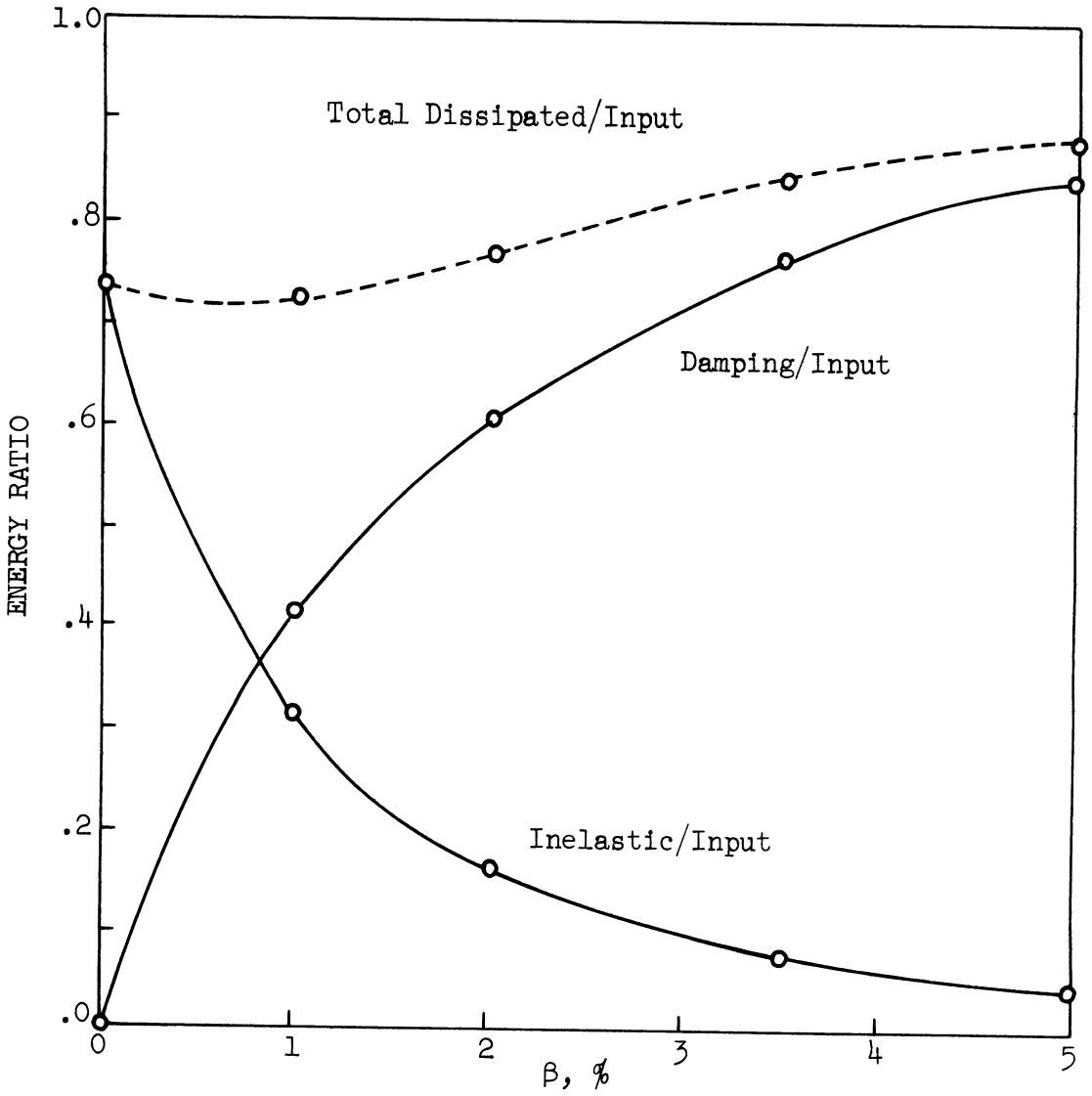

10-Story Standard R-0 Model, r = 10, T = 1.25; Taft 1952, S21°W x 3.0
Duration of Earthquake = 30 seconds.

Figure 5.22. Effect of damping ratio on energy dissipation.

Figure 5.18 shows a comparison of some of the significant response parameters for the three cases, i.e., with β = 0, 1, and 5 percent. A small fraction 1 percent of critical damping in the fundamental mode does not affect the displacements as much as it reduces the story shears, column moments and the girder ductility ratios. A five percent damping, which is a rather high figure, affects the displacements quite significantly while reducing the other three parameters by as much as 50 percent in some floors. Another significant point worth noticing in this figure is that even one percent damping is sufficient to eliminate the accentuation of response near the top, i.e., the "whiplash" effect.

The input and the dissipated energy versus time curves for the case of no damping and β = 1 percent are shown in Figure 5.19(a) and (b), respectively. A similar comparison of the displacements of the third and the tenth floor is presented in Figure 5.20. The small value of damping, β = 1 percent, has an insignificant effect upon these curves in general. But it can be clearly noticed that this amount of damping is sufficient enough to eliminate the contribution of higher modes in the response after about 10 or 15 seconds. This appears as smoothing of small wiggles in the input energy and the displacement curves for the damped case.

The total dissipated energy in the damped case (Figure 5.19) shows a more steady increase and seems to pass through the upper tips of the steps of the corresponding curve in the undamped case. The result is that the stored energy in the damped model is in general less than that in the undamped case. Figure 5.19(b) also shows the individual

shares of the damping and the inelastic action in the total dissipated energy at any instant of time. In the first ten seconds of response the share of the inelastic action is more than the damping. But after this time the inelastic energy remains more or less constant whereas the damping energy grows steadily with time. It appears in this case that the energy dissipation through inelastic deformation is more significant in the beginning of the response after which almost all the dissipation of energy is through viscous damping. The same observation was made for higher damping ratios also, the results of which are shown in Figure 5.22.

The effect of duration of the earthquake upon the individual shares of inelastic action and damping in the total dissipated energy for damping ratios ranging from 0 to 5 percent can be seen in Figure 5.21. Here the two energy ratios, i.e., inelastic/total dissipated and damping/total dissipated for all values of β , are plotted at 10, 20 and 30 seconds of the response. It is clear from these curves that for all values of damping the share of the inelastic energy in the total dissipated energy is higher at 10 seconds response and decreases gradually as the duration of the earthquake increases.

In Figure 5.22 three energy ratios, i.e., damping/input, inelastic/input, and total dissipated/input were plotted at the end of the 30 seconds of response to the Taft accelerogram for the cases, β = 0, 1, 2, 3.5 and 5 percent. These points were joined by three smooth curves. The first two ratios show an increase and an exponential decrease respectively, with increasing damping. The ratio of the total dissipated energy/the total input energy shows a slight decrease in the

beginning followed by an increase for higher damping ratios. It was also found that the total input energy varied with damping similarly as the above ratio of the total dissipated energy to the total input energy.

On the basis of these very limited analyses it can be said that even one percent of critical damping in the fundamental mode can cause a considerable reduction in the inelastic response of a multistory structure. This reduction is much more pronounced near the top stories indicating that the contribution from higher modes is more sensitive to damping than that from the lower modes. This is perhaps due to the fact that the fraction of critical damping is higher in the higher modes for the interfloor dashpot model used. For the Taft earthquake most of the inelastic deformation occurs in the first few seconds and thereafter the damping is primarily responsible for the additional energy dissipation.

CHAPTER 6

SUMMARY AND CONCLUSIONS

This dissertation presents a study of the inelastic behavior of unbraced multistory building frames when subjected to earthquake ground motion. A basic assumption made in the analysis was that the columns would behave elastically while all the energy dissipation of the structure would be provided by girders having stable hysteresis loops. A Ramberg-Osgood type moment-curvature relationship was assumed for the girders. The lateral strength of the structure was proveded by the flexural resistance of the frame members only. The effect of shear and axial strains, the sidesway effect of the gravity loads (P-Δ effect), and non-structural or material damping were not included in the analysis for the first phase of the study. However, the P-Δ effect, the effect of axial deformation of columns, and the effect of viscous damping in the form of inter-floor dashpots were studied in the later phase of the work.

A description of the method of analysis, which was developed for use on a high-speed digital computer, was given in Chapter 2. The equations of motion for the multistory building frame, treated as a lumped mass system, were solved by a Runge-Kutta fourth order numerical procedure. Each lumped mass was assumed to have only one degree of freedom, i.e., in lateral translation only. The response of the frame to the horizontal component of ground motion parallel to the frame was computed by an incremental technique. A special hysteresis law was defined for the transient hysteresis behavior of the girders during the lateral vibration of the structure.

The program of investigation, including the generation of the mathematical models of test frames, the choice of earthquake records, and the schedule of structural parameters whose influence upon the response was to be studied, were presented in Chapter 3. A wide range of significant structural parameters was selected. Three accelerograms, whose acceleration ordinates were multiplied by appropriate factors to give equal spectrum intensities for each earthquake, were selected because they have distinctly different elastic velocity response spectrum characteristics. In Chapter 4 the results of the scheduled computer analyses for the first phase were presented along with the discussion and the observations derived therefrom.

The second phase of the work consisted of modifying the method of analysis described in Chapter 2 to include the sidesway effect of gravity loads (the $P\text{-}\Delta$ effect), the axial deformation of columns, and interfloor viscous damping. Analyses were performed on 10-story models and on a 25-story model. This study gave an evaluation of the influence of these effects (considered separately) upon the inelastic response of the frames. The earthquakes considered in this part of the research were Taft 1952 and El Centro 1940. This phase of the work was described in Chapter 5.

The results, as presented in the foregoing chapters and the observations based upon them under the limitations of the assumptions made in the analysis, are strictly applicable to the types of structures and the earthquakes considered in the study. Summarized below are some important aspects of the results which need emphasis:

1. The assumption of elastic columns is well documented by the results for earthquakes as severe as 1.5 times the intensity of El Centro 1940 or 3.0 times that of Taft 1952 with the behavior of members determined on the basis of a yield level as low as 18 ksi. Thus, it appears feasible that the columns of multistory steel buildings may be designed as elastic even for earthquakes as severe as the ones considered here.
2. The inelastic action of girders tends to decrease the response by as much as 50 percent as compared with the results of the undamped elastic analysis. Thus, the hysteresis behavior of girders alone can be a potential source of energy dissipation in typical high-rise buildings during earthquake excited oscillation.
3. The assumption of the elasto-plasic hysteresis behavior tends to overestimate the response as compared with that of a Ramberg-Osgood type hysteresis behavior which is fairly typical of steel flexural members. An elasto-plastic structure may also be expected to show larger permanent distortion.
4. The elastic fundamental period of a multistory structure and the general features of the elastic velocity response spectrum of the earthquake have a marked influence upon the inelastic response of the structure and can provide significant information about the expected results.

Thus, an earthquake having spectrum peaks in the short period range may be expected to produce greater forces and deformations in the short-period, lower structures, and an earthquake having spectrum peaks in the long-period range will have greater effect upon the taller structures having their fundamental periods in that region of the velocity spectrum.

5. The accentuation of the response near the top of a normal stiffness-tapered multistory structure, commonly referred to as the "whiplash" effect, may be recognized as the contribution from the first few higher modes. This, therefore, is greatly influenced by the velocity spectrum values of the earthquake in the short-period region.

6. Height or the number of stories does not seem to be a very significant factor to influence the response, except for the fact that a taller structure would normally have a longer period so that more higher modal periods would lie on the significant portion of the velocity spectrum of the earthquake, thus, resulting in an increased contribution from the higher modes. However, the column moments and the seismic base shear coefficient may be expected to be smaller in a taller structure than in a short one, irrespective of their fundamental periods.

7. A uniform stiffness structure shows slightly increased lateral displacements as compared with those of a normal stiffness-tapered frame of the same period. The ductile deformations and forces in the members in the uniform structure are larger near the bottom, diminishing sharply toward the top, whereas the stiffness-tapered frame has relatively uniform distribution. The "whiplash" effect is absent in the response of the uniform structure.
8. A reduction in the yield strength of members cuts down the lateral displacements and the moments and shears in the columns. But the ductile deformations are increased in the girders.
9. The P-Δ effect influences the elastic response by as much as ten percent, whereas its effect on the inelastic response is insignificant, the change being of the order of one percent or so. Also, the magnitude of the change seems to be unaffected by the height of the structure or the type of the earthquake.
10. The effect of axial deformation of columns is to make the structure softer so that the columns and girders response can be affected by as much as 10 to 20 percent. This effect may not be predicted by an equivalent change in the elastic stiffness of the structure.
11. The maximum axial loads in the columns of a multistory structure subjected to a severe earthquake can be as high as three and one-half times the static loads.

12. Interfloor viscous damping as small as one percent of critical in the first mode can cause a considerable reduction in the inelastic response. The reduction is much more pronounced in the upper few stories indicating that the contribution of higher modes - the "whiplash" effect, is very sensitive to damping as provided by interfloor viscous dashpots of equal magnitude in each story.

13. For the Taft 1952 earthquake most of the inelastic deformation of a structure occurs in the first few seconds, thereafter, the damping is primarily responsible for the additional energy dissipation.

The investigation was designed to cover a fairly wide range of structural and ground motion characteristics in order to study their influence upon the inelastic behavior of multistory building frames. The results and the observations based upon them are strictly valid for the types of structures and the earthquakes considered in this study. Care must be taken not to draw too broad and general conclusions. Nevertheless, the author feels that some aspects of the results are very significant and contribute to an overall improved understanding of the inelastic behavior of high-rise buildings during strong motion earthquakes, thus, fulfilling the basic objective of this dissertation.

APPENDIX

HYSTERESIS LAW*

Any procedure for the computation of inelastic response of a system subjected to random vibration needs a suitable law which would control the hysteresis loops as the system vibrates. Such a law takes a very simple form for the conventional elasto-plastic or bilinear hysteresis models. But for a curvilinear shape, as is the Ramberg-Osgood model considered here, the problem of defining a suitable hysteresis law is rather complex. A simple and convenient law, which was used in the present study, is illustrated in Figure A and explained below.

Let the moment-curvature property of a structural member be given by the Ramberg-Osgood relationships as shown in Figure 2.1(b). In the first installment of loading let the point P_1 be reached on the skeleton curve C_o . Equation (2.2) will control the M-ϕ behavior so far. On reversal at point P_1 the descending branch C_1 will be generated which will be described by the Equation (2.3) with P_1 as its point of origin. If the descent along C_1 is continued beyond the point P_1' , point symmetrically opposite to P_1 , the branch curve C_1 will slip on to the descending skeleton

*This formulation of the general hysteresis behavior was developed and used in force-deflection terms by Professor G. V. Berg for his study of single-degree-of-freedom systems.(13) The hysteresis law, as presented here, was used in the present analysis to describe the moment-rotation hysteresis behavior of the girders of multistory frames subjected to earthquake motion.

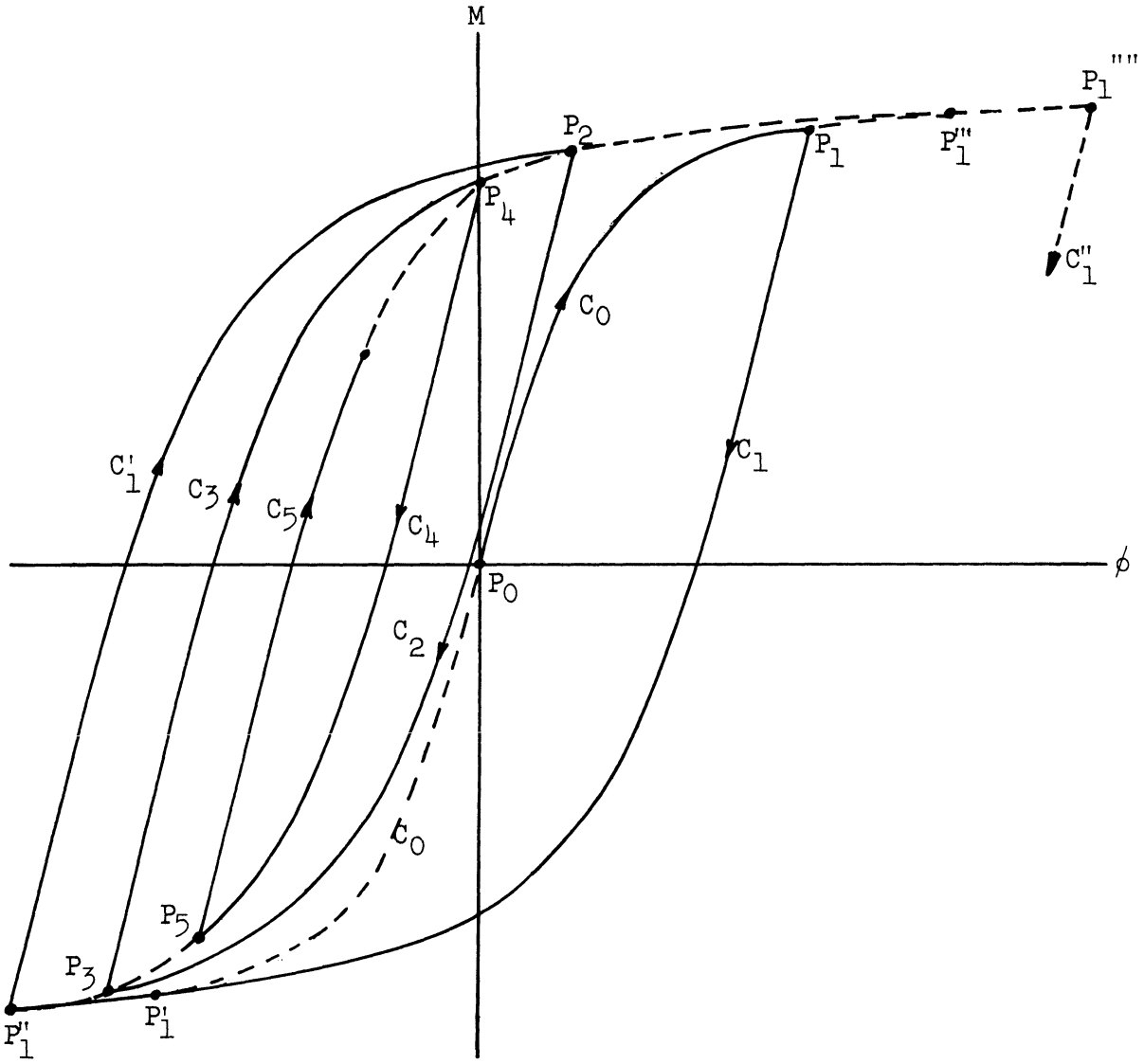

Figure A. General hysteresis behavior

curve P_oP_1' , the Equation (2.2) coming into action until the next point of reversal. Let this point be P_1'' , the new maximum on the skeleton curve C_o .

A fresh branch curve C_1' will now emerge from P_1'' controlled by Equation (2.3), which will be valid up to P_1''' , a point mirror image of P_1'' . If the motion reverses before the curve C_1 extends up to P_1''', a descending branch curve C_2 will emerge from the point of reversal P_2 as shown in the figure. This branch curve will pass through P_1'' (by the closure property of these curves)[12] and then slip on to the skeleton curve $P_oP_1'P_1''$ unless the motion reverses before reaching P_1'' . Let the point of reversal on C_2 be P_3 which will form the originating point for a new ascending branch curve C_3 .

Let the curve C_3 define the motion until it reverses at P_4 before reaching its closrue point P_2 . C_4 will be the new curve descending from P_4 up to the next point of reversal P_5 . The ascending branch curve C_5 will describe the motion up to the point P_4 , point of origin for the previous descending branch C_4 and the point of closure of the loop C_4C_5 . If the amplitude tends to increase further, the point P_4 will act as terminus for the curve C_5 beyond which the previous ascending branch C_3 will carry the motion up to P_2 , the terminus for C_3 . If the ascent still continues, the curve C_1' will take over from C_3 beyond P_2 , which will remain valid if the reversal does not occur before P_1''' , the terminus for the curve C_1' . The curve C_1' beyond this point will then slip on to the original ascending skeleton curve C_o ,

the reversal on which will mark a fresh point of maximum deformation P_1'''', on the curve C_o and the beginning of a fresh descending curve C_1'' as before. In other words, whenever a point of maxima is exceeded in any direction on the skeleton curve, a whole new set of branch curves will be generated until a similar thing occurs again.

The scheme as illustrated in Figure A and explained above is a fairly simple one which can be easily programmed for a numerical solution. It is believed that this law will very closely predict the actual hysteresis loops which a structural steel member would generate under a similar deformation history. The points of reversals of all the branch curves after the most recent point of maxima on the skeleton curve was reached, of course, have to be retained for guiding the new branch curves, until the previous absolute maximum on the skeleton curve is exceeded in either direction of loading.

REFERENCES

1. Housner, G. W., Martel, R. R., and Alford, J. L. "Spectrum Analysis of Strong Motion Earthquakes." Bulletin, Seismological Society of America, Vol. 43, April 1953.

2. Clough, R. W. "On the Importance of Higher Modes of Vibration in the Earthquake Response of a Tall Building." Bulletin, Seismological Society of America, Vol. 45, October 1955.

3. Degenkolb, H. J. "Structural Observations of the Kern County Earthquake." Transactions, ASCE, Vol. 120, 1955, pp. 1280-1294.

4. Penzien, J. "Dynamic Response of Elasto-Plastic Frames." Journal of the Structural Division, ASCE, Vol. 86, No. ST7, July 1960.

5. Veletsos, A. S. and Newmark, N. M. "Effect of Inelastic Behavior on the Response of Simple Systems to Earthquake Motions." Proceedings, 2nd World Conference on Earthquake Engineering, Tokyo, 1960, Vol. II.

6. Penzien, J. "Elasto-Plastic Response of Idealized Multistory Structures During Earthquakes." Proceedings, 2nd World Conference on Earthquake Engineering, Tokyo, 1960, Vol. II.

7. Berg, G. V. "The Analysis of Structural Response to Earthquake Forces." Ph.D. Thesis, The University of Michigan, May 1958.

8. Berg, G. V. and Thomaides, S. S. "Energy Consumption in Strong Motion Earthquakes." Proceedings, 2nd World Conference on Earthquake Engineering, Tokyo, 1960, Vol. II.

9. Clough, R. W., Benuska, K. L. and Wilson, E. L. "Inelastic Earthquake Response of Tall Buildings." Proceedings, 3rd World Conference on Earthquake Engineering, New Zealand, 1965.

10. Clough, R. W. and Benuska, K. L. "Earthquake Performance of High-Rise Buildings." FHA Report, T. Y. Lin and Associates, Van Nuys, California, October 1965.

11. Popov, E. P. and Franklin, H. A. "Steel Beam-to-Column Connections Subjected to Cyclically Reversed Loading." Proceedings, Structural Engineers Association of California, October, 1965.

12. Jennings, P. C. "Response of Simple Yielding Structures to Earthquake Excitation." Ph.D. Thesis, California Institute of Technology, Pasadena, California, 1963.

13. Berg, G. V. "A Study of the Earthquake Response of Inelastic Systems." Proceedings, Structural Engineers Association of California, October, 1965.

14. Gill, S. "A Procedure for the Step-by-Step Integration of Differential Equations in an Automatic Computing Machine." Proceedings, Cambridge Philosophical Society, 47:96, 1951.

15. Kaldjian, M. J. "Moment-Curvature of Beams as Ramberg-Osgood Functions." Jounral of the Structural Division, ASCE, October 1967.

16. Popov, E. P. "Low-Cycle Fatigue of Steel Beam-to-Column Connections." Proceedings, International Symposium on the Effects of Repeated Loading of Materials and Structural Elements, Mexico City, September 1966.

17. Housner, G. W. and Brady, A. G. "Natural Periods of Vibration of Buildings." Journal of the Engineering Mechanics Division, ASCE, August 1963.

18. Nielsen, N. Norby. "Vibration Tests of a Nine-Story Steel Frame Building." Journal of the Engineering Mechanics Division, ASCE, February 1966.

19. Rea, Bouwkamp, J. G. and Clough, R. W. "Dynamic Behavior of Steel Frame and Truss Buildings." Structures and Materials Report No. 62-24, University of California, Berkeley, California, September 1966.

20. Housner, G. W. "Behavior of Structures During Earthquakes." Journal of the Engineering Mechanics Division, ASCE, October 1959.

21. Arnold, P., Adams, P. F. and Lu, Le-Wu. "The Effect of Instability on the Cyclic Behavior of a Frame." Proceedings, International Symposium on the Effects of Repeated Loading of Materials and Structural Elements, Mexico City, September 1966.

22. Yarimci, E. "Incremental Inelastic Analysis of Framed Structures and Some Experimental Verifications." Ph.D. Thesis, Lehigh University, Bethlehem, Pennsylvania, May 1966.

23. Husid, R. "Gravity Effects on the Earthquake Response of Yielding Structures." Ph.D. Thesis, California Institute of Technology, Pasadena, California, June 1967.

24. Rubinstein, M. F. "Effect of Axial Deformation on the Periods of a Tall Building." Bulletin, Seismological Society of America, Vol. 54, No. 1, February 1964.